https://doi.org/10.1016/j.trc.2021.103337

A mixed-equilibrium model of individual and household activity–travel choices in multimodal transportation networks

Khoa D. Vo[a,*], William H. K. Lam[a], Zhi-Chun Li[b]

[a]*Department of Civil and Environmental Engineering, The Hong Kong Polytechnic University, Hong Kong*

[b]*School of Management, Huazhong University of Science and Technology, Wuhan, China*

Abstract

This paper develops a novel household-oriented activity-based mixed-equilibrium model for estimating individual and household activity–travel choices in multimodal transportation networks with interactions between private car and public transit modes. In the novel model, household members with heterogeneous errors of perception on the time-dependent utility of different activity types make daily joint/solo activity–travel choices in a mixed-equilibrium manner, which maximizes either perceived household utility or perceived individual utility. A logit-based stochastic choice model is developed to capture the mixed equilibrium with heterogeneous errors of perception and used to predict the choices of alternative joint activity–travel paths (JATPs) on a supernetwork platform. Based on this stochastic JATP choice model, the mixed-equilibrium model is formulated as an equivalent variational inequality (VI) problem and solved using a modified diagonalization method. This converts the time-dependent activity–travel scheduling problem into an equivalent static traffic assignment problem on JATPs. The conditions required for the existence and uniqueness of a solution to the equivalent VI problem in terms of a JATP flow pattern are also identified. Numerical examples are provided to illustrate the model's merits and its applications for examining the effect of the coronavirus disease 2019 (COVID-19) pandemic.

Keywords: Activity-based modeling, Intra-household interaction, Network equilibrium, Multimodal transportation network, COVID-19

1. Introduction

1.1. Background and motivation

In the modern life, it is a common thing that individuals perform daily activities and travel jointly with other members of the same household due to social factors (e.g., altruism and a desire for companionship) and/or resource constraints (Gliebe and Koppelman (2005); Bradley and Vovsha (2005); Bhat et al. (2013); Lin and Wang (2014)). Extensive survey evidence suggests that there are interactions between household members' joint activity–travel choices. For example, Srinivasan and Bhat (2008) found that almost one-third of individuals undertake one or more out-of-home activity and travel episodes with household members on weekdays, according to the American Time Use Survey data. Similarly, using the Hong Kong Travel Characteristics Survey data, Lai et al. (2019) showed that 18.7% of daily out-of-home activities by full-time working couples and 64.9% of those by retired couples are jointly conducted.

The process used for making decisions on joint activity–travel choices differs from that used for making decisions on solo activity–travel choices. Joint activity–travel choices require spatiotemporal coordination of the activity–travel schedules of the involved individuals (Zhang et al. (2005); Habib et al. (2008)). As a result, any change in the daily activity–travel schedule of an individual under a transportation policy can change the daily activity–travel schedules of his/her partners. However, such a secondary effect of the transportation policy cannot be captured if the joint activity and travel interactions between household members are not explicitly modeled (Srinivasan and Bhat (2008)). In addition, the analysis of joint activity–travel behavior is crucial for the accurate estimation of the effect of ridesharing policies, such as those related to high-occupancy vehicle lanes and tolls.

*Corresponding author

Email address: khoa.v.dang@gmail.com; khoa.vo@connect.polyu.hk (Khoa D. Vo[a,*])

The pandemic of coronavirus disease 2019 (COVID-19), the first reported case of which was recorded in November 2019 in Wuhan, Hubei province, China, has disrupted daily activities and travel worldwide, as widespread lockdowns and restrictions on activities and travel have drastically altered the daily routines of millions of people. For example, commuting to workplaces and in-store shopping have been replaced by telecommuting and online shopping, respectively, and thus the total travel demand for all modes of transportation has substantially been reduced (Beck and Hensher (2020); Parady et al. (2020); Shamshiripour et al. (2020); De Vos (2020)). The effects of the COVID-19 pandemic on activity–travel behavior and demand may persist over the long term, and at least not return to pre-pandemic levels in a short time. For example, it is expected that some work-at-home activities will continue after the pandemic has finished, and that the use of public transport will decrease slightly, because people will prefer to use active modes of transportation (e.g., a car) for health reasons. Moreover, the fear of infection with severe acute respiratory syndrome coronavirus 2 (SARS-CoV-2), the virus that causes COVID-19, will be a major long-term concern for people contemplating out-of-home activities, such as in-store shopping and face-to-face meetings (Public Transport Research Group (2020); Covidfuture (2020)). Thus, it is essential to investigate these effects of the COVID-19 pandemic when designing transportation arrangements for the short term (e.g., adjusting transit services according to the mode of transportation) and the long term (e.g., designing multimodal networks). In addition, although recurrent scenarios can be learned and solved via a long-term process (Arentze and Timmermans (2005); Zhang et al. (2016)), nonrecurrent scenarios related to COVID-19 pandemic restrictions or lockdowns cannot be learned and thus can substantially affect commuters' perceptions of risk and attitudes toward daily activity–travel choices. Thus, when examining the effects of the COVID-19 pandemic it is also crucial to account for the errors of perception on transportation network conditions that commuters may exhibit when making activity–travel choices.

Individuals' activity–travel schedules are highly interrelated in terms of the time of day, their intra-household interactions, and their knowledge about transportation network conditions. For example, if the wife in a one-car household is more familiar with the transit system, she will tend to use public transit for her daily commutes. Then, such a transit mode choice by the wife for a work trip in the morning will affect her choices of transportation mode for subsequent trips in her activity–travel schedule throughout the day. In turn, this will also affect her husband's activity–travel schedule and mode choices during the day, as he will be able to use the household's car for daily travel. Consequently, he may pick up his wife from her work, and they may dine together after work; these actions may themselves be affected by the couple's knowledge about characteristics of activity locations. Hence, an appropriate approach for evaluating the effects of transportation policies is to simultaneously investigate individuals' activity–travel scheduling behavior, their possible joint activity–travel behavior, their errors of perception on transportation network conditions, and the interactions between multiple transportation modes in which travel times of road-based transit modes (e.g., bus) are affected by road congestion.

To integrate activity-based modeling into dynamic traffic assignment for travel demand forecasting, various individual-oriented activity-based network equilibrium models have been developed to simulate the solo daily activity–travel schedules of individuals (e.g., Lam and Yin (2001); Lam and Huang (2002); Ramadurai and Ukkusuri (2010); Chow and Djavadian (2015); Liu et al. (2015, 2016); Li et al. (2018); Ouyang et al. (2011); Fu and Lam (2014); Fu et al. (2014); Fu and Lam (2018)). However, the effect of intra-household interactions on daily activity–travel scheduling behavior at a household level has rarely been studied (Fu and Lam (2018); Vo et al. (2020a)). The few studies that have been performed have mainly focused on public transit or private car modes and have ignored the interactions between different transportation modes, despite the fact that these can substantially affect households' activity–travel schedules. In addition, most of the above models have been developed based on the assumption that travelers have perfect knowledge about the traffic conditions throughout a transportation network and the congestion level at activity locations, which is clearly not realistic. Moreover, these models must be extended to investigate the effect of the COVID-19 pandemic in terms of the demand for working-at-home and the risk of infection with SARS-CoV-2 in public areas, such as at out-of-home activity locations and in public transit vehicles.

To address these research needs, this paper develops a novel household-oriented activity-based mixed-equilibrium model for the determination of individual and household activity–travel choices in multimodal transportation networks with interactions between private car and public transit modes. In the developed model, household members who have heterogeneous errors in their perception of the time-dependent utilities of different activity types, make joint/solo activity–travel choices in a mixed-equilibrium manner, which maximizes (or optimizes) their perceived household utility or individual utility. To consistently account for the intra-household interactions of joint/solo activity–travel choices, the activity–travel choices of a household's daily schedule are represented by a unified joint activity–travel

path (JATP) on a novel joint activity–time–space (JATS) supernetwork platform. Based on this platform, the JATP choice set can be generated using any conventional path-finding algorithms (e.g., Dijkstra's algorithm). We then develop a novel logit-based stochastic JATP choice model to capture the mixed equilibrium of individual and household activity–travel choices with considering the heterogeneous errors of perception. This mixed-equilibrium model is formulated as an equivalent variational inequality (VI) problem, based on the stochastic JATP choice model, and is solved using a diagonalization method. This solution method converts the time-dependent household activity–travel scheduling problem into an equivalent static traffic assignment problem with respect to JATPs on the supernetwork platform, and solves it within a unified framework.

1.2. Literature review

Many researchers have examined a wide range of aspects of interactions between household members, such as time allocation (Kato and Matsumoto (2009); Bernardo et al. (2015); Lai et al. (2019)), activity generation (Srinivasan and Bhat (2008); Bhat et al. (2013)), daily activity pattern types (Bradley and Vovsha (2005)), travel arrangement (Gliebe and Koppelman (2005); Gupta et al. (2014); Weiss and Habib (2018)), heterogeneous group decision-making mechanisms (Zhang et al. (2009)), and synchronization of work tour departure and arrival times (Gupta and Vovsha (2013)). These works have involved the development of models based on random utility maximization (RUM) theory, and the use of scale parameters to account for household members' heterogeneous or homogeneous errors in their perception of various dimensions of activity–travel choices. Nevertheless, as these models have typically been embedded in an external activity-based microsimulation framework (e.g., Bhat et al. (2004); Roorda et al. (2009); Dubernet and Axhausen (2015)), they must be extended to enable consideration of the daylong activity–travel schedules of household members.

Daylong household scheduling problems have been extensively investigated, and various models and methods have been used to generate households' daylong activity–travel schedules. Some household activity–travel scheduling models have been devised via a mathematical programming approach, such as that of Recker (1995) and its extensions (Gan and Recker (2008, 2013); Kang and Recker (2013); Chow and Nurumbetova (2015)), which formulate the household activity pattern problem as a pick-up and delivery problem with time windows. Other models have formulated the activity–travel scheduling problem with joint travel decisions in a multimodal system as a shortest path-finding problem in a multi-state supernetwork (Liao et al. (2013b); Liao (2019)). These supernetwork-based models with consideration of joint travel have been built upon the earlier comprehensive works on scheduling individuals' activity–travel patterns (see e.g., Liao et al. (2011, 2013a, 2014); Liao (2016); Lyu et al. (2021)). However, the aforementioned studies have mainly focused on generating disaggregated travelers' daily activity–travel schedules and have commonly assumed that travel times and/or activities are of fixed duration, without considering the endogenous effects of transportation network congestion. To extend their works, this paper aims to model explicitly the network congestion effects on joint travel and activity participation, and vice versa.

Other approaches for modeling intra-household interactions have been based on agent-based microsimulation frameworks, such as Albatross (Arentze and Timmermans (2004a)), TASHA (Roorda et al. (2009)), ADAPTS (Auld and Mohammadian (2012)), and MATSim (Dubernet and Axhausen (2015)). In these microsimulation models, the activity–travel choices of individuals have been generated using various approaches, such as computational processes, production rules, and/or utility maximization, to manage the complexity of time–space constraints in intra-household interactions. The activity–travel scheduling processes in these models have typically been based on the concept of skeleton schedules with given and fixed attributes, such as activity start time, duration, destination, and location (Habib et al. (2008)). As a result, the linkages in these models between different choice dimensions in households' activity–travel schedules are weak. In addition, to integrate activity-based modeling and traffic assignment, these agent-based microsimulation models have usually been based on external traffic assignment models in which the feedback between activity–travel scheduling and traffic assignment is iteratively updated in a separate and ad hoc manner.

To account for the effects of transportation network congestion on individuals' activity–travel scheduling behaviors within a unified framework, several individual-oriented activity-based network equilibrium models have been proposed for congested road networks (Lam and Yin (2001); Lam and Huang (2002); Ramadurai and Ukkusuri (2010); Ouyang et al. (2011); Nourinejad et al. (2016); Liu et al. (2018)), transit networks (Li et al. (2010); Fu and Lam (2014); Fu et al. (2014)), multimodal transportation networks (Chow and Djavadian (2015); Liu et al. (2015, 2016); Li et al. (2018); Najmi et al. (2020); Liu et al. (2020)), and bottlenecks (Li et al. (2014, 2017); Li and Zhang (2020); Cantelmo and Viti (2019)). These models can capture the interrelation of various choice facets and aspects of the activity–travel

scheduling behavior of travelers (e.g., their activity/trip chain, activity duration, departure time, path/mode at various times of day, day-to-day need-based activity–travel dynamics, and/or network uncertainty), and the endogenous effects of transportation network congestion. However, they are built upon either a deterministic user equilibrium (UE), (tolerance-based) dynamic user equilibrium (DUE), or stochastic user equilibrium (SUE) principle with respect to activity–travel choices at an individual level. Thus, the activity–travel choices and the possible intra-household interactions of joint activities and travel in these models are determined independently for each individual. In view of these, this paper proposes a novel model to explicitly account for household members' errors of heterogeneous perception on time-dependent activity–travel utility, and the interactions between private car and public transit modes in which travel times of road-based transit modes (e.g., buses) are in fact affected by road congestion.

Recently, a few attempts have been made to model the joint activity–travel choices of household members. Fu and Lam (2018) performed this modeling for two household members, using the concept of JATP on a JATS supernetwork platform. They modeled each household as a "user" and applied the UE principle at a household level to the activity–travel choices of all individuals of each household to maximize the household utility. They also simplified the modeling of joint activities and travel by allowing each individual's schedule to have a maximum of one joint activity (e.g., shopping) and one travel episode. In addition, their model only accounted for one user class of full-time working couples and transit modes. Vo et al. (2020a) later refined the UE principle used by Fu and Lam (2018) at a household level as a household utility optimum (HO) principle to model the joint activity–travel choices of car users. Their model could manage more generalized intra-household interactions of the joint activity–travel choices of various household types using different transportation modes (i.e., a private car or public transit). Nevertheless, the transit path choices in their model were not explicitly modeled, as the transit travel demand for each origin–destination (OD) pair was captured using a constant demand-excess function. Thus, Vo et al. (2020a) did not explicitly and endogenously model the transit congestion effects. Furthermore, neither of these mentioned household-oriented activity-based equilibrium models (Fu and Lam (2018); Vo et al. (2020a)) accounted for household members' errors of perception on time-dependent activity–travel utility, their need to work at home, or the risk of SARS-CoV-2 infection at activity locations and in transit vehicles.

Table 1 compares different approaches that have been used in previous works for generating households' daylong activity–travel schedules. These approaches have commonly assumed that households make decisions regarding their daily activity–travel schedules based on given exogenous and fixed network travel times. In contrast, we propose a network equilibrium approach in which households' decisions regarding their daily activity–travel schedules are based on the congestion effects of multimodal transportation networks, which are considered endogenously. Our approach leads to a consistent and stable solution for households' daily activity–travel schedules and the corresponding network equilibrium conditions, which is useful for strategic planning purposes. Table 2 contrasts the novel model developed in this paper with the previously established individual- and household-oriented activity-based network equilibrium models. These previous models focus on either individual or household activity–travel choices for either private car or transit modes. However, the novel model accounts for the mixed equilibrium of individual and household activity–travel choices, with mixed-mode interactions between private car and public transit modes and household members' heterogeneous errors of perception on activity–travel utility by time of day.

1.3. Contributions

In contrast to Vo et al. (2020a), who investigated intra-household interactions in congested road networks, this paper focuses on (i) a mixed equilibrium of individual and household activity–travel choices with homogeneous errors of perception, and (ii) interactions between private car and public transit modes. The contributions of this paper are as follows.

- Development of a novel household-oriented activity-based mixed-equilibrium model for estimating individual and household activity–travel choices in multimodal transportation networks, with interactions between private car and public transit modes.
- Development of a logit-based stochastic choice model with respect to JATPs on a supernetwork platform to capture a mixed equilibrium of individual and household activity–travel choices with heterogeneous errors of perception on the time-dependent utility of different activity types.
- A proof of the existence and uniqueness of a solution for the mixed-equilibrium problem in terms of a JATP flow pattern. As a result, this proof also implies the existence and uniqueness of link and path flows, and of households' activity–travel scheduling and time allocations.

Table 1: Comparison of different activity-based approaches used for generating households' daylong activity–travel schedules.

Modeling approach	References	Considering network congestion	
		Road	Transit
Mathematical programming	Recker (1995); Gan and Recker (2008, 2013); Kang and Recker (2013); Chow and Nurumbetova (2015)	No	No
Shortest path-finding	Liao et al. (2013b); Liao (2019)	No	No
Agent-based microsimulation	Arentze and Timmermans (2004a); Roorda et al. (2009); Auld and Mohammadian (2012); Dubernet and Axhausen (2015)	No	No
Network equilibrium	Fu and Lam (2018)	No	Yes
	Vo et al. (2020a)	Yes	No
	This paper	Yes	Yes

Note: "Yes" indicates that the model considers network congestion effects endogenously when households' activity–travel are made, and "No" indicates that the network congestion effects are given exogenously when household's activity–travel schedules are made.

Table 2: Comparison of the novel model developed in this paper with relevant individual- and household-oriented activity-based network equilibrium models.

Reference	User class	Travel mode	Considering mixed-mode interactions*	Considering perception error
Lam and Yin (2001)	Individual	Private car	No	Homogeneous
Ramadurai and Ukkusuri (2010)	Individual	Private car	No	No
Fu and Lam (2014)	Individual	Public transit	No	No
Liu et al. (2015)	Individual	Multimodal	No	No
Chow and Djavadian (2015)	Individual	Multimodal	No	Homogeneous
Liu et al. (2016)	Individual	Multimodal	No	No
Li et al. (2018)	Individual	Multimodal	No	No
Najmi et al. (2020)	Individual	Multimodal	No	No
Fu and Lam (2018)	Household	Public transit	No	No
Vo et al. (2020a)	Mixed	Private car	No	No
This paper	Mixed	Multimodal	Yes	Heterogeneous

*: "No" indicates that the model either does not consider transit modes or assumes given and fixed transit travel times, and "Yes" indicates that the model accounts for endogenous effects of road congestion on travel times of road-based transit modes.

The remainder of this paper is organized as follows. The assumptions used in the development of the novel model and some useful concepts are discussed in Section 2, and the novel model formulation and solution method are presented in Sections 3 and 4, respectively. The numerical results, which illustrate the merits of the novel model, are shown in Section 5. The applicability of the novel model for assessing the effects of the COVID-19 pandemic is illustrated in Section 6. Finally, conclusions and recommendations for further study are given in Section 7.

Some notation

Sets

A	set of road links
B	set of transit links $B = B_1 \cup B_2 \cup B_3 \cup B_4$, respectively including access, egress, transfer, and vehicle links
S	set of nodes including activity and/or drop-off/pickup locations
I	set of activities
P^w	set of feasible paths between OD pair w used by car users

$\hat{P}^w$	set of feasible paths between OD pair w used by transit passengers
Q^h	set of feasible JATPs chosen by household type h
Indices	
k	a time interval
m	a household member
h	a household type
g	a group of household members
q	a JATP
i	an activity
x	an activity type
s	a location
p	a path used by car users or transit passengers
a	a road link
b	a transit link, including access, egress, transfer, or vehicle link
w	an OD pair
K	number of time intervals in the study period
H	number of household types
G^h	number of groups in household type h
M^h	number of members in household type h
Parameters	
θ^h	household scale parameter associated with the percieved utility of household type h
η_x^{hm}	individual scale parameter associated with the percieved utility of type x activities of member m of household type h
α_{is}^{hg}	household preference parameter for joint activity i at location s of group g of household type h
β_a^{hg}	household preference parameter for joint travel on road link a of group g of household type h
$\hat{\beta}_b^{hg}$	household preference parameter for joint travel on transit link b of group g of household type h
$\varrho^{hg}, \hat{\varrho}^{hg}$ (\$/h)	household risk-perception parameter for joint out-of-home acitivities and travel by public transit of group g of household type h
$\varrho^{hm}, \hat{\varrho}^{hm}$ (\$/h)	individual risk-perception parameter for solo out-of-home acitivities and travel by public transit of member m of household type h
$u_{is}^{hm}(k)$ (\$)	marginal utility of member m of household type h performing activity i alone at location s during interval k
γ (\$/h)	value of travel time of car users
$\hat{\gamma}_1$–$\hat{\gamma}_4$ (\$/h)	coefficients to convert different quantities of the transit time components to a monetary unit
$\phi_a^{hg}(k)$ (\$)	operating travel cost on road link a during interval k of group g of household type h
φ_b (\$)	transit fare on vehicle link b
C_{is} (persons)	capacity of activity i at location s
$\tilde{C}_a$ (veh/h)	capacity of road link a
$\hat{C}_b$ (pax/veh)	capacity of each transit vehicle associated with vehicle link b
D_b (veh/h)	transit frequency associated with vehicle link b
t_σ (h)	length of each time interval
F^h	number of households with type h
R	infection ratio (i.e., expected number of confirmed cases divided by total population in the design year)
Variables	
f_q^h	number of households with type h choosing JATP q
$v_{is}(k)$	number of persons participating in activity i at location s during interval k
$\tilde{v}_a(k)$	number of private cars on road link a during interval k
$\hat{v}_b(k)$	number of transit passengers on transit link b during interval k
$v_{is}^{hmg}(k)$	number of persons being member m in group g of household type h participating in activity i at location s during interval k

$v_a^{hmg}(k)$	number of car users being member m in group g of household type h on road link a during interval k
$\hat{v}_b^{hmg}(k)$	number of transit passengers being member m in group g of household type h on transit link b during interval k
$\delta_{qis}^{hmg}(k)$	equals 1 if member m in group g of household type h choosing JATP q participates in activity i at location s during interval k, and 0 otherwise
$\xi_{qpw}^{hmg}(k)$	equals 1 if member m in group g of household type h choosing JATP q enters path p by private car between OD pair w during interval k, and 0 otherwise
$\hat{\xi}_{qpw}^{hmg}(k)$	equals 1 if member m in group g of household type h choosing JATP q enters path p by public transit between OD pair w during interval k, and 0 otherwise
$\zeta_{ap}^{wk}(k')$	equals 1 if private cars entering path p between OD pair w during interval k arrive at road link a during interval k', and 0 otherwise
$\hat{\zeta}_{bp}^{wk}(k')$	equals 1 if transit passengers entering path p between OD pair w during interval k arrive at transit link b during interval k', and 0 otherwise
$\tilde{\zeta}_{ab}^{k}(k')$	equals 1 if transit passengers entering vehicle link b associated with bus line l during interval k arrive at road link a during interval k', and 0 otherwise
$\xi_{qpwak}^{hmg}(k')$	equals 1 if $\xi_{qpw}^{hmg}(k)\zeta_{ap}^{wk}(k') = 1$, and 0 otherwise
$\hat{\xi}_{qpwbk}^{hmg}(k')$	equals 1 if $\hat{\xi}_{qpw}^{hmg}(k)\hat{\zeta}_{bp}^{wk}(k') = 1$, and 0 otherwise
Functions	
u_q^h (\$)	utility of household type h choosing JATP q under normal condition
$\tilde{u}_q^h$ (\$)	mapping function in the VI problem
$\bar{u}_q^h(R)$ (\$)	utility of household type h choosing JATP q when the infection ratio is R (i.e., $\bar{u}_q^h(R) = u_q^h - \rho_q^h(R)$)
$\rho_q^h(R)$ (\$)	disutility of risk percived by household type h choosing JATP q when the infection ratio is R
$u_{is}^{hmg}(k)$ (\$)	utility of member m in group g of household type h performing activity i at location s during interval k
$c_{pw}^{hmg}(k)$ (\$)	travel disutility of member m in group g of household type h entering path p by private car between OD pair w during interval k
$\hat{c}_{pw}^{hmg}(k)$ (\$)	travel disutility of member m in group g of household type h entering path p by public transit between OD pair w during interval k
$c_a^{hmg}(k)$ (\$)	travel disutility of member m in group g of household type h on road link a during interval k
$\hat{c}_b^{hmg}(k)$ (\$)	travel disutility of member m in group g of household type h on transit link b during interval k
$\rho_{is}^{hmg}(k,R)$ (\$)	disutility of risk perceived by member m in group g of household type h participating in activity i at location s during interval k when the infection ratio is R
$\hat{\rho}_b^{hmg}(k,R)$ (\$)	disutility of risk perceived by member m in group g of household type h on vehicle link b during interval k when the infection ratio is R
$t_p^w(k)$ (h)	travel time of a private car entering path p between OD pair w during interval k
$\hat{t}_p^w(k)$ (h)	travel time of a transit passenger entering path p between OD pair w during interval k
$t_a(k)$ (h)	travel time of a private car on road link a during interval k
$\hat{t}_b(k)$ (h)	travel time of a transit passenger on transit link b during interval k
$\psi_b(k)$	transit crowding discomfort factor on transit link b during interval k
χ_q^h	probability of household type h choosing JATP q

2. Basic considerations

2.1. Model assumptions

In order to facilitate presentation of basic ideas, without loss of generality, the following assumptions are made:

A1 A daily time period $[0,T]$ is discretized into constant time intervals $k = 1 \dots K$ with duration t_σ, such that $t_\sigma \times K = T$ (Lam and Yin (2001); Ouyang et al. (2011); Fu and Lam (2018); Vo et al. (2020a)).

A2 Different individuals can obtain different utilities for participating in the same activity, depending on the time of day (Ettema et al. (2007); Zhang et al. (2009); Lai et al. (2019)), regardless of the same value of travel time (Sheffi (1985)). In addition, individuals exhibit heterogeneous errors of perception on the utilities of different types of activities (Bhat et al. (2013)).

A3 Individuals make daily joint/solo activity–travel choices in a mixed-equilibrium manner, which maximizes either their perceived household utility or individual utility.

A4 Two main modes of transportation (private car and public transit) are considered, with two subtransit modes (bus and metro). The metro travel time is constant, whereas the bus travel time depends on the road congestion associated with the bus line (Wu and Lam (2003)). Bus routes are fixed without consideration of road congestion, and the number of buses is preloaded on the road links relating to their routes.

A5 The physical capacity constraints of activities are not considered in this paper; instead, positive and negative congestion effects at activity locations are modeled (Fu and Lam (2018); Liu et al. (2016, 2020)). Activity congestion effects have various physical interpretations, which depend on the activity type. A negative congestion effect associated with a maintenance activity (e.g., out-of-home shopping or a personal appointment) results in a penalty (a disutility) due to the uncomfortable physical proximity to others and/or the decline in the quality of services at the activity location (e.g., shopping malls and restaurants). A negative congestion effect associated with a subsistence activity (e.g., out-of-home work) results in a reduction in the activity utility due to poor task performance and a feeling of being crowded in a busy workplace (Paulus et al. (1976); Sinha and Sinha (1991)). In contrast, positive congestion effects are associated with social activities (Kim et al. (2018)), as an increased number of participants in these activities leads to a higher activity utility. In addition, the activity congestion utility/disutility is separable, and strictly increasing with the total number of persons at the activity location.

A6 In-vehicle crowding discomfort is modeled to capture the negative congestion effect in a transit vehicle, such as a loss of privacy, uncomfortable physical proximity, or the risk of sexual harassment (Sumalee et al. (2009); Li et al. (2010); Fu and Lam (2018)), whereas the physical capacity constraint of the transit vehicle is ignored. Moreover, the in-vehicle crowding discomfort is separable and strictly increasing with the total number of passengers in the transit vehicle.

A7 The road link travel time is separable and strictly increasing with the total number of private cars and transit vehicles on the link (Lam and Yin (2001); Liu et al. (2015)). Besides, the first-in–first-out condition, which prohibits private cars from arriving at a destination earlier by leaving later, is adopted (Janson (1991); Chen and Hsueh (1998); Boyce et al. (2001)).

A8 An individual conducts his/her trip between each OD pair by taking one of the following four roles: a solo driver (SD), a ridesharing driver (RD), a ridesharing passenger (RP) (when using a private car), or a transit passenger (TP) (when using public transit). On different trip legs of the trip chain, a driver can alternately adopt the SD and RD roles, whereas the passengers must choose between the RP and TP roles (Vo et al. (2020a)).

A9 An RD may pick up or drop off RPs from their own household at certain prespecified locations, and the capacity of the private car is sufficient for all household members. In addition, parking restrictions are excluded (Vo et al. (2020a)).

2.2. Heterogeneous household types

Consider multiple heterogeneous household types $h = 1 \dots H$ in a multimodal transportation network, where each household type h is associated with multiple members $m = 1 \dots M^h$, a number of households $F^h > 0$, and a set of JATP choices Q^h. Household type h represents F^h specific households with the same sociodemographic characteristics (e.g., household size, income, presence of children, age, education level, and employment status). Let I denote a set of activities conducted by household members, S be the set of activity and/or drop-off/pickup locations, and W be a set of OD pairs each of which connects two locations $s \in S$. Let P^w and $\hat{P}^w$ denote the sets of feasible paths between OD pair $w \in W$ for car users and transit passengers, respectively. Member m of household type h can participate in activity i at location s and travel on path p by private car or public transit ($p \in P^w$ or $p \in \hat{P}^w$) between OD pair w in multiple groups $g = 1 \dots G^h$, where each group g is a subset of members within household type h with group size $|g|$ (i.e., the number of household members in the group).

2.3. JATP concept

The key concept of the novel model is its use of a unified choice to simultaneously capture the multidimensional choice facets of household members' daily activity–travel schedules and their intra-household interactons in a multi-

modal transportation network. We adopt the concept of JATP choice, which was introduced by Fu and Lam (2018) and extended by Vo et al. (2020a). Fig. 1 illustrates the choice dimensions included within a JATP choice. It can be seen in Fig. 1 that a household type h chooses a JATP q, in which each member $m = 1 \dots M^h$ in each group $g = 1 \dots G^h$ of household type h chooses to either participate in an activity $i \in I$ at a location $s \in S$ or travel between an OD pair $w \in W$ using path $p \in P^w \cup \hat{P}^w$ (by private car or public transit) during each time interval $k = 1 \dots K$. Then, there is a joint activity/travel during a certain interval if the number of household members in group g is greater than one (i.e., $|g| > 1$), and otherwise a solo activity/travel. By adopting the concept of JATP choice, the proposed model in this paper can deal explicitly with intra-household interactions in terms of joint activity–travel choices by mode and by time of day, car ownership, and car allocation (i.e., the travel role taken by each member within the household in each private car trip).

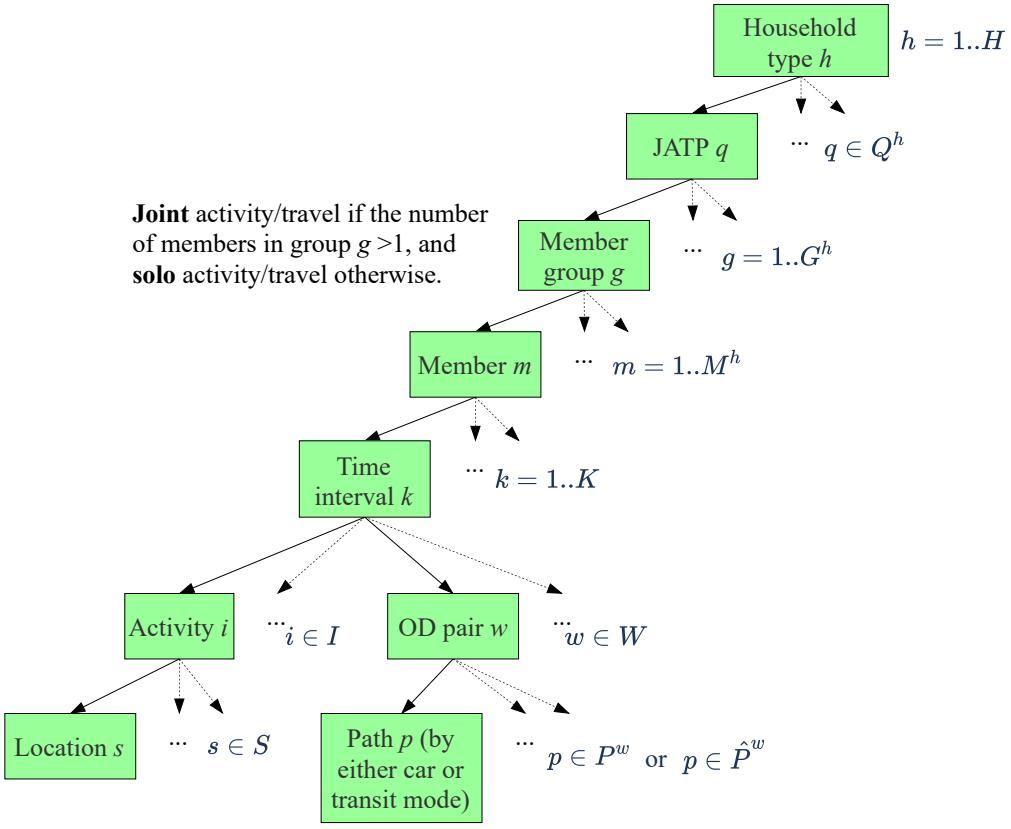

Figure 1: Choice dimensions included within a JATP choice.

2.4. Multimodal transportation network

Let $(\mathcal{S}, \mathcal{A}, L)$ denote a multimodal transportation network, in which $\mathcal{S}$, $\mathcal{A}$, and L are the sets of nodes, links, and transit lines, respectively. The multimodal network can be partitioned into two subnetworks, namely subnetwork (S, A) for private cars and subnetwork $(\hat{S}, B, L)$ for public transit where $\mathcal{S} = S \cup \hat{S}$ and $\mathcal{A} = A \cup B$. In the subnetwork (S, A), a *location node* $s \in S$ can be a road intersection, an activity, or a drop-off/pickup location, whereas a link $a \in A$ represents a *road link*. In the subnetwork $(\hat{S}, B, L)$, a transit line $l \in L$ is a fixed route on which transit vehicles run periodically on fixed schedules, and a *transit node* $s \in \hat{S}$ represents a line visiting a stop. In a case where several lines visit the same stop, each line forms a distinct transit node.

Let $B = B_1 \cup B_2 \cup B_3 \cup B_4$ be the sets of transit links, including access, egress, transfer, and vehicle links, respectively. Let $\tilde{b}$ and $\bar{b}$ denote the tail and head nodes, respectively, of transit link $b \in B$. Then, the flow on transit link b is from $\tilde{b}$ to $\bar{b}$. Let $N(s)$ and $L(s)$ denote the transit stop and line, respectively, associated with transit node $s \in \hat{S}$. Each pair of consecutive transit nodes along a transit line creates a *vehicle link* $b \in B_4$, which represents the passage of a transit vehicle from stop n to stop $(n+1)$ on line l, where $n = N(\tilde{b}), n+1 = N(\bar{b})$, and $l = L(\tilde{b}) = L(\bar{b})$. A location node $s \in S$ is connected to a transit node $s' \in \hat{S}$ through an *access link* $b \in B_1$, which involves a walk from the origin to stop n on line l, and then a period of waiting before boarding a vehicle on line l, where $n = N(\bar{b})$ and

$l = L(\bar{b})$. In contrast, a transit node $s \in \hat{S}$ is connected to a location node $s' \in S$ through an *egress link* $b \in B_2$, which involves a walk from stop n on line l to the destination, with $n = N(\tilde{b})$ and $l = L(\tilde{b})$. Two transit nodes of different lines form a *transfer link* $b \in B_3$, which involves a walk from stop n on line l to stop n' on line l' (if $l \neq l'$), and then a period of waiting before boarding the first vehicle arriving on line l', where $n = N(\tilde{b}), n' = N(\bar{b}), l = L(\tilde{b})$, and $l' = L(\bar{b})$.

In view of the above, a sequence of links in the multimodal transportation network connecting two location nodes $s \in S$, which form an OD pair $w \in W$, represents a feasible path p between OD pair w for car users ($p \in P^w$) or transit passengers ($p \in \hat{P}^w$). The path sets P^w and $\hat{P}^w$ between each OD pair w can then be generated using conventional path-finding algorithms, via the above representation of the multimodal transportation network.

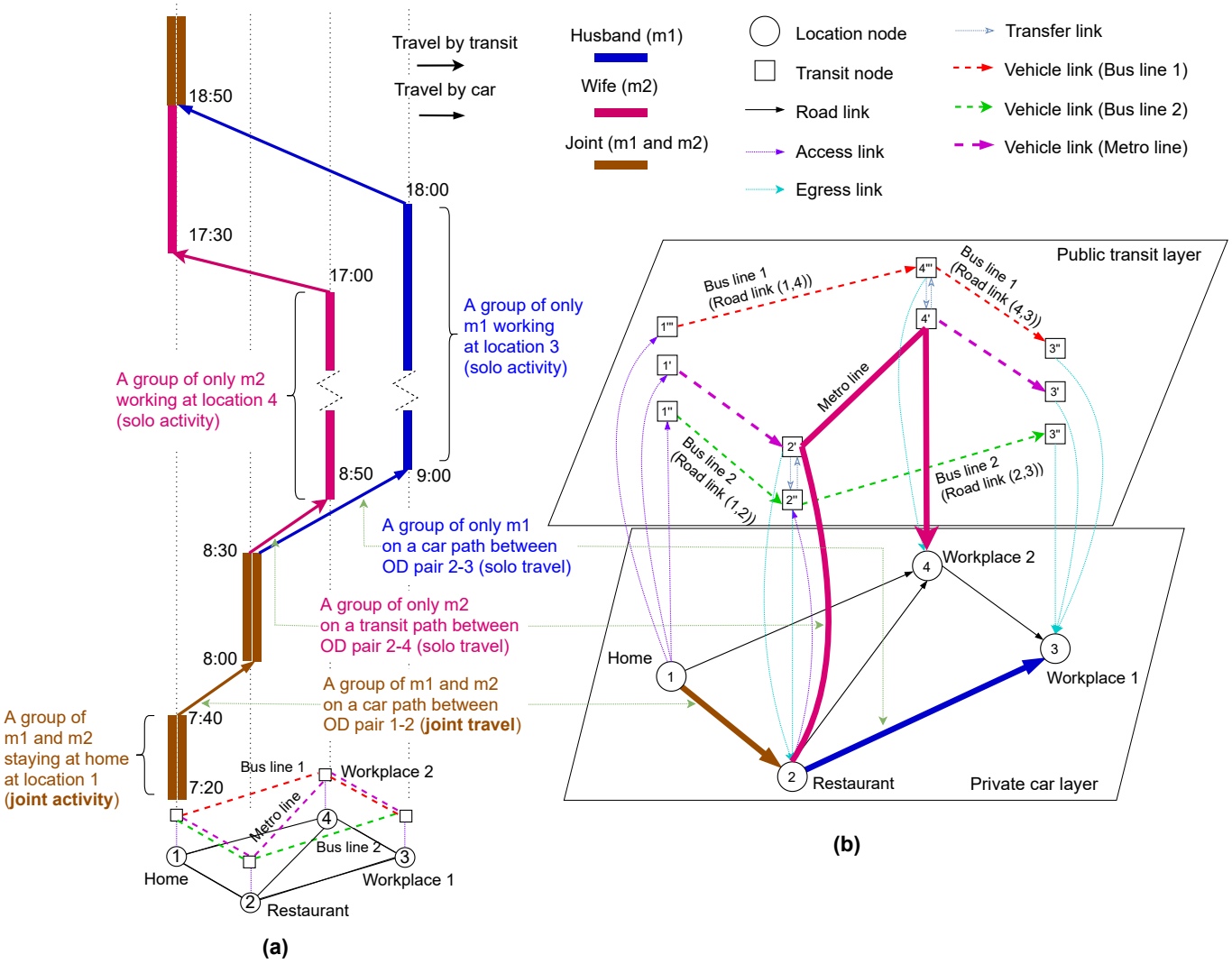

Figure 2: Illustration of (a) a joint activity–travel path (JATP) of a working couple, and (b) a representation of a simple multimodal transportation network.

Fig. 2a illustrates a JATP of a working couple (or a dual-earner couple), where for traveling between activity locations during the day, the husband switches between taking the RD and SD roles, and the wife takes the RP and TP roles (according to **A8**). In this example, the couple jointly travel by car (during which the husband takes the RD role and the wife takes the RP role) for a joint breakfast at the restaurant. Then, the wife switches to the metro line for commuting to her workplace (i.e., takes the TP role), and the husband drives to work alone (i.e., takes the SD role). After work, the wife takes bus line 1 for her travel home (takes the TP role), and the husband drives home alone (takes the SD role). Fig. 2b shows a representation of a simple multimodal transportation network used by the couple. In the network representation, path $1 \rightarrow 2$ is used for the joint car trip taken by the couple from their home to the restaurant, path $2 \rightarrow 2' \rightarrow 4' \rightarrow 4$ is used for the solo trip taken via the metro line by the wife from the restaurant to workplace 2, and path $2 \rightarrow 4$ is used for the solo trip taken by car by the husband from the restaurant to workplace 1. For

simplification, the multimodal transportation network is limited to the path choices of car users and transit passengers for their morning commutes.

2.5. Dynamic path travel times of car users and transit passengers

In a dynamic setting, the path choice of a car user includes the departure interval at the origin and the arrival time at each node along the path. The path travel time of a private car is the sum of travel times of its road links, with consideration of the interval during which the private car enters each link along the path (Janson (1991); Chen and Hsueh (1998); Boyce et al. (2001)). The travel time of a car user entering path p between OD pair w during interval k can be expressed as

$$t_p^w(k) = \sum_{a \in A} \sum_{k'=k}^{K} t_a(k') \zeta_{ap}^{wk}(k') \quad \forall p \in P^w, \tag{1}$$

where $t_a(k')$ is the travel time on road link a during interval k', and $\zeta_{ap}^{wk}(k')$ is a 0–1 integer variable that equals 1 if private cars entering path p between OD pair w during interval k arrive at road link a during interval k', and 0 otherwise. In addition, $\zeta_{ap}^{wk}(k')$ must satisfy

$$(k + \lceil t_{pa}^w(k) \rceil - k') \zeta_{ap}^{wk}(k') \leqslant 0, \tag{2}$$

$$(k + \lceil t_{pa}^w(k) \rceil - k' + 1) \zeta_{ap}^{wk}(k') \geqslant 0, \tag{3}$$

where $\lceil . \rceil$ is a function used to convert the travel time to an integer time interval, in which $\lceil t \rceil = k$ if $k \leqslant t/t_\sigma < k+1$. The above two constraints force a path to use a link during the time interval that is compatible with the travel time from the origin to the tail node of the link, and $t_{pa}^w(k)$ is the travel time of a private car entering path p between OD pair w during interval k and the tail node of road link a (Janson (1991)) which is expressed as

$$t_{pa}^w(k) = t_a(k + \lceil t_{pa'}^w(k) \rceil) + t_{pa'}^w(k), \tag{4}$$

where a' is the link preceding link a on path p. When a is the last link on path p, $t_p^w(k) = t_a(k + \lceil t_{pa}^w(k) \rceil) + t_{pa}^w(k)$.

In a dynamic context, the path choice of a transit passenger consists of the departure interval at the origin, an access link, a sequence of vehicle links (associated with different lines), an egress link, and the arrival time at each link. We consider the following components of the transit travel time: access, egress, transfer, and in-vehicle time (Tong and Wong (1999); Sumalee et al. (2009); Li et al. (2010)). The travel time of a transit passenger on path p between OD pair w with departure interval k is then formulated as

$$\hat{t}_p^w(k) = \sum_{b \in B} \sum_{k'=k}^{K} \hat{t}_b(k') \hat{\zeta}_{bp}^{wk}(k') \quad \forall p \in \hat{P}^w, \tag{5}$$

where $\hat{\zeta}_{bp}^{wk}(k')$ is a 0–1 integer variable that equals 1 if transit passengers entering path p between OD pair w during interval k use transit link b during interval k', and 0 otherwise. The transit time components are given as follows.

- For an access link $b \in B_1$ on which $n = N(\bar{b})$ and $l = L(\bar{b})$,

$$\hat{t}_b(k) = t_b^{(\text{walk})}(k) + \frac{1}{2D_b} \quad \forall b \in B_1, \tag{6}$$

  where the first term indicates the constant walking time from origin node $\tilde{b}$ to stop n on line l during interval k, the second term indicates the average waiting time prior to boarding the next vehicle arriving on line l, and D_b is the frequency of transit line l.
- For an egress link $b \in B_2$ on which $n = N(\tilde{b})$ and $l = L(\tilde{b})$,

$$\hat{t}_b(k) = t_b^{(\text{walk})}(k) \quad \forall b \in B_2, \tag{7}$$

  where $t_b^{(\text{walk})}(k)$ is the constant walking time from stop n on line l during interval k to destination node $\bar{b}$.

- For a transfer link $b \in B_3$ on which $n = N(\bar{b})$, and $l = L(\bar{b})$,

$$\hat{t}_b(k) = \frac{1}{2D_b} \quad \forall b \in B_3, \tag{8}$$

which is the average waiting time prior to boarding the next vehicle arriving on line l.

- For a vehicle link $b \in B_4$ on which $n = N(\tilde{b})$ and $l = L(\tilde{b})$, we have

$$\hat{t}_b(k) = \begin{cases} \hat{t}_b^{(\text{metro})}(k) & \text{if } l \text{ is a metro line} \\ \sum_{a \in A} \sum_{k'=k}^{K} t_a(k') \tilde{\zeta}_{ab}^{k}(k') & \text{if } l \text{ is a bus line} \end{cases} \quad \forall b \in B_4, \tag{9}$$

where $\hat{t}_b^{(\text{metro})}(k)$ is the constant travel time of metro line l from stop n to $(n+1)$ during interval k, and the bus travel time depends on the road travel time, and $\tilde{\zeta}_{ab}^{k}(k')$ is a 0–1 integer variable that equals 1 if transit passengers entering vehicle link b associated with bus line l during interval k arrive at road link a during interval k', and 0 otherwise. Note that a vehicle link may comprise multiple road links.

2.6. JATP utility

Let u_q^h be the daily activity–travel net utility of household type h choosing JATP q, which is calculated as the difference between the total utility of activities and the total disutility of travel by different modes for all household members:

$$u_q^h = \sum_{m=1}^{M^h} \sum_{g=1}^{G^h} \sum_{k=1}^{K} \left(\underbrace{\sum_{i \in I} \sum_{s \in S} u_{is}^{hmg}(k) \delta_{qis}^{hmg}(k)}_{\text{activity utility}} - \underbrace{\sum_{w \in W} \sum_{p \in P^w} c_{pw}^{hmg}(k) \xi_{qpw}^{hmg}(k)}_{\text{travel disutility by private car}} - \underbrace{\sum_{w \in W} \sum_{p \in \hat{P}^w} \hat{c}_{pw}^{hmg}(k) \hat{\xi}_{qpw}^{hmg}(k)}_{\text{travel disutility by public transit}} \right), \tag{10}$$

where $u_{is}^{hmg}(k)$ is the utility of member m in group g of household type h participating in activity i at location s during interval k, $c_{pw}^{hmg}(k)$ is the travel disutility of member m (taking the SD, RD, or TP role) in group g of household type h entering path p by private car between OD pair w during interval k, and $\hat{c}_{pw}^{hmg}(k)$ is the travel disutility of member m (taking the TP role) in group g of household type h entering path p by public transit between OD pair w during interval k.

In the JATP utility function (10), $\delta_{qis}^{hmg}(k)$ is a 0–1 integer variable that equals 1 if member m in group g of household type h choosing JATP q performs activity i at location s during interval k, and 0 otherwise; $\xi_{qpw}^{hmg}(k)$ is a 0–1 integer variable that equals 1 if member m in group g of household type h choosing JATP q enters path p by private car between OD pair w during interval k, and 0 otherwise, and $\hat{\xi}_{qpw}^{hmg}(k)$ is a 0–1 integer variable that equals 1 if member m in group g of household type h choosing JATP q enters path p by public transit between OD pair w during interval k, and 0 otherwise.

In what follows, we present how the utility/disutility components of the JATP utility function (10) are calculated.

2.6.1. Activity utility

The utility of an activity depends on its location and time of day (Ettema and Timmermans (2003); Ettema et al. (2007)), on the individuals participating in the activity (Zhang et al. (2005, 2009); Lai et al. (2019)), and on the congestion level at the activity location (Fu and Lam (2018); Liu et al. (2016, 2020)). A few studies have considered an extra utility to present the cases in which household members conduct joint activities (Bradley and Vovsha (2005); Lai et al. (2019); Vo et al. (2020a)). The utility of member m in group g of household type h participating in activity i at location s during interval k can be formulated as

$$u_{is}^{hmg}(k) = u_{is}^{hm}(k) + \varkappa_{is}^{hmg}(k) + \tilde{\varpi}_{is}(k) - \varpi_{is}(k), \tag{11}$$

where $u_{is}^{hm}(k)$ is the marginal utility obtained when member m of household type h participates in activity i alone during interval k, $\varkappa_{is}^{hmg}(k)$ is the extra utility gained when member m of household type h participates in activity i together with other household members in group g at location s during interval k, and $\tilde{\varpi}_{is}(k)$ and $\varpi_{is}(k)$ are the

activity congestion utility and disutility, respectively, that result from the positive and negative congestion effects experienced by persons participating in activity i at location s during interval k.

The marginal activity utility of member m of household type h participating in activity i alone is modeled by time of day as a bell-shaped function (Ettema and Timmermans (2003); Ashiru et al. (2004)):

$$u_{is}^{hm}(k) = U_{is}^{hm(0)} + \int_{kt_\sigma}^{(k+1)t_\sigma} \frac{\kappa_i^{hm} \upsilon_i^{hm} U_{is}^{hm}}{\exp\left(\kappa_i^{hm}\left(t-\tilde{t}_i^{hm}\right)\right)\left[1+\exp\left(-\kappa_i^{hm}\left(t-\tilde{t}_i^{hm}\right)\right)\right]^{\upsilon_i^{hm}+1}} \mathrm{d}t, \tag{12}$$

where $U_{is}^{hm(0)}$ and U_{is}^{hm} indicate the baseline and total utilities, respectively, for member m of household type h performing activity i at location s, $\tilde{t}_i^{hm}$ is the time at which the marginal utility reaches its maximum value, and κ_i^{hm} and υ_i^{hm} are the calibrated parameters.

According to **A5**, $\partial\tilde{\varpi}_{is}(k)/\partial v_{is}(k) > 0$ and $\partial\varpi_{is}(k)/\partial v_{is}(k) > 0$, where $v_{is}(k)$ is the number of persons participating in activity i at location s during interval k. The positive effect dominates the negative effect when $\partial\tilde{\varpi}_{is}(k)/\partial v_{is}(k) > \partial\varpi_{is}(k)/\partial v_{is}(k)$, and there is no congestion effect when $\partial\tilde{\varpi}_{is}(k)/\partial v_{is}(k) = \partial\varpi_{is}(k)/\partial v_{is}(k)$; otherwise, the negative effect dominates the positive effect. For simplicity, we ignore the positive effects at the activity locations, and model the activity congestion disutility as

$$\varpi_{is}(k) = w_{is} t_\sigma \left(\frac{v_{is}(k)}{C_{is}}\right)^{n_{is}}, \tag{13}$$

where C_{is} is the capacity of activity i at location s, t_σ is the length of each time interval, and w_{is} and n_{is} are the calibrated parameters associated with activity i at location s.

The extra utility of activity participation can be given by

$$\varkappa_{is}^{hmg}(k) = \begin{cases} 0 & \text{if } |g| = 1 \\ \alpha_{is}^{hg} u_{is}^{hm}(k) & \text{if } |g| > 1, \end{cases} \tag{14}$$

where α_{is}^{hg} is the household preference parameter for joint activity i at location s by group g of household type h.

2.6.2. *Travel disutilities of car users and transit passengers*

The travel disutility of member m in group g of household type h entering path p by private car between OD pair w during interval k is calculated as the sum of link disutilities in the interval during at which the private car enters each link along the path (Janson (1991); Chen and Hsueh (1998); Boyce et al. (2001)), as follows:

$$c_{pw}^{hmg}(k) = \sum_{a\in A} \sum_{k'=k}^{K} c_a^{hmg}(k') \zeta_{ap}^{wk}(k') \quad \forall p \in P^w, \tag{15}$$

where $c_a^{hmg}(k')$ is the travel disutility of member m in group g of household type h on road link a during interval k'.

The link travel disutility of car users comprises three components: the travel time disutility; the extra utility of joint travel; and the operating cost (e.g., fuel cost and toll), which can be averagely allocated among the group's members. Then, the travel disutility of member m in group g of household type h on road link a during interval k is given by

$$c_a^{hmg}(k) = \gamma t_a(k) - \vartheta_a^{hmg}(k) + \frac{1}{|g|}\phi_a^{hg}(k) \quad \forall a \in A, \tag{16}$$

where γ indicates the value of the travel time of car users, $t_a(k)$ is the travel time of private cars on road link a during interval k, $\vartheta_a^{hmg}(k)$ is the extra utility gained when member m of household type h travel together with other household members in group g on road link a during interval k, and $\phi_a^{hg}(k)$ is the shared operating cost that each car user in group g of household type h has to pay for traveling on road link a during interval k.

Based on **A7**, we have $\partial t_a(k)/\partial \tilde{v}_a(k) > 0$ where $\tilde{v}_a(k)$ is the number of private cars on road link a during interval k. We adopt the Bureau of Public Roads (BPR) function to model the link travel time of a private car:

$$t_a(k) = t_a^{(0)}\left(1 + \tilde{w}\left(\frac{\tilde{v}_a(k) + \hat{v}_a(k)}{(1/t_\sigma)\tilde{C}_a}\right)^{\tilde{n}}\right) \quad \forall a \in A, \tag{17}$$

where $\tilde{w}$ and $\tilde{n}$ are the calibrated parameters, $t_a^{(0)}$ is the free-flow travel time on road link a, $\tilde{C}_a$ is the capacity of road link a, $\hat{v}_a(k)$ is the preloaded number of transit vehicles on road link a during interval k (which can be calculated from transit service frequency), and $1/t_\sigma$ is used to convert the unit of $\tilde{C}_a$ from veh/h to veh/interval.

Similar to the time components considered in the transit path travel time (5), the travel disutility of member m in group g of household type h entering path p by public transit between OD pair w during interval k is calculated as

$$\hat{c}_{pw}^{hmg}(k) = \sum_{b\in B}\sum_{k'=k}^{K} \hat{c}_b^{hmg}(k')\hat{\zeta}_{bp}^{wk}(k') \quad \forall p \in \hat{P}^w, \tag{18}$$

in which

$$\hat{c}_b^{hmg}(k) = \begin{cases} \hat{\gamma}_1\hat{t}_b(k) - \hat{\vartheta}_b^{hmg}(k) & \forall b \in B_1 \\ \hat{\gamma}_2\hat{t}_b(k) - \hat{\vartheta}_b^{hmg}(k) & \forall b \in B_2 \\ \hat{\gamma}_3\hat{t}_b(k) - \hat{\vartheta}_b^{hmg}(k) & \forall b \in B_3 \\ \hat{\gamma}_4\hat{t}_b(k)\psi_b(k) - \hat{\vartheta}_b^{hmg}(k) + \varphi_b & \forall b \in B_4, \end{cases} \tag{19}$$

where $\hat{\gamma}_1$–$\hat{\gamma}_4$ are the coefficients that are required to convert different quantities of the transit time components to a monetary unit; $\psi_b(k)$ is the scale factor of in-vehicle travel time, which accounts for the in-vehicle crowding discomfort disutility incurred by transit passengers using vehicle link b during interval k; $\hat{\vartheta}_b^{hmg}(k)$ is the extra utility gained when member m of household type h travels together with other household members in group g on transit link b during interval k, and φ_b is the transit fare for using vehicle link b.

By reference to **A6**, we have $\partial\psi_b(k)/\partial\hat{v}_b(k) > 0$, where $\hat{v}_b(k)$ represents the number of transit passengers on vehicle link b during interval k. The transit crowding discomfort factor can be expressed as the following form of the BPR function (Fu and Lam (2014, 2018))

$$\psi_b(k) = 1 + \hat{w}\left(\frac{\hat{v}_b(k)}{(1/t_\sigma)\hat{C}_b D_b}\right)^{\hat{n}} \quad \forall b \in B_4, \tag{20}$$

where $\hat{w}$ and $\hat{n}$ are the calibrated parameters, $\hat{C}_b$ is the transit vehicle capacity, D_b is the transit frequency associated with vehicle link b, and $1/t_\sigma$ is used to convert the unit of $\hat{C}_b$ from pax/h to pax/interval.

The extra utilities of joint travel by private car and by public transit can be formulated as

$$\vartheta_a^{hmg}(k) = \begin{cases} 0 & \text{if } |g| = 1 \\ \beta_a^{hg}\gamma t_a^{(0)} & \text{if } |g| > 1 \end{cases} \quad \forall a \in A, \tag{21}$$

$$\hat{\vartheta}_b^{hmg}(k) = \begin{cases} 0 & \text{if } |g| = 1 \\ \hat{\beta}_b^{hg}\hat{\gamma}_1\hat{t}_b(k) & \text{if } |g| > 1, b \in B_1 \\ \hat{\beta}_b^{hg}\hat{\gamma}_2\hat{t}_b(k) & \text{if } |g| > 1, b \in B_2 \\ \hat{\beta}_b^{hg}\hat{\gamma}_3\hat{t}_b(k) & \text{if } |g| > 1, b \in B_3 \\ \hat{\beta}_b^{hg}\hat{\gamma}_4\hat{t}_b^{(0)} & \text{if } |g| > 1, b \in B_4, \end{cases} \tag{22}$$

where β_a^{hg} and $\hat{\beta}_b^{hg}$ are the household preference parameters for joint travel on road link a and on transit link b, respectively, by group g of household type h, and $t_a^{(0)}$ and $\hat{t}_b^{(0)}$ are the free-flow travel times on road link a and vehicle link b, respectively.

Fig. 3 summarizes the relationship between different utility/disutility components of the JATP utility function (10) presented in this Section 2.6. In particular, JATP utility u_q^h increases with activity utility $u_{is}^{hmg}(k)$, and decreases with path travel disutilities by private car $c_{pw}^{hmg}(k)$ and by public transit $\hat{c}_{pw}^{hmg}(k)$. The components of activity utility $u_{is}^{hmg}(k)$ are calculated by (11)–(14). Then, $u_{is}^{hmg}(k)$ increases with marginal utility $u_{is}^{hm}(k)$ and extra utility of joint activity participation $\varkappa_{is}^{hmg}(k)$, and decreases with activity congestion disutility $\varpi_{is}(k)$. Note that activity congestion utility $\tilde{\varpi}_{is}(k)$ is ignored here so as to illustrate the essential ideas presented in this paper. However, it can be extended to consider the positive effect of capacity constraint at the activity destination if necessary.

In addition, the components of path travel disutilities $c_{pw}^{hmg}(k)$ and $\hat{c}_{pw}^{hmg}(k)$ are given via (15)–(22). It should be noted that path travel disutility by private car $c_{pw}^{hmg}(k)$ is positively related to road link travel disutility $c_a^{hmg}(k')$, which in turn increases with road link travel time $t_a(k')$, and decreases with extra utility of car joint travel $\vartheta_a^{hmg}(k')$ $(k' \geqslant k)$. Similarly, path travel disutility by public transit $\hat{c}_{pw}^{hmg}(k)$ is also positively related to transit link travel disutility $\hat{c}_b^{hmg}(k')$, which increases with transit link travel time $\hat{t}_b(k')$ and crowding discomfort factor $\psi_b(k')$, and decreases with extra utility of transit joint travel $\hat{\vartheta}_b^{hmg}(k')$ $(k' \geqslant k)$.

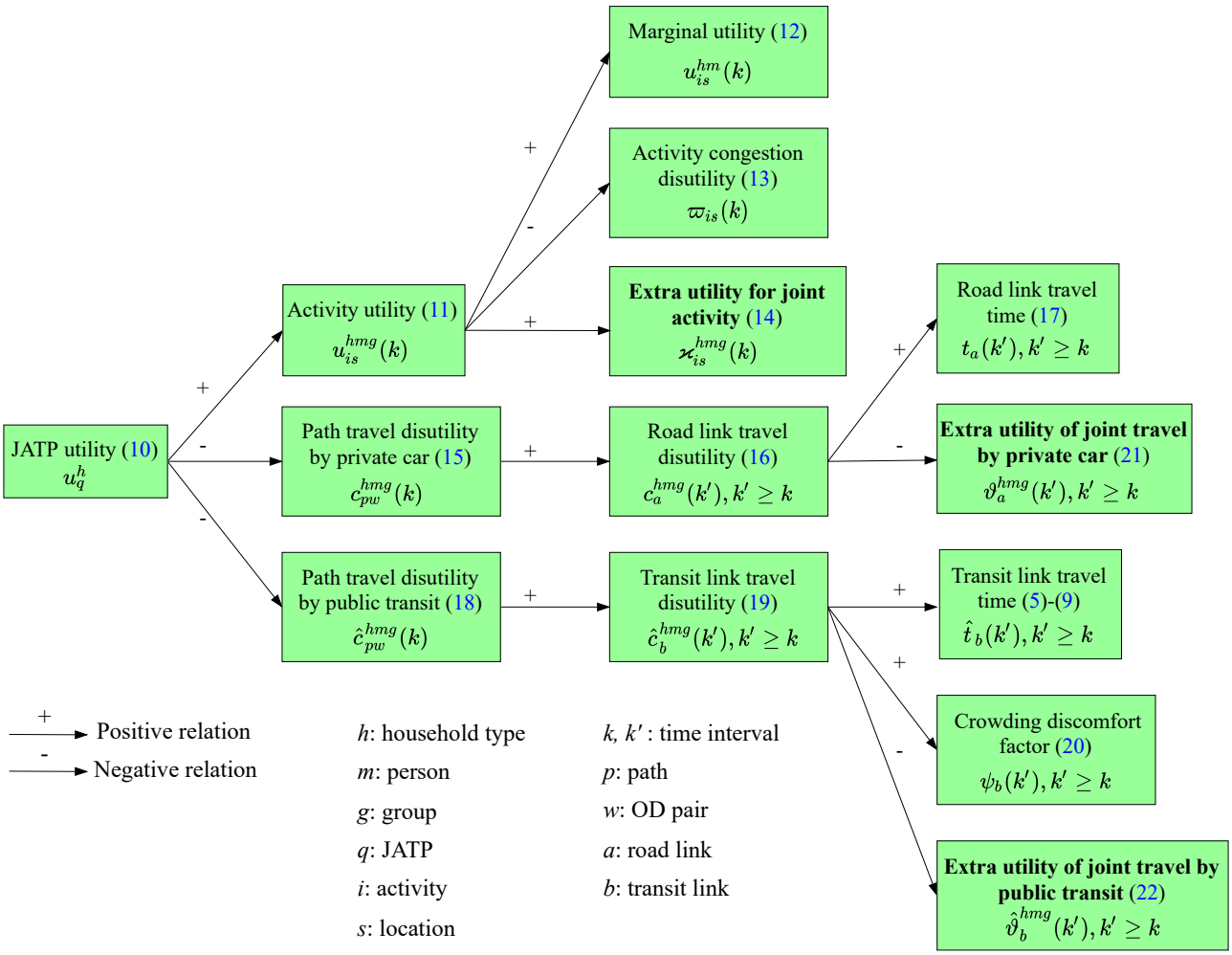

Figure 3: Relationship between different utility/disutility components of the JATP utility function.

Remark 1. Our novel activity-based model uses not only common parameters of conventional trip-based models, such as the value of travel times by modes (i.e., γ, and $\hat{\gamma}_1$–$\hat{\gamma}_4$), operating cost (i.e., $\phi_a^{hg}(k)$), and transit fare (i.e., φ_b), but also household-related parameters that are associated with the marginal time-dependent activity utility function (i.e., $u_{is}^{hm}(k)$), and the preferences for joint activities and travel (i.e., α_{is}^{hg}, β_a^{hg}, and $\hat{\beta}_b^{hg}$). These household-related parameters have certain effects on household members' aggregate activity–travel behaviors by time of day. For example, a higher value of $u_{is}^{hm}(k)$, $\forall h, m$, leads more household members to participate in activity i at location s during interval k, whereas a higher value of α_{is}^{hg}, $\forall h, g$, leads to more joint activity i at location s. Similarly, higher values of β_a^{hg} and $\hat{\beta}_b^{hg}$, $\forall h, g$, encourage more joint travel on road link a and on vehicle link b, respectively. Readers can refer to Ettema and Timmermans (2003); Ettema et al. (2007) for the information on calibrating the household-related parameters for the marginal activity utility function by time of day, and to Allahviranloo and Axhausen (2018); Lai et al. (2019) for the information on calibrating joint activity and/or travel utilities between household members.

3. Model formulation

In this section, we formulate the household-oriented activity-based mixed-equilibrium problem concerned. First, we develop a logit-based stochastic JATP choice model to capture a mixed equilibrium with heterogeneous errors of perception on the utility of different activity types. We then propose an equivalent VI problem for the mixed-equilibrium problem concerned. Finally, we investigate the interactions between between different-sized travel groups and different transportation modes, the model properties, and the existence and uniqueness of the solution to the proposed VI problem.

Fig. 4 shows the relationship between different model components in the proposed household-oriented activity-based mixed-equilibrium framework. First, the household-oriented activity-based mixed-equilibrium problem formulated in this Section 3 requires the input from (1) parameters for utilities/disutilities of solo/joint activities and travel (Section 2.6), (2) the multimodal transportation network (Section 2.4), (3) household demographic characteristics (Section 2.2), and (4) household members' heterogeneous errors of perception (Section 3.1). Based on these input, the utility/disutility components of the JATP utility function (10) are then calculated (Section 2.6), and the JATS supernetwork platform is constructed (Section 4.1). Finally, the output of the household-oriented activity-based mixed-equilibrium model would be a predicted daily JATP flow pattern (i.e., a vector of numbers of households with type h choosing JATP q, for all $h = 1 \dots H, q \in Q^h$).

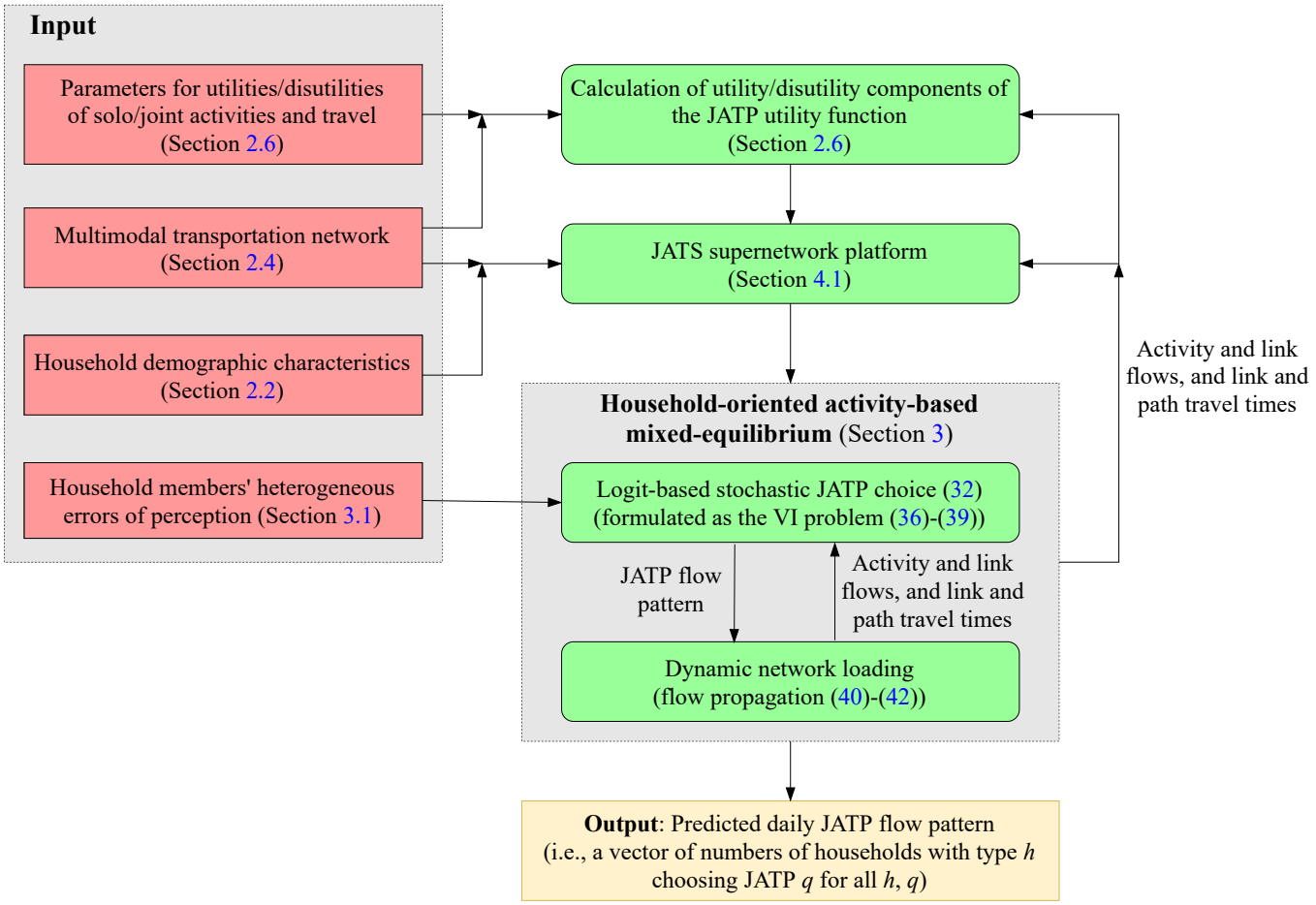

Figure 4: The proposed household-oriented activity-based network equilibrium framework.

3.1. Logit-based stochastic JATP choice model

Let U_q^h denote the perceived activity–travel net utility of household type h choosing JATP q. The perceived utility can be decomposed into deterministic and error terms, as follows:

$$U_q^h = u_q^h + \varepsilon_q^h. \tag{23}$$

From the RUM theory, the probability of household type h choosing JATP q can be expressed as

$$\chi_q^h = \Pr\left(U_q^h > U_e^h : \forall q \neq e \in Q^h\right). \tag{24}$$

The JATP choice model (24) results in a stochastic household utility optimum (SHO) principle based on which household members make JATP choices to maximize (or optimize) their *perceived household utility*.

If error term ε_q^h follows a Gumbel distribution with a zero mean and is identical and independently distributed, the JATP choice model (24) has the following closed-form expression:

$$\chi_q^h = \frac{\exp\left(\theta^h u_q^h\right)}{\sum_{e \in Q^h} \exp\left(\theta^h u_e^h\right)}, \tag{25}$$

where $\theta^h > 0$ is the household scale parameter that is associated with the perceived utilities of household type h, and θ^h is inversely proportional to the variance σ_{ε^h} of error term ε^h. It is well-known that $\theta^h = \pi/\sqrt{6\sigma_{\varepsilon^h}}$ where $\pi \approx 3.14$. If θ^h increases (i.e., the deterministic term of the perceived household utility is scaled up), then the household's error of perception decreases, and vice versa.

We next modify the deterministic term of the perceived utility (23) to account for household members' errors of perception on the utilities obtained from different activity types, and thus retain the closed-form expression of the multinomial logit (MNL) model. The closed-form expression is useful for investigating the properties of the stochastic choice model (24) and deriving an equivalent VI problem for the corresponding mixed-equilibrium problem. We now decompose u_q^h into different utility components, which are associated with different activity types:

$$u_q^h = \sum_{m=1}^{M^h} \sum_{x=1}^{X^{hm}} \eta_x^{hm} u_{qx}^{hm}, \tag{26}$$

where u_{qx}^{hm} is the activity–travel net utility obtained from type x activities by member m of household type h choosing JATP q, X^{hm} represents the number of activity types conducted by member m of household type h, and $\eta_x^{hm} > 0$ is the individual scale parameter associated with the utility of type x activities. Note that $u_{qx}^{hm} > 0$ results from the difference between the utility of performing type x activities and the travel disutility for reaching these activities. By substituting (26) into (25), the JATP choice model (25) can be expressed as

$$\chi_q^h = \frac{\prod_{m=1}^{M^h} \prod_{x=1}^{X^{hm}} \exp\left(\theta^h \eta_x^{hm} u_{qx}^{hm}\right)}{\sum_{e \in Q^h} \prod_{m=1}^{M^h} \prod_{x=1}^{X^{hm}} \exp\left(\theta^h \eta_x^{hm} u_{ex}^{hm}\right)}. \tag{27}$$

According to (27), the changes in the utility scale can be accommodated through changes in household and individual scale parameters θ^h and η_x^{hm}, respectively. Thus, similar to θ^h, as η_x^{hm} increases (i.e., the deterministic term of the perceived utility obtained by member m conducting type x activities is scaled up), the household's error of perception decreases, and vice versa. This implies that η_x^{hm} is also inversely proportional to variance σ_{ε^h}. Then, a higher value of η_x^{hm} leads to a lower error of perception being exhibited by member m of household type h regarding the utility associated with type x activities, and vice versa.

The scale parameters θ^h and η_x^{hm} in (27) are confounded as different combinations of the two parameters can lead to the same $\tilde{\eta}_x^{hm} = \theta^h \eta_x^{hm}$. Thus, $\tilde{\eta}_x^{hm}$ is commonly estimated in practice, instead of θ^h and η_x^{hm} separately. This means that θ^h and η_x^{hm} cannot be identified separately unless one parameter is fixed and the other is identified based on this fixed parameter. This confounding identification problem of scale parameters is well-known in conventional MNL models, and the scale parameter has usually been normalized to 1.0 (see e.g., Swait and Louviere (1993); Hess and Rose (2012)). This problem has no effect on the predicted probability (27) if the error assumptions on the distribution of ε^h are satisfied. However, in this paper, θ^h and η_x^{hm} must be separately identified to enable the mixed-equilibrium problem to be formulated as an equivalent VI problem. To address this matter, for a given set of estimated parameters $\left\{\tilde{\eta}_x^{hm} : \forall m, x\right\}$ the household scale parameter in this paper is fixed as

$$\theta^h = \max\left\{\tilde{\eta}_x^{hm} : \forall m, x\right\}, \tag{28}$$

and the individual scale parameter is derived as

$$\eta_x^{hm} = \frac{\tilde{\eta}_x^{hm}}{\theta^h}, \tag{29}$$

where η_x^{hm} ranges between 0 and 1.0, and $\max\left\{\eta_x^{hm} : \forall m, x\right\} = 1.0$.

Remark 2. The individual scale parameter η_x^{hm} in (27) can also represent the bargaining power of member m of household type h in jointly making the activity–travel choices relating to type x activities (Zhang et al. (2009); de Palma et al. (2015); Lai et al. (2019). Thus, the household members' errors of perception and bargaining powers are interpreted to be inversely proportional. Household members' heterogeneous errors of perception on activity–travel utility have rarely been investigated. However, this relationship allows us to link household members' errors of perception with their bargaining powers, which have been extensively investigated. For example, the wives in dual-earner households tend to have more bargaining power—and thus exhibit fewer errors of perception—than men (de Palma et al. (2015); Lai et al. (2019)).

Remark 3. Various classifications of activity types conducted by household members in (26) can be used. Gliebe and Koppelman (2002) classified daily household activities into four representative types: subsistence activities (e.g., out-of-home work, school, or college activities), maintenance activities (e.g., out-of-home shopping, personal activities, and appointments), leisure activities (e.g., out-of-home free-time and visiting), and home activities (e.g., unspecified home activities). Similarly, Bradley and Vovsha (2005) divided daily activities into three types: mandatory, non-mandatory, and home. As household members perceive various activity types differently, it is reasonable to assume that they tend to exhibit lower (or at least equal) errors of perception regarding mandatory and home activities than regarding nonmandatory activities.

Similar to the MNL model, the JATP choice model (27) has the property of independent and irrelevant alternatives. In other words, the ratio of the choice probabilities of two JATPs remains entirely unaffected by the utilities of other JATPs:

$$\frac{\chi_q^h}{\chi_e^h} = \prod_{m=1}^{M^h} \prod_{x=1}^{X^{hm}} \exp\left(\theta^h \eta_x^{hm} (u_{qx}^{hm} - u_{ex}^{hm})\right). \tag{30}$$

Thus, the JATP choice model (27) cannot account for the overlap or correlation between JATP choices.

To solve the overlapping problem, we extend the choice model (27) by using the following commonality factor, which is also used in the well-known C-logit model proposed by Cascetta et al. (1996):

$$CF_q^h = \nu_0 \ln \sum_{e \in Q^h} \left(\frac{L_{qe}^h}{\sqrt{L_q^h L_e^h}} \right)^{\nu_1}, \tag{31}$$

where ν_0 and ν_1 are the calibrated parameters; L_q^h and L_e^h are the lengths of JATPs q and e chosen by household type h, respectively; L_{qe}^h is their common "*length*". We define the length of JATP q as the total number of intervals for all household members that elapse in q (i.e., $L_q^h = M^h K$). Then, two JATPs overlap if they contain the same choices regarding activity participation (i.e., activity location, start time, and duration) and travel (i.e., departure time, path, and mode choices) made by the same household member during the same interval.

The JATP choice model (27) that considers the correlation between various JATPs can be expressed as

$$\chi_q^h = \frac{\exp\left(-\theta^h CF_q^h\right) \prod_{m=1}^{M^h} \prod_{x=1}^{X^{hm}} \exp\left(\theta^h \eta_x^{hm} u_{qx}^{hm}\right)}{\sum_{e \in Q^h} \left[\exp\left(-\theta^h CF_e^h\right) \prod_{m=1}^{M^h} \prod_{x=1}^{X^{hm}} \exp\left(\theta^h \eta_x^{hm} u_{ex}^{hm}\right) \right]}. \tag{32}$$

We next examine the direct and cross elasticities of the developed choice model. Direct elasticity represents a change in the probability of a particular JATP being chosen in response to a change in the utility of that JATP. Cross-elasticity represents the extent to which the probability of a particular JATP being chosen changes as the utility of another JATP changes. Consider the following derivative of the JATP choice probability (32):

$$\frac{\partial \chi_q^h}{\partial u_{ex}^{hm}} = \left(\theta^h \eta_x^{hm} \frac{\partial u_{qx}^{hn}}{\partial u_{ex}^{hm}}\right) \chi_q^h - \frac{\sum_{j \in Q^h} \left[\left(\theta^h \eta_x^{hm} \frac{\partial u_{jx}^{hm}}{\partial u_{ex}^{hm}}\right) \exp\left(-\theta^h CF_j^h\right) \prod_{n=1}^{M^h} \prod_{z=1}^{X^{hm}} \exp\left(\theta^h \eta_z^{hn} u_{jz}^{hn}\right) \right]}{\sum_{j \in Q^h} \left[\exp\left(-\theta^h CF_j^h\right) \prod_{n=1}^{M^h} \prod_{z=1}^{X^{hm}} \exp\left(\theta^h \eta_z^{hn} u_{jz}^{hn}\right) \right]} \chi_q^h, \tag{33}$$

and obtain the direct and cross-elasticities

$$\frac{\partial \chi_q^h}{\partial u_{qx}^{hm}} = \theta^h \eta_x^{hm} \chi_q^h \left(1 - \chi_q^h\right) > 0, \tag{34}$$

$$\frac{\partial \chi_e^h}{\partial u_{qx}^{hm}} = -\theta^h \eta_x^{hm} \chi_q^h \chi_e^h < 0. \tag{35}$$

Note that the direct elasticity (34) is positive, whereas the cross elasticity (35) is negative. Thus, improving the utility obtained from type x activities by member m of household type h choosing JATP q will increase the probability of households of type h choosing JATP q, and the incremental probability of choosing JATP q originates from the reduced probabilities of all other JATPs $e \neq q$. Note that the cross elasticity is uniform for all JATPs $e \neq q$ (i.e., the probabilities of all other JATPs $e \neq q$ decrease by the same percentage).

3.2. VI problem

Consider the following VI formulation problem: finding a JATP flow pattern $\mathbf{f}^* = (\dots, f_q^{h*}, \dots) \in \Omega$ such that

$$\tilde{\mathbf{u}}(\mathbf{f}^*)\left(\mathbf{f}^* - \mathbf{f}\right) \geqslant 0 \quad \forall \mathbf{f} \in \Omega \tag{36}$$

where $*$ denotes an equilibrated solution, f_q^h is the number of households with type h choosing JATP q, $\tilde{\mathbf{u}}(\mathbf{f}) = (\dots, \tilde{u}_q^h(\mathbf{f}), \dots)$ is the mapping with

$$\tilde{u}_q^h(\mathbf{f}) = \sum_{m=1}^{M^h} \sum_{x=1}^{X^h} \eta_x^{hm} u_{qx}^{hm}(\mathbf{f}) - \frac{1}{\theta^h}\left(1 + \ln f_q^h\right) - CF_q^h, \tag{37}$$

and Ω is a compact set of feasible JATP flow patterns that satisfy

$$\sum_{q \in Q^h} f_q^h = F^h, \tag{38}$$

$$f_q^h \geqslant 0, \tag{39}$$

where F^h is the number of households with type h.

Proposition 1. *The solution to the VI problem (36) is equivalent to the JATP flow pattern derived from the logit-based stochastic choice model (32).*

Proof. See Appendix B. □

According to Vo et al. (2020a), the JATP flow propagation that is required to ensure a consistent movement of household members forward in space and time through activity locations, paths, and links during a day can be expressed as follows:

$$v_{is}^{hmg}(k) = \underbrace{\sum_{q \in Q^h} f_q^h \delta_{qis}^{hmg}(k)}_{\text{activity person flow}} \tag{40}$$

$$v_a^{hmg}(k) = \underbrace{\sum_{w\in W}\sum_{p\in P^w}\sum_{k'=k}^{K}\underbrace{\left(\sum_{q\in Q^h} f_q^h \xi_{qpw}^{hmg}(k')\right)}_{\text{car user flow on car path}}\zeta_{ap}^{wk'}(k)}_{\text{car user flow on road link}} = \sum_{w\in W}\sum_{p\in P^w}\sum_{k'=k}^{K}\sum_{q\in Q^h} f_q^h \xi_{qpwak'}^{hmg}(k) \quad \forall\, a\in A, \tag{41}$$

$$\hat{v}_b^{hmg}(k) = \underbrace{\sum_{w\in W}\sum_{p\in \hat{P}^w}\sum_{k'=k}^{K}\underbrace{\left(\sum_{q\in Q^h} f_q^h \hat{\xi}_{qpw}^{hmg}(k')\right)}_{\text{passenger flow on transit path}}\hat{\zeta}_{bp}^{wk'}(k)}_{\text{passenger flow on transit link}} = \sum_{w\in W}\sum_{p\in \hat{P}^w}\sum_{k'=k}^{K}\sum_{q\in Q^h} f_q^h \hat{\xi}_{qpwbk'}^{hmg}(k) \quad \forall\, b\in B, \tag{42}$$

where $\xi_{qpwak'}^{hmg}(k)$ is a 0–1 integer variable that equals 1 if $\xi_{qpw}^{hmg}(k')\zeta_{ap}^{wk'}(k) = 1$, and 0 otherwise; $\hat{\xi}_{qpwbk'}^{hmg}(k)$ is a 0–1 integer variable that equals 1 if $\hat{\xi}_{qpw}^{hmg}(k')\hat{\zeta}_{bp}^{wk'}(k) = 1$, and 0 otherwise; $v_{is}^{hmg}(k)$ is the number of persons being member m in group g of household type h participating in activity i at location s during interval k; $v_a^{hmg}(k)$ is the number of car users being member m in group g of household type h using road link a during interval k; and $\hat{v}_b^{hmg}(k)$ is the number of transit passengers being member m in group g of household type h using transit link b during interval k.

Finally, we define $v_{is}(k)$ as the total number of persons participating in activity i at location s during interval k, $\tilde{v}_a(k)$ as the total number of private cars using road link a during interval k, and $\hat{v}_b(k)$ as the total number of transit passengers using transit link b during interval k:

$$v_{is}(k) = \sum_{h=1}^{H}\sum_{m=1}^{M^h}\sum_{g=1}^{G^h} v_{is}^{hmg}(k), \tag{43}$$

$$\tilde{v}_a(k) = \sum_{h=1}^{H}\sum_{m=1}^{M^h}\sum_{g=1}^{G^h} \frac{1}{|g|} v_a^{hmg}(k) \quad \forall a\in A, \tag{44}$$

$$\hat{v}_b(k) = \sum_{h=1}^{H}\sum_{m=1}^{M^h}\sum_{g=1}^{G^h} \hat{v}_b^{hmg}(k) \quad \forall b\in B. \tag{45}$$

The flow propagation (40)–(42) ensures the feasibility of the time–space trajectories of household members through a JATP by using 0–1 integer variables. These variables are not indices, but instead depend on the (continuous) link travel times of both private cars and transit vehicles, which in turn are affected by road congestion (see Vo et al. (2020a)). Please refer to Appendix A for the relationship between the 0–1 integer variables and the path and link travel times.

Remark 4. The solution to the VI problem (36) is only equivalent to the JATP flow pattern derived from the stochastic choice model (25) under the assumption that flow propagation condition (40)–(42) and travel times of road links are fixed (Janson (1991); Chen and Hsueh (1998); Boyce et al. (2001); Vo et al. (2020a)). If the fixed flow propagation relation is also the relation realized at equilibrium, the solution to the VI subproblem is also the JATP flow pattern derived from the stochastic choice model. Hereafter, we investigate the model properties and the existence and uniqueness of a solution to the particular VI problem based on the assumption that the flow propagation (40)–(42) and travel times are fixed.

3.3. Interactions between different-sized travel groups and different transportation modes

We next investigate the interactions between users belonging to different-sized travel groups and using different transportation modes considered in our problem.

Interaction 1. There exists an interaction between car users and transit passengers on road links, such that the car users may affect the travel disutility of transit passengers, but the reverse effect is not necessarily true.

Based on (16) and (19), Interaction 1 can be expressed as

$$\frac{\partial \hat{c}_b^{hmg}(k)}{\partial v_a^{jnz}(k)} = \frac{\hat{\gamma}_4}{|z|}\frac{\partial \hat{t}_b(k)}{\partial \tilde{v}_a(k)}\psi_b(k) \geqslant 0 \quad \forall a \in A, b \in B_4, \tag{46}$$

$$\frac{\partial c_a^{jnz}(k)}{\partial \hat{v}_b^{hmg}(k)} = 0 \quad \forall a \in A, b \in B_4, \tag{47}$$

where $\partial \hat{c}_b^{hmg}(k)/\partial v_a^{jnz}(k)$ indicates the effect of the number of car users being member n in group z of household type j on road link a on the travel disutility of transit passengers being member m in group g of household type h on vehicle link b during interval k, and the reverse effect $\partial c_a^{jnz}(k)/\partial \hat{v}_b^{hmg}(k)$ is negligible due to **A4**; and $\partial \hat{c}_b^{hmg}(k)/\partial v_a^{jnz}(k) \geqslant 0$ because the travel time of the bus mode is affected by the road travel time, which is in turn separable and strictly increasing with the number of vehicles on the link.

Interaction 2. There is an asymmetric interaction between car users on road links, such that the car users in different-sized travel groups may affect the travel disutilities of other car users in different ways.

Because the road link travel time is separable and strictly increasing with the number of vehicles on the link (i.e., $\partial t_a(k)/\partial \tilde{v}_a(k) > 0$), from (16) we have

$$\frac{\partial c_a^{hmg}(k)}{\partial v_a^{jnz}(k)} = \frac{\gamma}{|z|}\frac{\partial t_a(k)}{\partial \tilde{v}_a(k)} > 0 \quad \forall a \in A, \tag{48}$$

where $\partial c_a^{hmg}(k)/\partial v_a^{jnz}(k)$ is the effect of the number of car users being member n in group z of household type j on road link a during interval k on the travel disutility of other car users being member m in group g of household type h on the road link during the same interval. Interaction 2 is asymmetric, as various travel groups z yield different group sizes $|z|$.

Interaction 3. There is a symmetric interaction between the transit passengers on transit vehicles, such that transit passengers in different-sized travel groups may affect the travel disutilities of other transit passengers in similar ways.

As the in-vehicle crowding discomfort disutility is strictly increasing with the number of passengers in the transit vehicle (i.e., $\partial \psi_b(k)/\partial \hat{v}_b(k) > 0$), based on (19), Interaction 3 can be expressed as

$$\frac{\partial \hat{c}_b^{hmg}(k)}{\partial \hat{v}_b^{jnz}(k)} = \hat{\gamma}_4 \hat{t}_b(k)\frac{\partial \psi_b(k)}{\partial \hat{v}_b(k)} > 0 \quad \forall b \in B_4, \tag{49}$$

where $\partial \hat{c}_b^{hmg}(k)/\partial \hat{v}_b^{jnz}(k)$ indicates the effect of the number of transit passengers being member n in group z of household type j on vehicle link b during interval k on the travel disutility of other transit passengers being member m in group g of household type h on the vehicle link associated with the same vehicle.

Given the interactions between users belonging to different-sized travel groups and using different transportation modes mentioned above, the novel model developed in this paper includes the model proposed by Vo et al. (2020a) as a special case, as the congestion effects of transit modes are ignored. That is, the interaction between car users and transit passengers on road links and that between transit passengers in transit vehicles were relaxed in Vo et al. (2020a).

3.4. Model properties

In this section, we investigate the properties of the solution to the VI problem (36). Property 1 shows that the proposed SHO principle includes the conventional SUE principle as a special case, in which there are no intra-household interactions. Then, under the SUE principle, the household members make JATP choices to maximize their *perceived individual utility*. Thus, the mixed equilibrium of activity–travel choices at both individual and household levels can be solely stated by the SHO principle at the household level where each individual without intra-household interactions can be regarded as a one-member household. However, because of the asymmetric interactions of different

household types via their travel disutilities (Interactions 1, 2, and 3), the maximum utility for a given household type at equilibrium (under the SHO or SUE principles) can be affected (improved or worsened) by the choices of other household types. Thus, the system's expected total utility can also be improved or worsened under a mixed equilibrium condition, depending on the proportion of household members following the SHO or SUE principle. A similar phenomenon was observed by Vo et al. (2020a) where household members of heterogeneous household types follow a deterministic HO principle.

Property 1. In the absence of intra-household interactions, the solution to the VI problem (36) satisfies a SUE principle.

Proof. See Appendix B. □

Property 2 shows that the SHO principle considered in this paper includes the HO principle in Vo et al. (2020a) as a special case, in which household members' errors of perception on the utility of different activity types are ignored. Property 3 highlights a special case in which household members have no knowledge about the utility, and therefore, tend to make random JATP choices. In such a case, the first term of the mapping (37) will be negligible. Consequently, the VI problem (36) uniformly distributes the household travel demand to all available JATPs.

Property 2. When $\theta^h \to +\infty, \forall h$, the solution to the VI problem (36) satisfies a deterministic HO principle (Vo et al. (2020a)).

Proof. See Appendix B. □

Property 3. When $\theta^h \to 0, \forall h$, the household travel demand tends to be uniformly distributed to the available JATPs (i.e., the JATP choice is independent of the JATP utility).

Proof. See Appendix B. □

Property 4 highlights the importance of accounting for heterogeneity in errors of perception on the utility of different activity types. In particular, when member m of household type h has a higher error of perception on the utility obtained from type x activities than member n in the same household has on the utility obtained from type z activities, the type x activities conducted by member m are less important than the type z activities conducted by member n in the JATP choices of household type h. Moreover, when member m of household type h has no knowledge on the utility of any activity types (i.e., $\eta_x^{hm} \to 0, \forall x$), he/she tends to not participate in decision-making on the JATP choices of household type h. This property is reasonable from a behavioral viewpoint, as household members with less knowledge about the network conditions tend to depend on others with more knowledge to make activity–travel decisions.

Property 4. When $\eta_x^{hm} < \eta_z^{hn}, \forall m \neq n$, the change in utility obtained by member m from type x activities has a smaller effect on the JATP probabilities chosen by household type h than the change in the utility obtained by member n from type z activities.

Proof. See Appendix B. □

3.5. Existence and uniqueness of a solution

We now discuss the existence and uniqueness of a solution to the VI problem (36) in terms of a JATP flow pattern. Proposition 2 indicates the existence of a solution to the VI problem as mapping $\tilde{\mathbf{u}}(\mathbf{f})$ is continuous with JATP flow pattern $\mathbf{f}$.

Proposition 2. *There exists at least one solution* $\mathbf{f}^* \in \Omega$ *to the VI problem* (36).

Proof. See Appendix B. □

As mentioned above, because of the interactions between users belonging to different-sized travel groups and using different transportation modes in terms of link travel disutilities, the link travel disutility functions $c_a^{hmg}(k)$ for car users and $\hat{c}_b^{hmg}(k)$ for transit passengers may not be strictly monotonic with their link flow. In addition, the household members' errors of perceptions are heterogeneous. Hence, the monotonicity of mapping $\tilde{\mathbf{u}}(\mathbf{f})$ in terms of JATP flow pattern $\mathbf{f}$ does not hold in general cases. This indicates that a solution to the VI problem (36) in terms of JATP flow pattern $\mathbf{f}^*$ may be not unique.

To establish a condition for the uniqueness of a solution to the VI problem (36), we define $\check{\mathbf{v}} = (\dots, v_{is}(k), \dots)$ as a vector of person flows participating in activities, $\mathbf{v} = (\dots, v_a(k), \dots)$ as a vector of car user flows on road links, $\tilde{\mathbf{v}} = (\dots, \tilde{v}_a(k), \dots)$ as a vector of private car flows on road links, and $\hat{\mathbf{v}} = (\dots, \hat{v}_b(k), \dots)$ as a vector of transit passenger flows on vehicle links deduced from JATP flow pattern $\mathbf{f}$. We also define $\varpi(\check{\mathbf{v}}) = (\dots, \varpi_{is}(k), \dots)$, and $\tilde{\varpi}(\check{\mathbf{v}}) = (\dots, \tilde{\varpi}_{is}(k), \dots)$ as the vectors of activity congestion disutilities and utilities under $\check{\mathbf{v}}$, respectively; $\mathbf{t}(\tilde{\mathbf{v}}) = (\dots, t_a(k), \dots)$ as the vector of travel times on road links under $\tilde{\mathbf{v}}$, $\psi(\tilde{\mathbf{v}}, \hat{\mathbf{v}}) = (\dots, \psi_b(k)\hat{t}_b(k), \dots)$ as the vector of crowding discomfort disutilities on vehicle links under $\tilde{\mathbf{v}}$ and $\hat{\mathbf{v}}$; and $\mathbf{e}(\mathbf{f}) = \left(\dots, (\ln f_q^h)/\theta^h, \dots\right)$ as the vector of entropy terms.

Proposition 3. *Assuming that individuals are homogeneous in terms of individual scale parameter $\eta_x^{hm}, \forall h, m, x$, which is denoted η, the VI problem (36) has exactly one solution $\mathbf{f}^* \in \Omega$ if*

$$Z_1(\mathbf{f}^{(1)}, \mathbf{f}^{(2)}) - Z_2(\mathbf{f}^{(1)}, \mathbf{f}^{(2)}) + Z_3(\mathbf{f}^{(1)}, \mathbf{f}^{(2)}) + Z_4(\mathbf{f}^{(1)}, \mathbf{f}^{(2)}) + Z_5(\mathbf{f}^{(1)}, \mathbf{f}^{(2)}) > 0 \quad \forall \mathbf{f}^{(1)} \neq \mathbf{f}^{(2)} \in \Omega, \tag{50}$$

where

$$Z_1(\mathbf{f}^{(1)}, \mathbf{f}^{(2)}) = \eta \left(\varpi(\check{\mathbf{v}}^{(1)}) - \varpi(\check{\mathbf{v}}^{(2)})\right) \left(\check{\mathbf{v}}^{(1)} - \check{\mathbf{v}}^{(2)}\right) \tag{51}$$

$$Z_2(\mathbf{f}^{(1)}, \mathbf{f}^{(2)}) = \eta \left(\tilde{\varpi}(\check{\mathbf{v}}^{(1)}) - \tilde{\varpi}(\check{\mathbf{v}}^{(2)})\right) \left(\check{\mathbf{v}}^{(1)} - \check{\mathbf{v}}^{(2)}\right) \tag{52}$$

$$Z_3(\mathbf{f}^{(1)}, \mathbf{f}^{(2)}) = \eta\gamma \left(\mathbf{t}(\tilde{\mathbf{v}}^{(1)}) - \mathbf{t}(\tilde{\mathbf{v}}^{(2)})\right) \left(\mathbf{v}^{(1)} - \mathbf{v}^{(2)}\right) \tag{53}$$

$$Z_4(\mathbf{f}^{(1)}, \mathbf{f}^{(2)}) = \eta\hat{\gamma}_4 \left(\psi(\tilde{\mathbf{v}}^{(1)}, \hat{\mathbf{v}}^{(1)}) - \psi(\tilde{\mathbf{v}}^{(2)}, \hat{\mathbf{v}}^{(2)})\right) \left(\hat{\mathbf{v}}^{(1)} - \hat{\mathbf{v}}^{(2)}\right) \tag{54}$$

$$Z_5(\mathbf{f}^{(1)}, \mathbf{f}^{(2)}) = \left(\mathbf{e}(\mathbf{f}^{(1)}) - \mathbf{e}(\mathbf{f}^{(2)})\right) \left(\mathbf{f}^{(1)} - \mathbf{f}^{(2)}\right). \tag{55}$$

Proof. See Appendix B. □

We now discuss the meanings and signs of the five terms defined in Proposition 3, which are related to the monotonicity of the utility and disutility components of mapping $\tilde{\mathbf{u}}(\mathbf{f})$ in the set of feasible JATP flow patterns $\mathbf{f} \in \Omega$. In particular, Z_1 and Z_2 represent the monotonicity of activity congestion disutilities and utilities, respectively; Z_3 represents the monotonicity of travel times on road links; and Z_4 represents the monotonicity of crowding discomfort disutilities in transit vehicles. In addition, $Z_1 \geqslant 0$ and $Z_2 \geqslant 0$ because the activity congestion disutilities and utilities are strictly increasing with the number of persons at the activity location (according to **A5**); that is

$$Z_1(\mathbf{f}^{(1)}, \mathbf{f}^{(2)}) \begin{cases} > 0 & \text{if } \check{\mathbf{v}}^{(1)} \neq \check{\mathbf{v}}^{(2)} \\ = 0 & \text{if } \check{\mathbf{v}}^{(1)} = \check{\mathbf{v}}^{(2)}, \end{cases} \tag{56}$$

$$Z_2(\mathbf{f}^{(1)}, \mathbf{f}^{(2)}) \begin{cases} > 0 & \text{if } \check{\mathbf{v}}^{(1)} \neq \check{\mathbf{v}}^{(2)} \\ = 0 & \text{if } \check{\mathbf{v}}^{(1)} = \check{\mathbf{v}}^{(2)}. \end{cases} \tag{57}$$

The sign of Z_3 is unknown because there may exist joint travel of car users on road links that have a lower number of car users but a higher number of private cars; that is

$$Z_3(\mathbf{f}^{(1)}, \mathbf{f}^{(2)}) \begin{cases} > 0 & \text{if } \left(t_a(k)^{(1)} - t_a(k)^{(2)}\right)\left(v_a(k)^{(1)} - v_a(k)^{(2)}\right) > 0 \quad \forall a, k \\ = 0 & \text{if } \tilde{\mathbf{v}}^{(1)} = \tilde{\mathbf{v}}^{(2)} \text{ or } \mathbf{v}^{(1)} = \mathbf{v}^{(2)} \\ \textit{unknown} & \text{otherwise.} \end{cases} \tag{58}$$

Condition $Z_3 > 0$ holds if a larger number of car users $v_a(k)$ leads to a longer travel time $t_a(k)$ for each road link a. The sign of Z_4 is also unknown because there exists the interaction between private cars and transit vehicles on road

links; that is

$$Z_4(\mathbf{f}^{(1)},\mathbf{f}^{(2)})\begin{cases}>0 & \text{if } \left(\hat{t}_b(k)^{(1)}\psi_b(k)^{(1)}-\hat{t}_b(k)^{(2)}\psi_b(k)^{(2)}\right)\left(\hat{v}_b(k)^{(1)}-\hat{v}_b(k)^{(2)}\right)>0 \quad \forall b,k\\ =0 & \text{if } \hat{\mathbf{v}}^{(1)}=\hat{\mathbf{v}}^{(2)} \text{ and } \tilde{\mathbf{v}}^{(1)}=\tilde{\mathbf{v}}^{(2)}\\ \textit{unknown} & \text{otherwise.}\end{cases} \tag{59}$$

The condition for $Z_4 > 0$ holds if a higher number of transit passengers $\hat{v}_b(k)$ leads to a higher crowding discomfort disutility $\hat{t}_b(k)\psi_b(k)$ for all vehicle link b. In addition, $Z_5 > 0$ for any $\mathbf{f}^{(1)} \neq \mathbf{f}^{(2)}$ because $(1/\theta^h)\ln f_q^h$ is an increasing function. In summary, for any $\mathbf{f}^{(1)} \neq \mathbf{f}^{(2)} \in \Omega$, $Z_1 \geqslant 0$, $Z_2 \geqslant 0$, $Z_5 > 0$, the signs of Z_3 and Z_4 are unknown due to the joint travel and interaction between private cars and transit vehicles sharing same road links.

Proposition 3 states a condition under which the VI problem (36) has a unique solution in terms of a JATP flow pattern. This condition is independent of the nonmonotonicity of the link disutility functions $c_a^{hmg}(k)$ for car users and $\hat{c}_b^{hmg}(k)$ for transit passengers resulting from the asymmetric interactions between users belonging to different-sized travel groups and using different transportation modes. The homogeneous individual scale parameter η_x^{hm} in Proposition 3 does not indicate that individuals from different households make homogeneous errors of perception, as the error in the perception of member m of household type h is not only parameterized by η_x^{hm} but also by θ^h.

Remark 5. Condition (50) in Proposition 3 is expected to hold in practice. First, aside from social activities, which have positive congestion effects (i.e., more participants result in a higher activity utility), most daily activities have negative congestion effects (i.e., more participants result in lower activity utility). Thus, Z_1 often dominates Z_2. Second, activity duration is in reality much longer than travel time. For example, the UK Department for Transport reported in 2017 (Department for Transport (2017)) that people spent an average of an hour a day traveling, which included 36 min traveling by car. In addition, the Hong Kong Transport Department reported in 2011 (Transport Department (2011)) that the average total mechanized trip rate on a weekday was 1.83 trips/person, while the mean journey time per trip was 40 min. Hence, as activities are usually longer in duration than travel, the congestion effects of activities are in practice likely to be much larger than the traffic congestion effects of travel by different modes (i.e., Z_1 dominates Z_3 and Z_4). Consequently, the monotonicity of mapping $\tilde{\mathbf{u}}(\mathbf{f})$ of the VI problem (36) is often governed by the monotonicity of activity congestion disutility Z_1. Due to the uniqueness of a solution in terms of a JATP flow pattern, condition (50) also ensures the uniqueness of the link and path flows by different travel groups and transportation modes, and of households' daily activity–travel schedules and time allocations. This can be regarded as a merit of our activity-based approach, as the uniqueness of path and link flows cannot be ensured in conventional trip-based traffic assignment models because of asymmetric interactions between users who participate in different-sized travel groups and use different transportation modes.

4. Solution method

The VI problem (36) is solved using the predetermined JATP choice set. We first develop a JATS supernetwork platform, on which we can apply the column generation method to generate feasible JATPs when needed. We then develop a modified diagonalization method to solve the VI problem (36).

4.1. JATS supernetwork platform

The novel supernetwork platform is a time–space network, in which each time–space link represents participation of an activity or a dynamic path choice between an OD pair for a travel mode during a certain time interval, which involves a possible interaction with joint activity–travel choices. We extend the joint activity–time–space (JATS) supernetwork platform, proposed by Vo et al. (2020a) for road users, to represent a unified JATP choice with multimodal travel options as a path in the supernetwork. Crucially, this extended supernetwork explicitly accounts for multiple transit path choices for each OD pair, rather than a single demand-excess transit link with constant cost, as used by Vo et al. (2020a). The details of the supernetwork platform are as follows.

Let $\mathbf{G}^h(\mathbf{N}^h,\mathbf{L}^h)$ be the JATS supernetwork of household type h, where $\mathbf{N}^h$ and $\mathbf{L}^h$ are the sets of JATS nodes and links, respectively. The sets of JATS nodes and links can be decomposed with respect to their time intervals as

$$\mathbf{N}^h=\bigcup_{k=1}^{K+1}\mathbf{N}^h(k) \quad \text{and} \quad \mathbf{L}^h=\bigcup_{k=1}^{K}\mathbf{L}^h(k) \quad \forall h, \tag{60}$$

where $\mathbf{N}^h(k)$ is the set of JATS nodes at interval k, and $\mathbf{L}^h(k) = \mathbf{N}^h(k) \times \mathbf{N}^h(k+1)$ is the set of JATS links during interval k. We can express the sets of JATS nodes and links with respect to the sets of ATS nodes and links as

$$\mathbf{N}^h(k) = \left\{ \mathbf{n} \in \bigtimes_{m=1}^{M^h} \mathcal{N}^m(k) \right\} \quad \text{and} \quad \mathbf{L}^h(k) = \left\{ \mathbf{l} \in \bigtimes_{m=1}^{M^h} \mathcal{L}^m(k), \mathbf{l} \text{ is feasible} \right\} \quad \forall h, k, \tag{61}$$

where "$\times$" is the Cartesian product, $\mathcal{N}^m(k)$ is the set of activity–time–space (ATS) nodes at interval k, and $\mathcal{L}^m(k) = \mathcal{N}^m(k) \times \mathcal{N}^m(k+1)$ is the set of ATS links during interval k. The sets of ATS nodes and links for member m during interval k are given by

$$\mathcal{N}^m(k) = \bigcup_{j=1}^{2} \mathcal{N}_j^m(k), \quad \forall m, \tag{62}$$

$$\mathcal{L}^m(k) = \bigcup_{j=1}^{6} \mathcal{L}_j^m(k), \quad \forall m, \tag{63}$$

where $\mathcal{N}_1^m(k)$ and $\mathcal{N}_2^m(k)$ are the sets of ATS nodes for member m at interval k who takes the driver (SD or RD) and passenger (RP or TP) roles, respectively; $\mathcal{L}_1^m(k)$ and $\mathcal{L}_2^m(k)$ are the sets of activity links for member m participating in activities during interval k who takes the SD or RD and RP or TP roles, respectively; $\mathcal{L}_3^m(k)$, $\mathcal{L}_4^m(k)$, and $\mathcal{L}_5^m(k)$ are the sets of travel links for member m using private car paths during interval k who takes the SD, RD, and RP roles, respectively; and $\mathcal{L}_6^m(k)$ is the set of travel links for member m using transit paths during interval k who takes the PT role. Note that a household member can switch between taking the SD and RD roles (if he/she takes the driver role), or between the RP and TP roles (if he/she takes the passenger role) at activity locations (according to **A8**). Thus, one set of activity links is used by the SD and RD roles, and another set is used by the RP and TP roles. Additional details on supernetwork construction are given in Vo et al. (2020a).

In the above-defined JATS supernetwork, a JATS link in $\mathbf{L}^h(k)$ represents the activity and travel choices of all members of household type h and their interactions during interval k, and a sequence of JATS links in JATS supernetwork $\mathbf{G}^h$ for household type h represents a JATP choice that satisfies the feasibility constraints shown in Appendix A. Thus, we can use this novel supernetwork and conventional path-finding algorithms (e.g., Dijkstra's algorithm) to generate the JATP choice set.

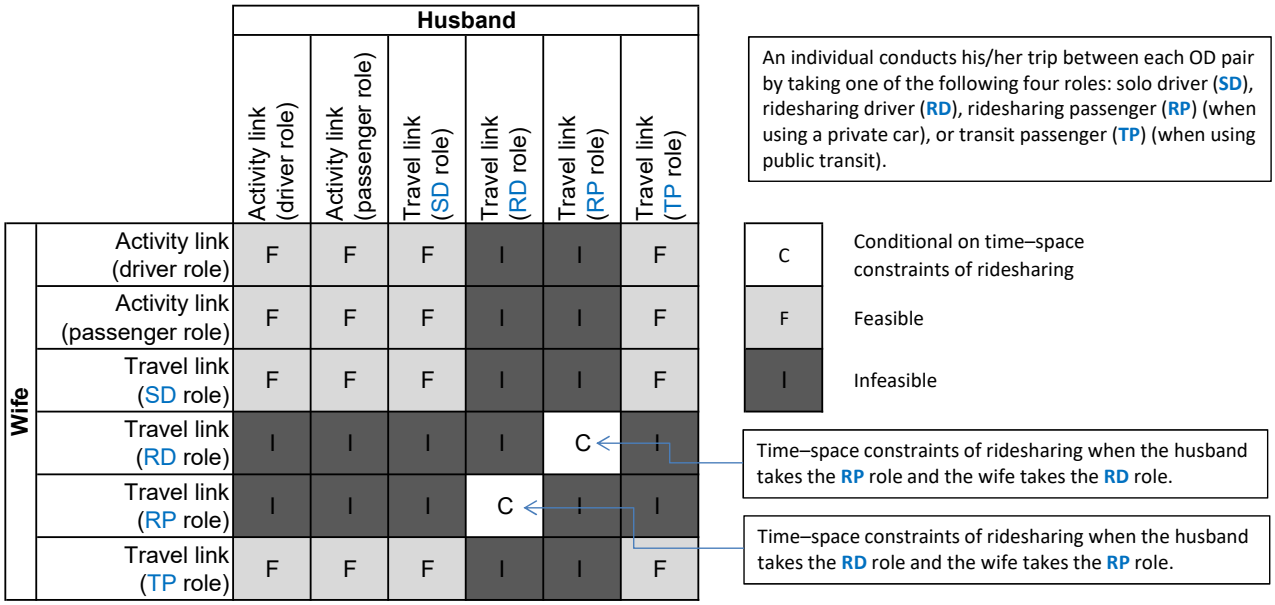

Figure 5: Feasibility rules for combining two activity–time–space (ATS) links of a working couple (modified from Vo et al. (2020a)).

As defined by (61), a JATS link during an interval comprises a vector (or combination) of ATS links during that interval, and not all combinations are feasible. The feasibility of a combination of ATS links can be determined using

predefined rules relating to the household context, such as the number of cars owned and/or car licenses possessed by the household. Fig. 5 shows the feasibility rules for combining two ATS links of a working couple who each has a car license and owns a car. In this figure, a dark gray cell indicates a infeasible combination (I), a light gray cell indicates a feasible combination (F), and a white cell indicates a *conditional* feasible combination (C), whose feasibility is conditional on the time–space constraints for ridesharing when the couple travel by private car. For example, if the ATS link of the husband is an activity link (for a RD or RP role) or a travel link (for a TP role), we can combine this link with any ATS link of the wife, except with travel links for the RD and RP roles. This is because travel links for the RD and RP roles are governed by the time–space constraints for ridesharing, in which a shared ride by private car can only occur if there is one RD and one RP. On the other hand, if the ATS link of the husband is a travel link for the RD role, we can only combine this link with a travel link for the RP role of the wife, provided that the two ATS links use the same path and have the same departure time.

Due to the complexity of the JATS supernetwork of the household, we illustrate only the ATS supernetwork associated with one household member. Thus, Fig. 6 illustrates the ATS supernetwork related to the wife's daily activity–travel schedule, and her interactions in the RP and TP roles in the JATP shown in Fig. 2. For ease of illustration, the time intervals in the supernetwork are not evenly discretized, and each OD pair is connected by only one simplified travel link. In fact, a travel link in this example supernetwork comprises multiple travel links each of which represents a path choice by model between two activity locations for a travel role. For example, the travel link connecting the home location and the restaurant includes one path $1 \to 2$ for the RP role, and two transit paths $1 \to 1' \to 2' \to 2$ and $1 \to 1'' \to 2'' \to 2$ for the TP role. Similarly, the travel link connecting the restaurant and the workplace 2 consists of one car path $2 \to 4$ for the RP role and one transit path $2 \to 2' \to 4' \to 4$ for the TP role.

Next, we follow Vo et al. (2020a) by analyzing the size of the JATS supernetwork for each household type with respect to the household size (i.e., the number of household members), the network size (i.e., the numbers of activity locations and of paths between OD pairs), and the number of time intervals. Let $S^m \subseteq S$ be the set of activity and drop-off/pick-up locations, and $W^m \subseteq W$ be the set of OD pairs related to member m. For each interval k, there are $|S^m|$ activity links for member m for the SD and RD roles, $|S^m|$ activity links for member m for the RP and TP roles. In addition, for each combination of interval k and OD pair w, there are $|P^w|$ feasible trips for member m for the SD role, $|P^w|$ feasible trips for member m for the RD role, $|P^w|$ feasible trips for member m for the RP role, and $|\hat{P}^w|$ feasible trips for member m for the TP role. Moreover, each car trip using path $p \in P^w$ during interval k is discretized into $\lceil t_p^w(k) \rceil$ travel links, and each transit trip using path $p \in \hat{P}^w$ also consists of $\lceil \hat{t}_p^w(k) \rceil$ travel links. Recall that $t_p^w(k)$ and $\hat{t}_p^w(k)$ are the travel times for the private car and the transit path p, respectively, between OD pair w with departure interval k, and $\lceil . \rceil$ is a function used to convert path travel time to integer time intervals. The number of links in the ATS supernetwork $\mathcal{G}^m$ for member m during interval k is then calculated as

$$|\mathcal{L}^m(k)| = \sum_{j=1}^{6} |\mathcal{L}_j^m(k)| = \left[2|S^m| + \sum_{w \in W^m} \left(3 \sum_{p \in P^w} \lceil t_p^w(k) \rceil + \sum_{p \in \hat{P}^w} \lceil \hat{t}_p^w(k) \rceil \right) \right] \quad \forall m. \tag{64}$$

Based on (61), the number of links in JATS supernetwork $\mathbf{G}^h$ for household type h is given by

$$|\mathbf{L}^h| = \frac{1}{\Lambda} \sum_{k=1}^{K} \prod_{m=1}^{M^h} |\mathcal{L}^m(k)| = \frac{1}{\Lambda} \sum_{k=1}^{K} \prod_{m=1}^{M^h} \left[2|S^m| + \sum_{w \in W^m} \left(3 \sum_{p \in P^w} \lceil t_p^w(k) \rceil + \sum_{p \in \hat{P}^w} \lceil \hat{t}_p^w(k) \rceil \right) \right] \quad \forall h, \tag{65}$$

where $\Lambda > 1$ in practice because JATS links only represent *feasible* combinations of ATS links rather than all possible combinations.

Remark 6. In (65), the size of the JATS supernetwork for each household type depends on the household size, the number of daily activities, and the path choices. In practice, the daily activity–travel program of a household consists of a limited number of daily JATP choices (Vo et al. (2020a)). This is partly due to real-life spatiotemporal activity–travel constraints; specifically, each person can only be involved in a relatively small number of daily activities with different durations at various locations, within a small part of a real transportation network (so-called personalized network by Arentze and Timmermans (2004b); Liao et al. (2011, 2013a)). In addition, empirical studies have shown that the daily activity–travel program of a household can be simplified to a few representative activities per typical day (as noted in Remark 3). Thus, for strategic planning purposes, the JATS supernetwork can be confined to a very small

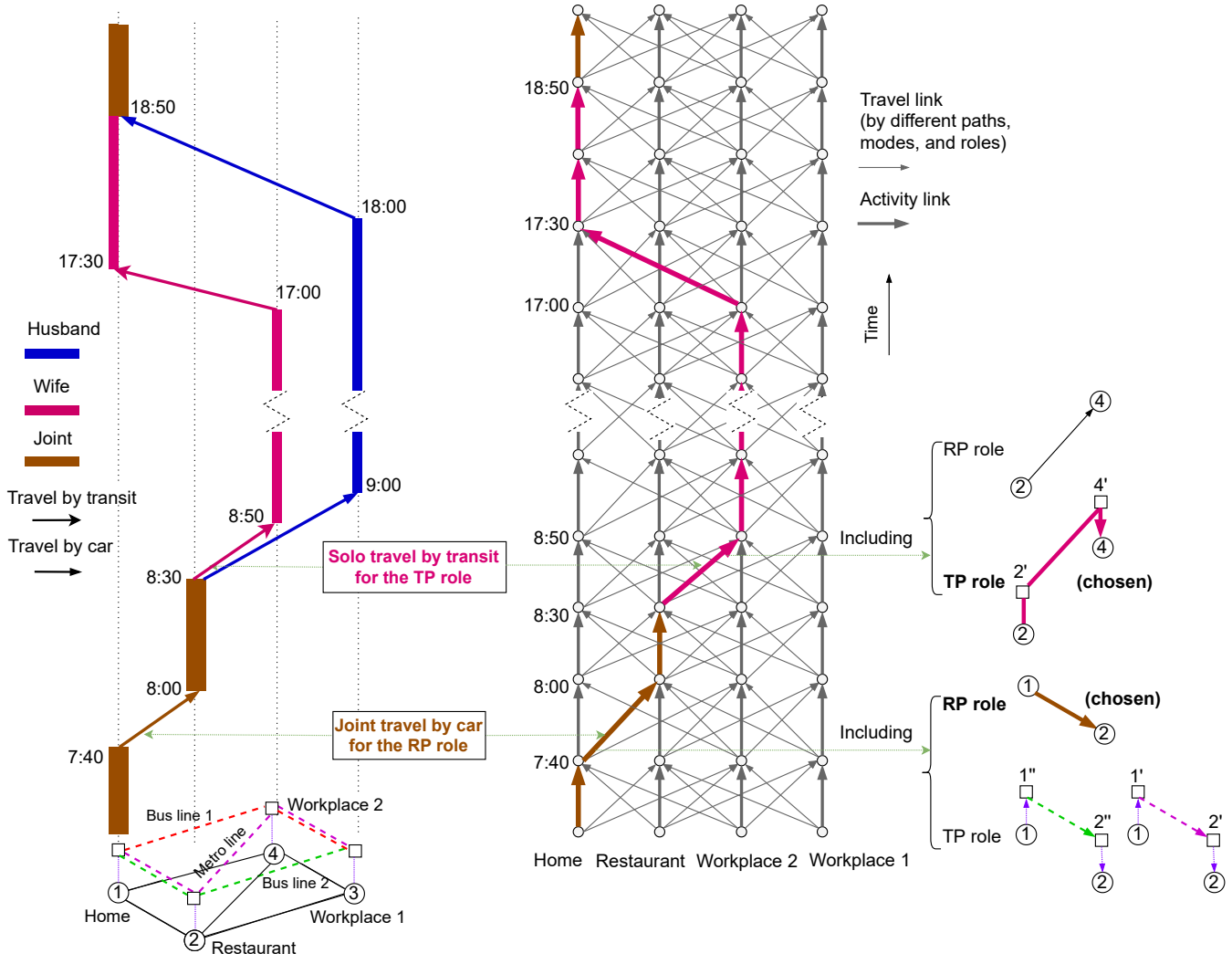

Figure 6: Activity–time–space (ATS) supernetwork of the wife, who may switch between the ridesharing passenger (RP) and transit passenger (TP) roles.

number of typical daily activities (e.g., an average of three or four daily activities) and path choices (fewer than 10) for each household type, rather than the large numbers of OD pairs and path choices for aggregated travel behaviors considered in conventional trip-based models. Moreover, most households comprise fewer than four persons (e.g., in 2017, approximately 69.8% of households in Hong Kong (Hong Kong Census and Statistics Department (2017)) and 77.4% of households in the US (US National Household Travel Survey (2017)) comprised fewer than four members). Recently, Vo et al. (2020b) used Wi-Fi tracking data to investigate the activity–travel patterns of pedestrians on the Hong Kong Polytechnic University campus, which has a reliable on-campus wireless network and a student population that extensively uses Wi-Fi-enabled devices. As we enter the 5G era, multiple types of sensors and fully connected infrastructure will become available. Our novel mixed-equilibrium model will thus benefit from the use of multiple sources of urban big data for constructing JATS supernetworks (see Siripirote et al. (2015)).

4.2. Diagonalization method

In this section, we develop a diagonalization method to solve the VI problem (36). This method was first proposed by Dafermos (1982) to solve static traffic assignment with asymmetric travel disutilities, and later adapted to manage the interactions of temporal link flows in dynamic traffic assignment (Chen and Hsueh (1998)), in dynamic activity-based traffic assignment (Lam and Yin (2001)), and in a household activity-based network equilibrium (Vo et al. (2020a)). The core strategy of our novel diagonalization method is to relax the interaction of link flows in flow propagation (40)–(42) and the interaction between car users and transit passengers sharing the same road links in the

VI problem (36) in order to yield subproblems that can be solved more effectively. The method involves the following steps:

Step 0: Initialization. Let $n = 0$.

Step 0.1: Initialize the *estimated* road link travel times $\bar{\mathbf{t}}^{(0)} = (\dots, \bar{t}_a^{(0)}(k), \dots)$ with the free-flow road link travel times $\mathbf{t}^{(0)}$.

Step 0.2: Use the estimated road link travel times $\bar{\mathbf{t}}^{(0)}$ to estimate the path travel times of car users and transit passengers using (1) and (5).

Step 1: Fix the flow propagation (40)–(42) with the estimated road link travel times $\bar{\mathbf{t}}^{(n)}$, and with the estimated path travel times of car users and transit passengers. Then, solve the VI problem (36) to determine the JATP flow pattern $\mathbf{f}^{(n)}$ and reproduce the *actual* road link travel times $\mathbf{t}^{(n)}$.

Step 2: Stabilize the estimated road link travel times. Let $n = n + 1$.

Step 2.1: Update the estimated road link travel times using the method of successive averages:

$$\bar{\mathbf{t}}^{(n)} = \bar{\mathbf{t}}^{(n-1)} + \frac{1}{n}\left(\mathbf{t}^{(n)} - \bar{\mathbf{t}}^{(n-1)}\right). \tag{66}$$

Step 2.2: Use the estimated road link travel times $\bar{\mathbf{t}}^{(n)}$ to update the estimated path travel times of car users and transit passengers using (1) and (5).

Step 3: Convergence check. If $\bar{\mathbf{t}}^{(n)} \approx \bar{\mathbf{t}}^{(n-1)}$, stop and consider $\mathbf{f}^{(n)}$ as the solution. Otherwise, go to **Step 1**.

Dafermos (1982) showed that sufficient conditions for the convergence of the diagonalization algorithm require the continuity of link costs in the presence of weak effects of the off-diagonal components on link costs. Such conditions are stringent and unnecessary for many practical applications, and do not hold in our mixed-equilibrium problem. The empirical results show that the diagonalization algorithm converges despite these conditions being violated (Friesz et al. (1984); Mahmassani and Mouskos (1988)). Hence, the developed method is expected to converge to a good-quality solution and thereby achieve network equilibrium.

The VI problem (36) in Step 1 of the diagonalization method is solved with a predetermined set of JATP choices. However, a different JATP choice set (satisfying the flow propagation (40)–(42)) should be generated for each JATP flow pattern because road link travel times vary according to the level of network congestion (Vo et al. (2020a)). Thus, it may be difficult to enumerate in advance the JATP choice sets for all feasible JATP flow patterns. To solve this problem, we couple the solution algorithm for the VI subproblem with a column generation strategy based on the shortest-path problem, which enables the JATP choice set to be generated when required (see also Ramadurai and Ukkusuri (2010); Ouyang et al. (2011); Fu and Lam (2014, 2018); Vo et al. (2020a)). Unlike the previous works where utility and disutility components are deterministic during column generation, in this paper utility and disutility components are stochastic due to households' errors of perception. Thus, during the column generation, we multiply the utility and disutility components of JATP utility u_q^h in (10) by a random factor $rand = (1 + unif(0, 0.1)/\theta^h)$, denoted by $rand \circ u_q^h$, where $unif(0, 0.1)$ is the uniform-distributed random value between 0 and 0.1. Then, the range of random factor $rand$ is proportional to the household's errors of perception (i.e., $1/\theta^h$).

Given that road link travel times are fixed by the diagonalization method to relax the interaction of link flows in flow propagation (40)–(42) and the interaction between car users and transit passengers sharing same road links, the VI subproblem (36) can be solved by a path-swapping algorithm (Vo et al. (2020a)). Under the assumption that the path cost function (which in this paper is equivalent to mapping $\tilde{u}_q^h$ given by (37)) is strictly monotonic, Huang and Lam (2002) proved that the path-swapping algorithm produces a converge solution. The mapping $\tilde{u}_q^h$ is strictly increasing in the VI subproblem due to the condition given by Proposition 3. Our developed path-swapping algorithm for the VI subproblem (36) is presented as below.

Step 0: Initialization. Let $n = 0$.

Step 0.1: Construct a JATS supernetwork for each household type h.

Step 0.2: Find JATP q with a highest $rand \circ u_q^h$ using the JATS supernetwork for each household type h under free-flow conditions.

Step 0.3: Let $Q^h = \{q\}$ and assign the flow $f_q^{h(0)} = F^h$ to obtain JATP flow pattern $\mathbf{f}^{(0)}$.

Step 1: Column generation.

Step 1.1: Find JATP q with a highest $rand \circ u_q^h$ using the JATS supernetwork for each household type h under JATP flow pattern $\mathbf{f}^{(n)}$.
Step 1.2: Update $Q^h = Q^h \cup \{q\}$.

Step 2: Convergence test. Stop if the relative gap (RGAP) satisfies

$$RGAP = \frac{\sum_{h=1}^{H} \sum_{q \in Q^h} f_q^{h(n)} \left(\mu^{h(n)} - \tilde{u}_q^{h(n)} \right)}{\sum_{h=1}^{H} \sum_{q \in Q^h} f_q^{h(n)} \mu^{h(n)}} < \varepsilon, \tag{67}$$

$$\mu^{h(n)} = \max \left\{ \tilde{u}_q^{h(n)} : q \in Q^h \right\}. \tag{68}$$

Step 3: JATP flow swapping.

$$f_q^{h(n+1)} = \begin{cases} \max \left\{ 0, f_q^{h(n)} - \Theta^{(n)} f_q^{h(n+1)} \left(\mu^{h(n)} - \tilde{u}_q^{h(n)} \right) \right\} & \forall q \notin \bar{Q}^{h(n)} \\ f_q^{h(n)} + \frac{\bar{F}^{h(n)}}{|\bar{Q}^{h(n)}|} & \forall q \in \bar{Q}^{h(n)} \end{cases}, \tag{69}$$

$$\bar{F}^{h(n)} = \sum_{q \notin \bar{Q}^{h(n)}} \left(f_q^{h(n)} - f_q^{h(n+1)} \right), \tag{70}$$

$$\bar{Q}^{h(n)} = \left\{ q \in Q^h : \tilde{u}_q^{h(n)} = \mu^{h(n)} \right\}, \tag{71}$$

$$\Theta^{(n)} = \frac{0.0001}{1 + n/10}. \tag{72}$$

Let $n = n + 1$. Go to **Step 1**.

5. Numerical examples

In relation to the contributions of this paper presented in Section 1.3, a small network is used below to illustrate (1) the effect of individual and household mixed equilibrium on the system's expected total utility and time allocation, (2) the effect of mixed-mode interactions on the modal split, and (3) the effect of household members' heterogeneous errors of perception on the time-dependent utility of different activity types. Then, the Sioux Falls network is used to illustrate (4) the monotonicity condition for the uniqueness of the solution to the VI problem, and (5) the convergence result of our solution method, and the practical computational feasibility of this method.

5.1. Example 1: small network

5.1.1. Settings

Fig. 7 shows a small multimodal network that comprises four nodes, 10 road links, two bus lines, one metro line, and four activity locations. We assume that the household comprises two full-time working members, who start and end their daily activity–travel schedules at home. There are four activities: work at workplaces 1 and 2, at home, and shopping. We set the duration of each time interval as $t_\sigma = 30$ min, which is sufficient for long-term transportation-planning purposes. For example, the adopted time resolution can be up to one hour (see e.g., Bradley and Vovsha (2005); Roorda et al. (2008); Lam and Yin (2001); Gupta and Vovsha (2013)), or four to five broad departure-time periods throughout a day (e.g., Arentze and Timmermans (2004a)).

Table 3 shows the input parameters for the marginal utility functions of different activities by time of day. The curves of the marginal utility functions of activities are illustrated in Fig. 8. We assume that the household members incur no activity congestion utility or disutility at home. The parameters for the activity congestion disutilities at the shopping mall and workplaces are set as $w_{(\text{shop})} = 30$ HK\$/h, $w_{(\text{work})} = 6$ HK\$/h, $n_{(\text{shop})} = 4$, and $n_{(\text{work})} = 2$. The capacities for the shopping mall the workplaces are set as $C_{(\text{shop})} = 20,000$ persons, and $C_{(\text{work})} = 20,000$ persons. The household preference parameters for joint activities and travel are set as $\alpha^{hg}_{(\text{home})} = 0.5\Delta$, $\alpha^{hg}_{(\text{shop})} = 0.6\Delta$,

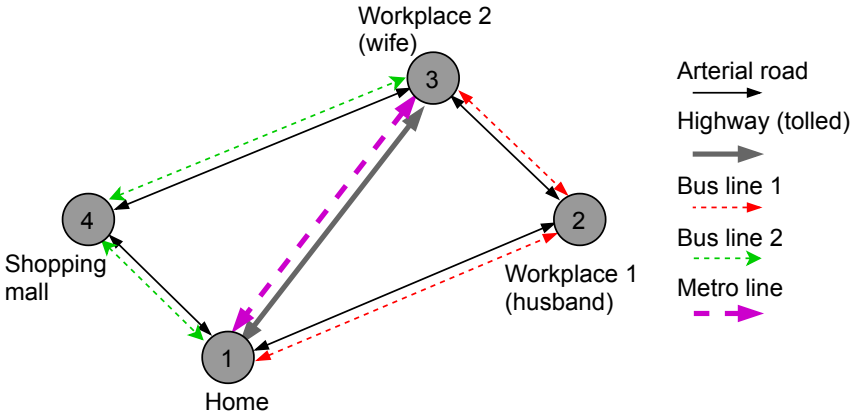

Figure 7: A small multimodal network.

Table 3: Input parameters for the marginal utility functions of different activities by time of day.

Activity	$U_{is}^{hm(0)}$ (HK$/min)	U_{is}^{hm} (HK$)	κ_i^{hm}	υ_i^{hm}	$\tilde{t}_i^{hm}$ (min)
At home	1.5	1000	−0.006	1	750
Work (husband)	0.0	2100	0.008	1	750
Work (wife)	0.0	1900	0.008	1	780
Shopping (husband)	0.0	900	0.015	1	1100
Shopping (wife)	0.0	1050	0.015	1	1130

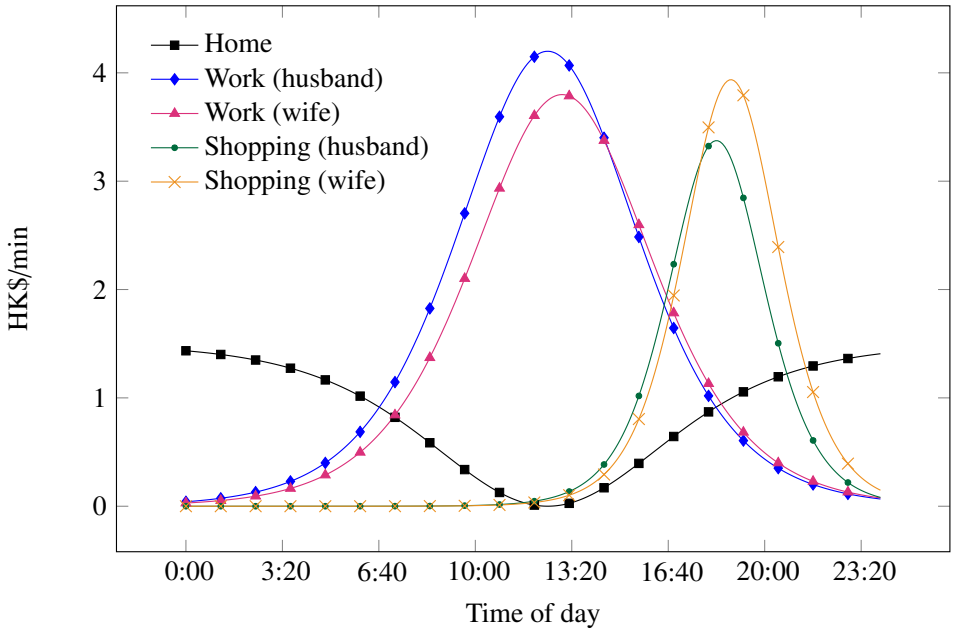

Figure 8: Marginal utility function curves of different activities by time of day.

$\beta_a^{hg} = 1.8\Delta$, and $\hat{\beta}_b^{hg} = 1.8\Delta$, where Δ is the normalized household preference parameter for joint activities and travel (i.e., $0 \leqslant \Delta \leqslant 1$), and is used for the illustrative purposes. Unless otherwise stated, $\Delta = 1$.

Table 4 shows the input parameters for the link travel times of private cars. The congestion parameters of private cars are set as $\tilde{w} = 1.5$, and $\tilde{n} = 4$. The value of the travel time of car users is $\gamma = 60$ HK$/h. The operating cost $\phi_a^{hg}(k)$ includes the fuel cost, which is set as 1.4 HK$/km, and a toll. A time-varying toll scheme is imposed on the highway, which has a HK$40 toll in the morning peak period [7:00, 9:00] and evening peak period [17:00, 19:00] and a HK$20 toll in other periods. All paths used by car users connecting activity and drop-off/pick-up locations are enumerated. Table 5 shows the input parameters for the transit travel disutilities. The congestion parameters of transit

passengers are $\hat{w} = 0.6$, and $\hat{n} = 4$. The coefficients of the transit time components are set as $\hat{\gamma}_1 = \hat{\gamma}_2 = \hat{\gamma}_3 = \hat{\gamma}_4 = 60$ HK$/h. The access/egress times to/from transit stops are set as 3 min. In addition, all paths used by transit passengers are enumerated.

Table 4: Input parameters for road link travel times.

Link	Free-flow travel time (h)	Free-flow speed (km/h)	Length (km)	Capacity (veh/h)	Fixed pre-loaded transit vehicle flow (veh/h)
1–2	0.3	50	15	1800	10
1–3	0.5	70	30	3600	0
2–3	0.3	50	15	1800	10
1–4	0.3	50	15	1800	10
3–4	0.3	50	15	1800	10

Note: Only one direction of the link is shown.

Table 5: Input parameters for transit disutilities.

Line*	Links	Link free-flow travel times (h)	Link fares (HK$)	Frequency (veh/h)	Capacity (pax/veh)
Bus line 1	1–2, 2–3	0.3, 0.3	5, 5	10	120
Bus line 2	1–4, 4–3	0.3, 0.3	5, 5	10	120
Metro line**	1–3	0.5	10	10	1500

*: only one direction of the transit line is shown.
**: the metro travel time is not affected by road congestion.

Unless otherwise stated, the husband's and wife's individual scale parameters associated with home, work, and shopping are $\eta^{\mathrm{H}}_{(\mathrm{home})} = 0.8, \eta^{\mathrm{H}}_{(\mathrm{work})} = 0.9, \eta^{\mathrm{H}}_{(\mathrm{shop})} = 0.7, \eta^{\mathrm{W}}_{(\mathrm{home})} = 0.9, \eta^{\mathrm{W}}_{(\mathrm{work})} = 1.0$, and $\eta^{\mathrm{W}}_{(\mathrm{shop})} = 0.8$, respectively. The household scale parameter is set as $\theta = 1.0$. The population is 20,000 households (or 40,000 persons) and all household members follow the SHO principle. The commonality factors are $\nu_0 = \nu_1 = 0$.

5.1.2. Effect of individual and household mixed equilibrium

We first investigate the effect of the mixed equilibrium of individual and household activity–travel choices on daily time allocation. In this scenario, household members are classified into two groups with different activity–travel behaviors. The first group follows the SHO principle, which maximizes the perceived household utility for each household, whereas the other follows the SUE principle, which maximizes the perceived individual utility for each household member. Table 6 compares the average daily time allocation for various activities per person for three proportions Γ of household members following the SHO principle: $\Gamma = 0$ (100% following the SUE principle), $\Gamma = 0.6$, and $\Gamma = 1.0$ (100% following the SHO principle). As observed, a higher Γ leads to a longer time spent on joint activities and travel. This is because the SHO principle, unlike the SUE principle, accounts for the extra benefits of joint activities and travel, which encourage more household members to conduct activities and travel together. A similar result was found by Vo et al. (2020a) for deterministic cases when households' errors of perception are ignored.

We further investigate the effect of the mixed equilibrium on the system's expected total utility versus the household preference Δ for joint activities and travel. In this experiment, Δ is varied between 0 and 1, where Δ is proportional to the extra benefits of joint activities and travel, and thus $\Delta = 0$ indicates no extra benefit. Fig. 9 shows a plot of the expected total household utility versus Γ and Δ. If Δ is low (i.e., $\Delta = 0$), as Γ increases to a certain limit (i.e., $\Gamma = 0.4$), the expected total household utility initially increases, and then decreases. This result indicates that if the extra benefits of joint activities and travel are relatively small and more household members follow the SHO principle, the expected total household utility may be worse off. This is because the extra benefits of joint activities and travel cannot compensate for the disutilities of additional pick-up and drop-off trips. In contrast, if Δ is high (i.e., $\Delta = 1.0$), as Γ increases, the expected total household utility increases because households benefit more from joint

Table 6: Average daily time allocation per person versus the proportion Γ of household members following the SHO principle.

Duration (h/person)	Γ = 0.0	Γ = 0.6	Γ = 1.0
Solo travel by car	1.5	1.4	1.3
Joint travel by car	**0.0**	**0.3**	**0.5**
Solo travel by transit	1.7	1.4	1.3
Joint travel by transit	**0.0**	**0.1**	**0.2**
Solo at-home	1.5	1.2	0.9
Joint at-home	**9.7**	**9.9**	**10.0**
Work	9.0	8.8	8.7
Solo shopping	0.6	0.3	0.2
Joint shopping	**0.1**	**0.6**	**0.8**
Total	24.0	24.0	24.0

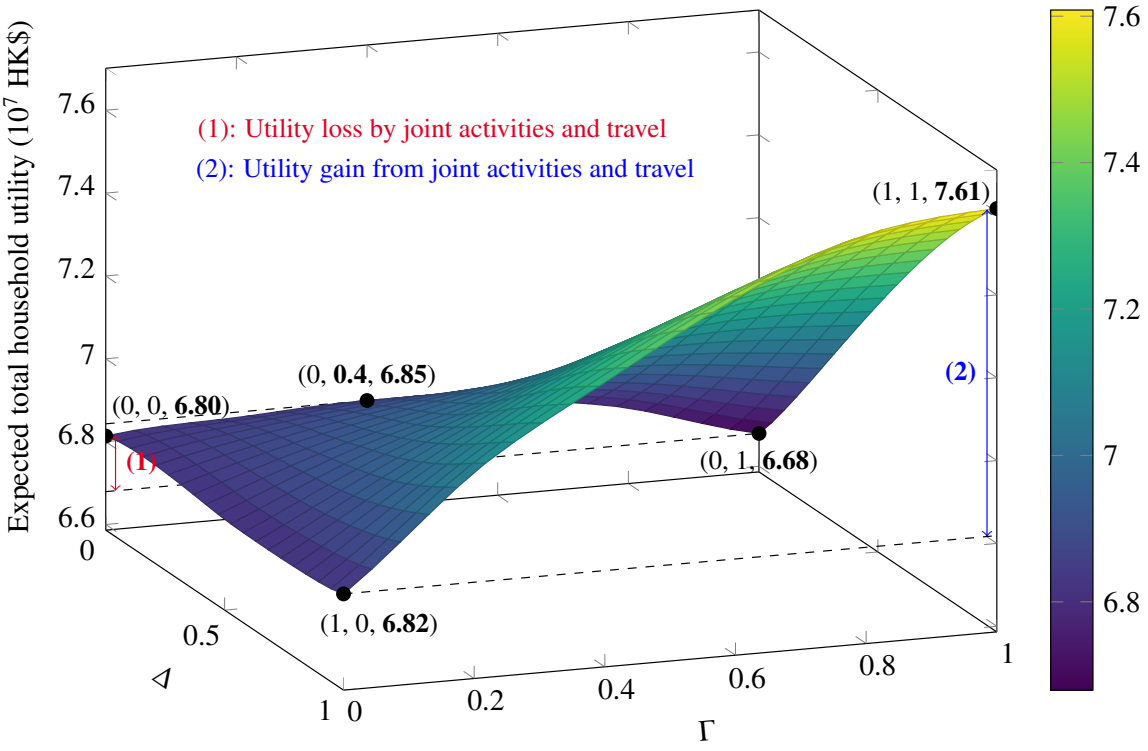

Figure 9: Expected total household utility versus the proportion Γ of household members following the SHO principle and the household preference Δ for joint activities and travel.

activity–travel choices. Clearly, the system benefits from certain values of Γ and Δ. This suggests that policies can be imposed to ensure that a mixed equilibrium contains appropriate proportions of household members who optimize their household and individual utilities, such that the benefits to the system can be maximized. Additional studies are needed to investigate the complex interactions between individual and household activity–travel choices in a mixed equilibrium.

5.1.3. Effect of mixed-mode interactions

In this section, we discuss the effect of mixed-mode interactions between private cars and public transit modes on the modal split. Our novel model fully considers the congestion effect of multiple modes, where the travel times of road-based transit modes (e.g., bus) are affected by road congestion. In contrast, previous household-oriented activity-based network equilibrium models (Vo et al. (2020a); Fu and Lam (2018)) have only considered the congestion effects of either private car or public transit modes, and have assumed that transit travel times are fixed and predetermined. However, ignoring mixed-mode interactions can lead to biased estimates of travel demand and transit use, as these

depend on how the travel times of road-based transit modes are predetermined.

Table 7: Modal split in the presence and absence of mixed-mode interactions.

	With mixed-mode interactions	Without mixed-mode interactions	
		BTT = 1×FTT	BTT = 5×FTT
Number of person trips by private car	52227 (46%)	52632 (41%)	62518 (61%)
Number of person trips by metro	30848 (27%)	24757 (19%)	28840 (28%)
Number of person trips by bus	**30523** (27%)	**51378** (40%)	**11470** (11%)
Total travel demand	**113598** (100%)	**128767** (100%)	**102828** (100%)

Note: "BTT" denotes the bus travel time, and "FTT" denotes the free-flow travel time on a road link.

Table 8: Average daily time allocation per person in the presence and absence of mixed-mode interactions.

Duration (h/person)	With mixed-mode interactions	Without mixed-mode interactions	
		BTT = 1×FTT	BTT = 5×FTT
Travel	3.4	**2.8**	**3.5**
Home	11.1	10.8	11.2
Work	8.7	8.8	8.7
Shopping	0.8	**1.6**	**0.6**
Total	24.0	24.0	24.0

Note: "BTT" denotes the bus travel time, and "FTT" denotes the free-flow travel time on a road link.

Table 7 compares the modal split in the presence and absence of mixed-mode interactions. If the predetermined bus travel time (BTT) is small (i.e., equal to the road free-flow travel time (FTT)), ignoring the mixed-mode interactions results in an overestimation of the use of the bus mode and thus an overestimation of the travel demand. In contrast, as BTT increases (i.e., to 5×FTT), ignoring the mixed-mode interactions results in an underestimation of the use of the bus mode and an underestimation of the travel demand. Note that the total travel demand is elastic in response to changes in BTT. We further investigate the effect of mixed-mode interactions on daily time allocation, as shown in Table 8. In particular, a shorter BTT leads to a longer time spent doing out-of-home activities (e.g., shopping), as more household members are encouraged to choose the bus mode for traveling.

The results in this section indicate that if the predetermined travel times of road-based transit modes are low (high), ignoring the mixed-mode interactions between private car and transit modes will lead to an overestimation (underestimation) of the transit use, travel demand, and out-of-home activity duration.

5.1.4. Effect of household members' heterogeneous perception errors

This section shows the effect of household members' heterogeneous errors of perception on the utility of different activity types. As household members' errors of perception are parameterized by household and individual scale parameters, we investigate the effect of these parameters on household and individual utilities.

Fig. 10 shows a plot of the expected total household utility versus the household scale parameter θ. As θ increases with a decrease in the household's error of perception, the expected total household utility increases, and then reaches a stable limit. After that, at a large value of θ, the stochastic effect of households' errors of perception decreases, at which point the SHO principle approaches the deterministic HO principle (Property 2). In this situation, household members have perfect information about the network conditions, and can therefore choose the most efficient JATPs with a highest expected utility, which increases the expected total household utility. In contrast, a smaller θ causes more households to choose JATPs with a smaller expected utility, and the JATP flows tend to be even (Property 3).

To investigate the effect of individual scale parameters on the individual utilities of different activity types, we vary the husband's and wife's individual scale parameters of shopping, which are $\eta^{\mathrm{H}}_{(\mathrm{shop})}$ and $\eta^{\mathrm{W}}_{(\mathrm{shop})}$, respectively,

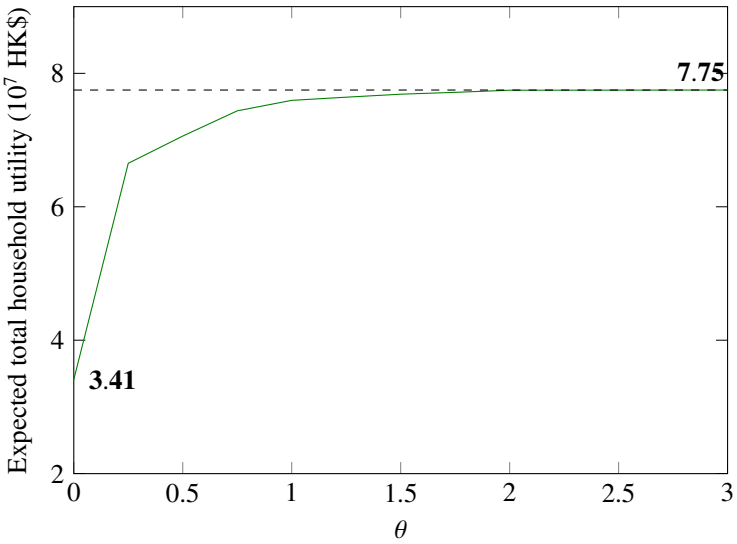

Figure 10: Expected total household utility versus the household scale parameter θ.

Table 9: Relationship between the expected total utility associated with different activity types and the individual scale parameters $\eta^{H}_{(shop)}$ and $\eta^{W}_{(shop)}$.

Utility (10^7 HK$)	Individual scale parameters $(\eta^{H}_{(shop)}, \eta^{W}_{(shop)})$						
	Decrease in $\eta^{W}_{(shop)}$				Decrease in $\eta^{H}_{(shop)}$		
	(0.8, 0.2)	(0.8, 0.4)	(0.8, 0.6)	(0.8, 0.8)	(0.6, 0.8)	(0.4, 0.8)	(0.2, 0.8)
Work (H)	2.44	2.54	2.50	2.50	2.51	2.52	2.53
Work (W)	2.74	2.74	2.73	2.71	2.70	2.71	2.71
At-home (H)	0.97	0.87	0.83	0.74	0.82	0.83	0.84
At-home (W)	1.10	1.00	0.96	0.89	0.90	0.93	0.91
Shopping (H)	0.17	0.21	0.23	**0.26**	**0.22**	**0.14**	**0.11**
Shopping (W)	**0.26**	**0.40**	**0.45**	**0.51**	0.48	0.46	0.43

Note: "H" stands for "husband", and "W" stands for "wife".

Table 10: Relationship between the average time allocation of activities per person and the individual scale parameters $\eta^{H}_{(shop)}$ and $\eta^{W}_{(shop)}$.

Duration (h/person)	Individual scale parameters $(\eta^{H}_{(shop)}, \eta^{W}_{(shop)})$						
	Decrease in $\eta^{W}_{(shop)}$				Decrease in $\eta^{H}_{(shop)}$		
	(0.8, 0.2)	(0.8, 0.4)	(0.8, 0.6)	(0.8, 0.8)	(0.6, 0.8)	(0.4, 0.8)	(0.2, 0.8)
Work (H)	8.7	8.6	8.7	8.6	8.6	8.7	8.7
Work (W)	9.0	9.1	9.0	8.8	8.9	8.9	8.9
At-home (H)	11.3	11.1	10.8	10.6	10.8	11.2	11.0
At-home (W)	12.0	11.6	11.4	11.3	11.3	11.3	11.2
Shopping (H)	0.4	0.6	0.7	**0.8**	**0.7**	**0.4**	**0.3**
Shopping (W)	**0.4**	**0.7**	**0.8**	**1.0**	0.9	0.9	0.8

Note: "H" stands for "husband", and "W" stands for "wife".

while fixing the household and individual scale parameters of other activities. Table 9 shows the relationship between the expected total individual utility of different activities and $\eta^{H}_{(shop)}$ and $\eta^{W}_{(shop)}$. If $\eta^{H}_{(shop)}$ or $\eta^{W}_{(shop)}$ decreases in value (i.e., the husband's or wife's individual errors of perception on shopping increase), the expected individual utility of shopping (for both the husband and wife) decreases. This leads to increases in the expected individual utilities

associated with other activities (i.e., at-home and work activities). Note that smaller values of $\eta^{\mathrm{H}}_{(\mathrm{shop})}$ or $\eta^{\mathrm{W}}_{(\mathrm{shop})}$ also indicate that more households choose JATPs with smaller expected individual utilities of shopping. This implies that smaller values of $\eta^{\mathrm{H}}_{(\mathrm{shop})}$ or $\eta^{\mathrm{W}}_{(\mathrm{shop})}$ result in a smaller effect of shopping on JATP choices (Property 4). Table 10 shows that a smaller expected shopping utility leads to shorter joint and solo shopping durations, which result in longer at-home and work durations.

These results suggest that the expected total utility in the system is overestimated if we assume that household members have erfect information about network conditions, especially if their heterogeneous perceptions of the utility associated with different activity types are highly inaccurate.

5.2. Example 2: Sioux Falls network

5.2.1. Settings

A second example is presented to illustrate the monotonicity condition for the uniqueness of a solution to the VI problem, the convergence of the developed diagonalization method, and the computational feasibility of this method in practice. The example network is a medium-sized Sioux Falls network (Leblanc (1973)), as shown in Fig. 11. The path set for private cars between OD pairs used in this example is taken from Bekhor et al. (2008), which was also used by Vo et al. (2020a). This path set is behaviorally generated using a combination of the link elimination method and a penalty method. In this example, the average number of private car paths for each OD pair is 7.2, and the maximum number of private car paths generated for any OD pair is 12. The road link capacity for each link is 1,800 veh/h. The fixed metro travel time is set as the road free-flow travel time. All transit paths connecting each OD pair are enumerated.

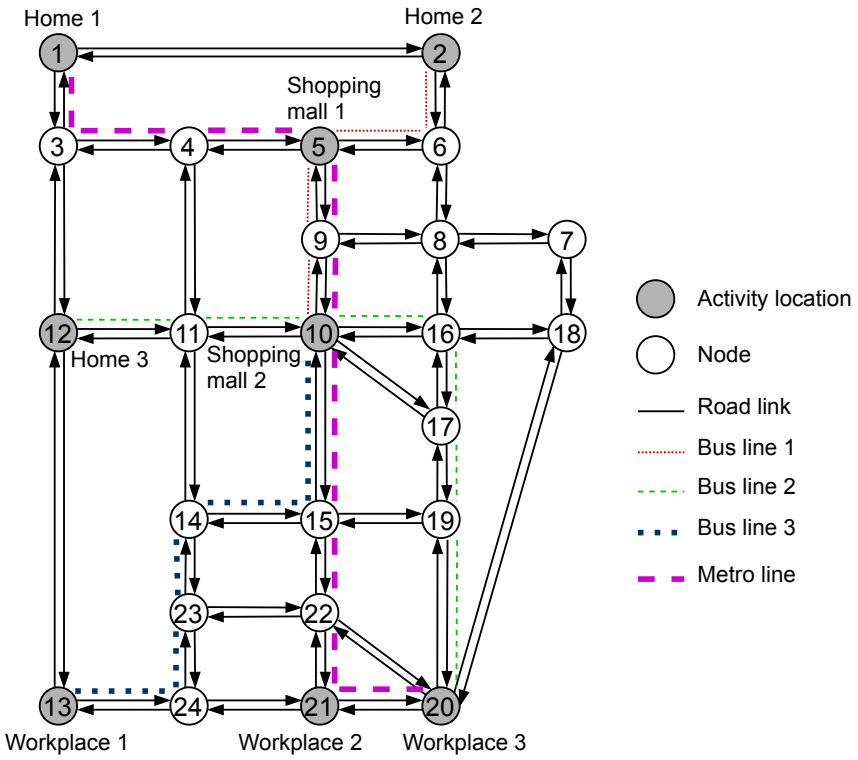

Figure 11: Sioux Falls network.

We assume that there are 10,000 households comprising two full-time workers, who start and end their daily activity–travel schedules at homes 1, 2, or 3. The parameters for the marginal utility functions of different activities by time of day for each couple are described in Table 3. The husband at home 1 works at workplace 1 and his wife works at workplace 2, the husband at home 2 works at workplace 1 and his wife works at workplace 3, and the husband at home 3 works at workplace 2 and his wife works at workplace 3. The household members can shop at either shopping mall 1 or 2. We also assume that each household owns two cars, and set $w_{(\mathrm{shop})} = 45$ HK\$/h, $w_{(\mathrm{work})} = 15$ HK\$/h, $C_{(\mathrm{shop})} = 10,000$ persons, and $C_{(\mathrm{work})} = 10,000$ persons. The congestion parameters of private

cars and transit passengers are set as $\tilde{w} = 0.3$, $\hat{w} = 0.15$, and $\tilde{n} = \hat{n} = 4$. The household preference parameter for joint activities and travel is $\Delta = 1$. Other parameters, if not mentioned, are the same as those in Example 1. The computer program is coded in Java SE 8 on Windows 10, on a machine with a 3.50 GHz Intel Core i5 and 8 GB of RAM. The threshold for the gap in the VI subproblem is 0.001.

5.2.2. Results

As discussed, it is not feasible to enumerate in advance the JATP choice set as road link travel times vary according to the level of network congestion. Thus, it is also difficult to verify the monotonicity condition (50) for the set of feasible JATP flow patterns Ω, which may not be available. According to Remark 5, the monotonicity condition (50) holds when the expected total activity congestion and entropy disutility (related to $Z_1 + Z_5$) dominate the expected total travel congestion disutility (related to $Z_3 + Z_4$). Table 11 shows that the expected total activity congestion and entropy disutility, in practice, may be much higher than the expected total travel congestion disutility. In addition, a smaller θ leads to a greater dominance of the expected total activity congestion and entropy disutility. This occurs because a smaller θ results in more households choosing JATPs with a smaller utility, which is attributable to the larger expected activity congestion disutility, and also results in a larger entropy disutility.

Table 11: Relationship between expected total congestion disutility components and the household scale parameter θ.

Disutility component (10^6 HK$)	HO	SHO	
	$\theta \to +\infty$	$\theta = 1.0$	$\theta = 0.1$
Activity congestion disutility (1)	35.46	36.20	35.88
Entropy disutility (2)	0.00	0.18	1.63
Travel congestion disutility (3)	6.68	6.47	6.04
Percentage difference $\frac{(1)+(2)-(3)}{(3)} \times 100$	**430.71**	**462.32**	**521.42**

Fig. 12 shows the convergence of the developed diagonalization method for the Sioux Falls network versus the household scale parameter θ. The method requires an average computational time of 7 min per iteration. The convergence index indicates the difference (in min) between the estimated travel times of road links for constructing the supernetwork platform of two consecutive iterations. It appears that a smaller θ leads to a faster convergence. This may be because of a more evenly distributed JATP flow pattern when θ decreases (see Property 3). As a result, traffic flows (and also congestion effects) tend to be distributed more evenly on various road links of the transportation network. This leads to a smaller difference between the travel times of road links, and thus a smaller difference between the estimated travel times of road links between two consecutive iterations of the diagonalization method. Additional studies should be performed to develop a better understanding of the convergence characteristics of the diagonalization method in solving the concerned mixed-equilibrium problem in this paper.

Remark 7. Based on Remark 6, for strategic planning purposes the constructed JATS supernetwork may be confined to a very small number of daily activities (e.g., an average of three or four daily activities) and path choices (fewer than 10) for each household type, rather than the large numbers of OD pairs and path choices for aggregated travel behaviors considered in the conventional trip-based models. Thus, the settings in the Sioux Falls network example (i.e., 24 nodes, 76 links, three activity types, eight activity locations, 30 OD pairs, an average of 7.2 private car paths per OD pair, and three household types) may be sufficient for demonstrating the computational feasibility of our model for strategic planning purposes, for at least three household types (see also Vo et al. (2020a)). However, because a JATS supernetwork is constructed for each household type, the computational time of our model increases linearly with the number of household types. This means that the computational time required for solving a problem related to realistic networks with numerous household types could become impracticably long. Nevertheless, the linearity of this increase means that the computational time may be acceptable for long-term planning purposes.

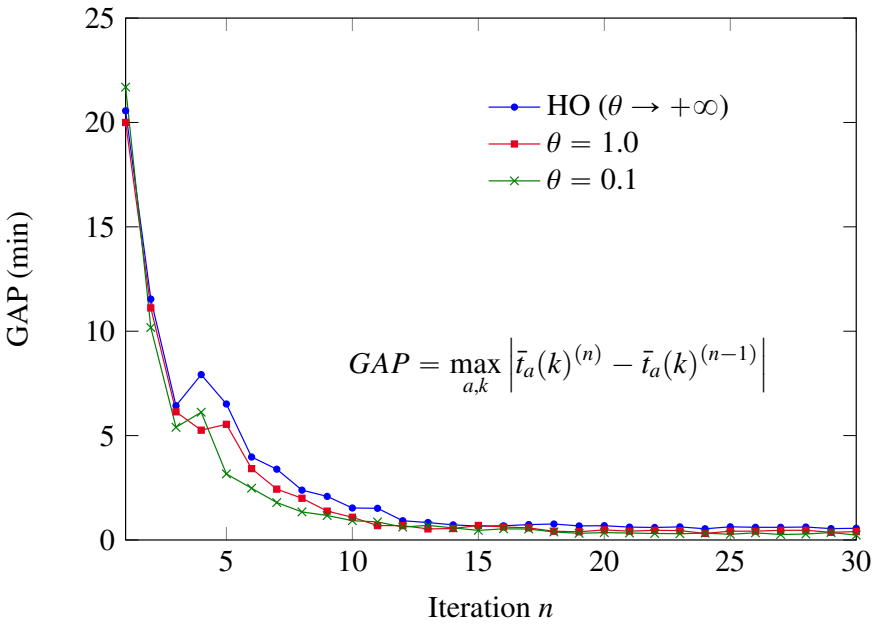

Figure 12: Plot of the convergence gap of the developed diagonalization method versus the household scale parameter θ.

6. Applicability of the novel model for assessing the effect of the COVID-19 pandemic

6.1. Extension of model formulation for modeling the specific effect of the COVID-19 pandemic

In addition to its main purpose of assessing the effects of alternative transport policies on long-term strategic planning in normal scenarios (Vo et al. (2020a)), the novel model can also capture the effect of the COVID-19 pandemic. We extend the model formulation as follows:

- risks of infection at out-of-home activity locations and in transit vehicles are incorporated into utility and disutility component functions to capture household members' preferences for teleworking and/or concerns about being infected while using public transport and participating in out-of-home activities;
- new types of at-home activities (e.g., working at home), which are not subject to infection risks, can be flexibly incorporated by redefining the supernetwork; and
- differential increases in household members' errors of perception in uncertain nonrecurrent scenarios can be specifically modeled by the heterogeneity in their errors of perception.

We adopt the following assumptions:

B1 As the novel model is mainly used for strategic planning, we assume that household members have perfect information about the SARS-CoV-2 infection ratio (i.e., expected number of confirmed cases of infection divided by the total population in the design year), which is one of the most important indicators of the effect of the COVID-19 pandemic (SCDHE's Key Indicators (2021); Worldometer's Coronavirus Update (2020)). Then, the effect of the COVID-19 pandemic on households' daily activity–travel choices, can be calibrated in terms of utility and disutility, and assumed to be a function of the infection ratio (Barbieri et al. (2021)).

B2 As taxi trips or carpooling are not considered, the risk of infection presents only at out-of-home activity locations and in transit vehicles. Moreover, the risk disutility is separable and increasing with the number of persons presented and the duration of time spent at an activity location or in a transit vehicle.

B3 Household members perceive that there is a higher infection risk when conducting joint out-of-home activities and joint travel, as they may have a greater fear that they or their close family will become infected.

Based on **B1**, we define the activity–travel net utility of household type h choosing JATP q when the infection ratio is R as the trade-off between the activity–travel utility and the disutility of risks:

$$\bar{u}_q^h(R) = u_q^h - \rho_q^h(R), \tag{73}$$

where u_q^h is the activity–travel net utility obtained by household type h choosing JATP q under normal (non-pandemic) conditions, and $\rho_q^h(R)$ is the disutility of risks which is an increasing function with respect to the infection ratio R. When $R = 0$, the disutility of the risk is eliminated with $\rho_q^h(0) = 0$, and the JATP utility function (73) is reduced to that for the normal case with $\bar{u}_q^h(0) = u_q^h$.

According to **B2**, there is a risk of infection only at out-of-home activity locations and in public transit vehicles. Thus, the disutility of risks perceived by household type h choosing JATP q when the infection ratio is R is formulated as

$$\rho_q^h(R) = \sum_{m=1}^{M^h}\sum_{g=1}^{G^h}\sum_{k=1}^{K}\left(\sum_{i\in I}\sum_{s\in S}\rho_{is}^{hmg}(k,R)\delta_{qis}^{hmg}(k) + \sum_{w\in W}\sum_{p\in\hat{P}^w}\sum_{b\in B_4}\sum_{k'=k}^{K}\hat{\rho}_b^{hmg}(k',R)\hat{\xi}_{qpwbk}^{hmg}(k')\right), \tag{74}$$

where $\rho_{is}^{hmg}(k,R)$ and $\hat{\rho}_b^{hmg}(k,R)$ are, respectively, the disutilities of risk perceived by member m in group g of household type h for participating in activity i at location s and for traveling on vehicle link b during interval k under infection ratio R.

As the disutility of risk at an activity location is separable and increasing with the number of persons at that location and the activity duration (due to **B2**), the disutility of risk perceived by member m of household type h for participating in activity i at location s during interval k when the infection ratio is R can be expressed as

$$\rho_{is}^{hmg}(k,R) = \varrho^{hmg}(R)t_\sigma\left(\frac{v_{is}(k)}{C_{is}}\right)^N, \tag{75}$$

where $\varrho^{hmg}(R)$ is the risk perception of member m in group g of household type h for out-of-home activity participation when the infection ratio is R, $v_{is}(k)$ is number of persons participating in activity i at location s during interval k, C_{is} is the activity capacity, t_σ is the duration of each interval, and N is a calibrated parameter. Similarly, the disutility of risk perceived by member m of household type h for traveling on vehicle link b during interval k when the infection ratio is R is defined as

$$\hat{\rho}_b^{hmg}(k,R) = \hat{\varrho}^{hmg}(R)\hat{t}_b(k)\left(\frac{\hat{v}_b(k)}{(1/t_\sigma)\hat{C}_b D_b}\right)^{\hat{N}} \quad b\in B_4, \tag{76}$$

where $\hat{\varrho}^{hmg}(R)$ is the risk perception of member m in group g of household type h for transit travel when the infection ratio is R, $\hat{v}_b(k)$ is the number of transit passengers on vehicle link b during interval k, $\hat{C}_b$ is the capacity of each transit vehicle, D_b is the transit frequency associated with vehicle link b, $\hat{t}_b(k)$ is the transit travel time, $1/t_\sigma$ is used to converted the unit of $\hat{C}_b$ from pax/interval, and $\hat{N}$ is a calibrated parameter.

The risk-perception parameters $\varrho^{hmg}(R)$ and $\hat{\varrho}^{hmg}(R)$ must satisfy the following two conditions:

- $\varrho^{hmg}(R)$ and $\hat{\varrho}^{hmg}(R)$ are increasing functions with respect to R, implying that when the infection ratio is higher, member m in group g of household type h is more risk-averse toward infection at out-of-home activity locations and in transit vehicles.
- $\varrho^{hmg}(0) = 0$ and $\hat{\varrho}^{hmg}(0) = 0$, implying that the risk of infection disappears at a zero infection ratio.

In addition, we assume that household members incur higher risks of infection when conducting joint activities and travel, as in such situations they may have a greater fear that they or their close family will be infected (according to **B3**). We thus formulate the risk attitudes as

$$\varrho^{hmg}(R) = \exp\left[\left(\varrho^{hm} + \varrho^{hg}\right)R\right] - 1, \tag{77}$$

$$\hat{\varrho}^{hmg}(R) = \exp\left[\left(\hat{\varrho}^{hm} + \hat{\varrho}^{hg}\right)R\right] - 1, \tag{78}$$

where $\varrho^{hm} \geqslant 0$ and $\hat{\varrho}^{hm} \geqslant 0$ are the individual risk-perception parameters, and ϱ^{hg} and $\hat{\varrho}^{hg}$ are the household risk-perception parameters for joint out-of-home activities and travel by public transit, where

$$\varrho^{hg}\begin{cases}\geqslant 0 & \text{if } g > 1\\ = 0 & \text{if } g = 1,\end{cases} \tag{79}$$

$$\hat{\varrho}^{hg} \begin{cases} \geqslant 0 & \text{if } g > 1 \\ = 0 & \text{if } g = 1. \end{cases} \tag{80}$$

The larger values of ϱ^{hg} and $\hat{\varrho}^{hg}$ in (79) and (80) indicate that the household member is more concerned about infecting their family when participating in joint activities and travel by transit modes.

According to **B1**, household members perceive the risks of infection at out-of-home activity locations and in transit vehicles based on the information they receive about the SARS-CoV-2 infection ratio during the COVID-19 pandemic. As the future value of the infection ratio is unknown, for long-term-planning purposes, we derive a value for this ration from the average infection ratio and its probability. For simplicity, we derive a sample of three infection levels from the provided information, as shown in Table 12, which are classified based on the list (sorted by infection ratio) reported in Worldometer's Coronavirus Update (2020). A low infection ratio is associated with countries at the bottom of the list, such as Hong Kong; a medium ratio is associated with countries in the middle of the list, such as the UK; and a high ratio is associated with those countries at the top of the list, such as the US. We denote the provided information $\mathcal{I} = (P_1, P_2, P_3)$ as a vector of probabilities of infection levels, where P_ℓ is the *prior probability* of infection level ℓ.

Table 12: Infection levels derived from the provided information on infection ratios.

Infection level	Average ratio (%)	Country
Low infection	$R_1 = 0.1$	Hong Kong
Medium infection	$R_2 = 4.0$	The UK
High infection	$R_3 = 6.0$	The US

Note: ratio $= \frac{\text{number of confirmed cases}}{\text{total population}} \times 100$.

In practice, household members may perceive a *posterior probability* of each infection level based on their past experiences. Let $P_{\mathcal{I}|\ell}$ represent the conditional probability of the provided information $\mathcal{I}$, with the infection level perceived by the household member being ℓ. Then, according to Bayes' theorem, we formulate the following posterior probability for infection level ℓ perceived by member m of household type h:

$$\tilde{P}^{hm}_{\ell|\mathcal{I}} = \frac{P^{hm}_{\mathcal{I}|\ell}}{\sum_{\ell'=1}^{3} P_{\ell'} P^{hm}_{\mathcal{I}|\ell'}} P_\ell. \tag{81}$$

Moreover, the following conservation of posterior probabilities holds: $\sum_{\ell=1}^{3} \tilde{P}^{hm}_{\ell|\mathcal{I}} = 1$.

Given the posterior probability of a specific infection-level occurrence defined in (81), the resultant random utility of household type h choosing JATP q based on different possible provided information $\mathcal{I}$ is a mixture distribution. From (73) and (74), the mean of the mixture distribution is given by

$$\bar{u}^h_{q|\mathcal{I}} = u^h_q - \sum_{\ell=1}^{3} \sum_{m=1}^{M^h} \sum_{g=1}^{G^h} \sum_{k=1}^{K} \left(\sum_{i\in I} \sum_{s\in S} \tilde{P}^{hm}_{\ell|\mathcal{I}} \rho^{hmg}_{is}(k, R_\ell) \delta^{hmg}_{qis}(k) + \sum_{w\in W} \sum_{p\in \hat{P}^w} \sum_{b\in B_4} \sum_{k'=k}^{K} \tilde{P}^{hm}_{\ell|\mathcal{I}} \hat{\rho}^{hmg}_{b}(k', R_\ell) \hat{\xi}^{hmg}_{qpwbk}(k') \right), \tag{82}$$

where R_ℓ is the average infection ratio at level ℓ, as shown in Table 12.

Remark 8. Given that the household risk-perception parameters given by (79) and (80) are zero, if we substitute the household JATP utility (73) during the COVID-19 pandemic into the mapping function of the VI problem (36), condition (50) will also ensure the uniqueness of a solution to the extended VI problem in terms of a JATP flow pattern. It is also straightforward to derive a stricter uniqueness condition related to the effect of the COVID-19 pandemic. Note that the individual scale parameters remain reserved for the utility components presented in (82).

6.2. Results

In the case study for investigating the effect of the COVID-19 pandemic, we use the small network in Example 1 with settings given in Section 5.1.1. The household scale parameter is reduced as $\theta = 0.5$, whereas the individual scale

parameter is the same as that under the normal condition. Household members are encouraged to work at home during the pandemic, and their marginal utility functions for working at home by time of day are listed in Table 13. Household members' errors of perception on working at home are found to be similar to their errors of perception on at-home activities; however, household members do not incur congestion effects at home. Three scenarios are assumed, based on the provided information about infection levels, as shown in Table 14. The individual risk-perception parameters are set as $\varrho^{hm} = 18$ HK$/h, $\hat{\varrho}^{hm} = 60$ HK$/h, and the household risk-perception parameters are set as $\varrho^{hg} = 6$ HK$/h, and $\hat{\varrho}^{hg} = 30$ HK$/h. The parameters for the risk disutility functions are $N = \hat{N} = 1$ The population is fixed at 20,000 households.

Table 13: Input parameters for the marginal utility functions for working at home during the COVID-19 pandemic by time of day.

Activity	$U_{is}^{hm(0)}$ (HK$/min)	U_{is}^{hm} (HK$)	κ_i^{hm}	υ_i^{hm}	$\tilde{t}_i^{hm}$ (min)
Work at home (husband)	0.0	1000	0.01	1	750
Work at home (wife)	0.0	1000	0.01	1	780

Table 14: Scenarios based on different provided information about infection levels during the COVID-19 pandemic.

Provided information	Prior probability			Conditional probability		
	P_1	P_2	P_3	$P_{\mathcal{I}\|1}$	$P_{\mathcal{I}\|2}$	$P_{\mathcal{I}\|3}$
Low infection	**0.6**	0.3	0.1	**0.5**	0.4	0.1
Medium infection	0.3	**0.5**	0.2	0.3	**0.4**	0.3
High infection	0.3	0.3	**0.4**	0.3	0.3	**0.4**

Table 15: Comparison of the average daily time allocation of different activities per person with the infection level, before and during the COVID-19 pandemic.

Duration (h/person)	Before COVID-19	During COVID-19		
		Low infection	Medium infection	High infection
Solo travel by car	1.3	1.4	0.9	0.8
Joint travel by car	0.5	0.5	0.5	0.2
Solo travel by transit	**1.3**	1.1	0.7	**0.4**
Joint travel by transit	**0.3**	0.1	0.0	**0.0**
Solo at-home	0.9	0.9	0.6	0.7
Joint at-home	**10.1**	10.1	11.5	**12.4**
Work (at-workplace)	**8.7**	7.8	5.7	**4.5**
work (at-home)	**0.0**	1.2	3.2	**4.4**
Solo shopping	0.2	0.2	0.2	0.2
Joint shopping	**0.7**	0.7	0.6	**0.3**
Total	24.0	24.0	24.0	24.0

Table 15 compares the average daily time allocation of different activities per person against the infection level. When the infection ratio is low (i.e., the number of confirmed cases is high), household members tend to spend more time together at home for teleworking and other at-home activities. In contrast, they spend less time at workplaces and in transit travel. This result is reasonable because it means that household members avoid the risk of infection in public areas. Furthermore, more people cancel joint shopping than solo shopping when the infection rate increases. This is because household members perceive that there is higher infection risk when conducting joint shopping (according to **B3**); this will lead to a decrease the congestion level at shopping malls, which will benefit people conducting solo shopping.

We further examine the effect of the COVID-19 pandemic at different population levels. Table 16 compares household members' activity–travel behaviors during the pandemic in terms of infection and population levels. When the infection level increases, the numbers of office workers and shop-goers decrease, which leads to reductions in the travel demands of all modes. There is also a shift from transit modes to private modes due to health concerns. These results are consistent with empirical findings (Beck and Hensher (2020); Parady et al. (2020); Shamshiripour et al. (2020); De Vos (2020)). Moreover, the effects of the pandemic are greater when the population increases, as the risk of infection at public areas is proportional to the population density.

Table 16: Comparison of the effect of COVID-19 pandemic on activity–travel behaviors in terms of infection and population levels.

Percentage (%)	During COVID-19								
	Population = 10,000			Population = 15,000			Population = 20,000		
	Low infection	Medium infection	High infection	Low infection	Medium infection	High infection	Low infection	Medium infection	High infection
Office workers	**89.0**	84.1	**72.5**	88.0	63.9	50.3	**68.3**	48.0	**38.4**
Shop goers	**97.6**	85.3	**71.2**	95.3	81.6	68.5	**86.7**	74.2	**62.4**
Travel demand	**95.6**	80.2	**60.5**	75.1	70.3	53.2	**76.5**	55.8	**42.4**
Person trips by private car	97.6	92.7	84.2	97.0	89.5	81.9	96.9	87.1	69.4
Person trips by transit	93.5	66.5	34.6	75.0	53.9	32.4	60.1	38.7	20.8

Note: 100% refers to the pre-pandemic situation, and the population is in number of households.

The above results show that our model provides better insights into the effect of the COVID-19 pandemic on specific joint/solo activity–travel behaviors than that has been achieved with conventional trip- or activity-based models. This is because the latter models have not explicitly modeled at-home activities and the risks of infection in public areas.

7. Conclusions and further studies

This paper develops a novel household-oriented activity-based mixed-equilibrium model for estimating the individual and household activity–travel choices in multimodal transportation networks with interactions between private car and public transit modes. In this novel model, household members with heterogeneous errors of perception on utility make daily joint/solo activity–travel choices in a mixed-equilibrium manner, which maximizes either their perceived household utility for each household (under the SHO principle) or their perceived individual utility for each household member (under the SUE principle). The novel mixed-equilibrium model is formulated as an equivalent VI problem, and solved using a diagonalization method. The solution method converts the time-dependent household activity–travel scheduling problem into an equivalent static traffic-assignment problem on JATPs on a supernetwork platform, and solves the problem within a unified framework.

The conditions for the existence and uniqueness of a solution to the mixed-equilibrium problem in terms of a JATP flow pattern are established. These conditions indicate the existence and uniqueness of link and path flows by different transportation modes, household activity–travel scheduling, and time allocation. This activity-based approach is superior to the trip-based approach, as the latter cannot ensure the uniqueness of link and path flows due to the asymmetric link cost functions resulting from joint travel and mixed-mode interactions in road-based multimodal networks. Such a monotonicity condition is also expected to hold in practice, if the congestion effects of activities with longer duration are greater than those of travel by different modes.

The applications of our novel mixed-equilibrium model are illustrated in numerical examples and lead to the following new insights and important findings. First, when the extra benefits of joint activities and travel are high, more household members follow the SHO principle, compared to those following the SUE principle, will improve the system's expected total utility. However, under the small extra benefits of joint activities and travel that cannot compensate the disutilities of additional pickup and drop-off trips, more household members following the SHO principle may worsen the system's expected total utility. Second, ignoring the mixed-mode interactions between the private car and public transit modes when the predetermined travel times of road-based transit modes are low (high) will lead to overestimations (underestimations) of the travel demand and transit use. Third, the system's expected

total utility is overestimated if we assume that the household members have perfect information on the network conditions, especially if their heterogeneous perceptions on the time-dependent utility of different activity types are highly inaccurate. Fourth, our novel model can be used to assess the effect of the COVID-19 pandemic, which exerts negative effects on the travel demand. Notably, the higher the number of confirmed cases and the higher population the level, the greater the effect of the COVID-19 pandemic. This effect is difficult to examine using conventional trip- or activity-based models, as these have been developed without explicit modeling of at-home activities or the risks of infection in public areas.

Our novel model does not consider some realistic aspects, which will be addressed in future work. These will involve calibrating the parameters of utility/disutility functions and household members' errors of perception under normal and COVID-19 pandemic conditions with survey data, and developing efficient solution algorithms and data structures for solving the JATP choice problem on the supernetwork platform. Our approach could also be used in a new avenue of research to investigate the effect of various types of land use and transportation planning, such as household location and high-occupancy vehicle lanes/tolls, on joint/solo activity–travel choices in multimodal transportation networks, and vice versa. Furthermore, our model could be extended to assess post-COVID-19 pandemic effects on land use and transportation planning to assist sustainable city development.

Acknowledgments

This study was supported by grants from the Research Grants Council of the Hong Kong Special Administrative Region, China (Project No. PolyU 152095/17E), the National Key Research and Development Program of China (2018YFB1600900), the National Natural Science Foundation of China (71890974/71890970), the NSFC-JPI Urban Europe (71961137001), and the Fundamental Research Funds for the Central Universities (2021GCRC014).

Appendix A. Feasibility of JATPs

In this appendix, we formulate the flow propagation relations between JATPs, paths, and links. Similar to Vo et al. (2020a), the 0–1 integer variables in constraints (40)–(42) satisfy the following constraints:

$$\underbrace{\sum_{g=1}^{G^h}\sum_{i\in I}\delta_{qis}^{hmg}(k)}_{\text{member } m \text{ at } s \text{ during } k} = \underbrace{\sum_{g=1}^{G^h}\sum_{i\in I}\delta_{qis}^{hmg}(k-1)}_{\text{member } m \text{ at } s \text{ during } k-1} - \underbrace{\sum_{g=1}^{G^h}\sum_{w\in W^-(s)}\sum_{p\in P^w}\xi_{qpw}^{hmg}(k-1) - \sum_{g=1}^{G^h}\sum_{w\in W^-(s)}\sum_{p\in \hat{P}^w}\hat{\xi}_{qpw}^{hmg}(k-1)}_{\text{car and transit users } m \text{ depart from } s \text{ during } k-1}$$
$$+ \underbrace{\sum_{g=1}^{G^h}\sum_{w\in W^+(s)}\sum_{p\in P^w}\xi_{qpw}^{hmg}(k-\lceil t_p^w(k')\rceil-1) + \sum_{g=1}^{G^h}\sum_{w\in W^+(s)}\sum_{p\in \hat{P}^w}\hat{\xi}_{qpw}^{hmg}(k-\lceil \hat{t}_p^w(k')\rceil-1)}_{\text{car and transit users } m \text{ arrive at } s \text{ during } k-1} \quad \text{(A.1)}$$

$$\underbrace{\sum_{g=1}^{G^h}\sum_{i\in I}\frac{1}{|g|}\delta_{qis}^{hmg}(k)}_{\text{private car carrying member } m \text{ at } s \text{ during } k} = \underbrace{\sum_{g=1}^{G^h}\sum_{i\in I}\frac{1}{|g|}\delta_{qis}^{hmg}(k-1)}_{\text{private car carrying member } m \text{ at } s \text{ during } k-1}$$
$$- \underbrace{\sum_{g=1}^{G^h}\sum_{w\in W^-(s)}\sum_{p\in P^w}\frac{1}{|g|}\xi_{qpw}^{hmg}(k-1)}_{\text{private car carrying member } m \text{ departs from } s \text{ during } k-1} + \underbrace{\sum_{g=1}^{G^h}\sum_{w\in W^+(s)}\sum_{p\in P^w}\frac{1}{|g|}\xi_{qpw}^{hmg}(k-\lceil t_p^w(k')\rceil-1)}_{\text{private car carrying member } m \text{ arrives at } s \text{ during } k-1} \quad \text{(A.2)}$$

where k' is the departure interval from the origin of OD pair w via path p to reach destination s during interval $(k-1)$. Constraints (A.1) and (A.2) ensure a consistent flow movement for member m of household type h and his/her private car on JATP q forward in space and time through location s during interval k where $W^-(s)$ and $W^+(s)$ are, respectively, the sets of OD pairs with s indicating origins and destinations.

In addition, the following constraints must hold.

$$\sum_{n\in g} \xi_{qpw}^{hng}(k)\varsigma_q^{hn} = \xi_{qpw}^{hmg}(k), \tag{A.3}$$

$$\sum_{i\in I} \delta_{qis}^{hmg}(k) \leqslant 1, \tag{A.4}$$

$$\sum_{k=1}^{K} \xi_{qpw}^{hmg}(k) \leqslant 1, \tag{A.5}$$

$$\sum_{k=1}^{K} \hat{\xi}_{qpw}^{hmg}(k) \leqslant 1, \tag{A.6}$$

$$\sum_{m=1}^{M^h} \varsigma_q^{hm} \leqslant V^h. \tag{A.7}$$

Constraint (A.3) is the ridesharing constraint, which forces each travel group of car users to have at least one driver from their household. Constraint (A.4) allows each JATP to have only one activity during one interval. Constraints (A.5) and (A.6) allow each JATP to use each of its private car paths and transit dummy links during only one departure interval. Constraint (A.7) is a car allocation constraint where ς_q^{hm} equals 1 if household type h choosing JATP q assigns a private car to member m during the day and 0 otherwise, and V^h is the number of cars owned by household type h.

Finally, the boundary constraint is

$$\delta_{qi_0s_0}^{hmg}(1) = \delta_{qi_0s_0}^{hmg}(K) = 1. \tag{A.8}$$

Constraint (A.8) shows that each member m within household type h choosing JATP q participates in activity i_0 at location s_0 during the initial and final intervals.

Appendix B. Proofs

Proof of Proposition 1. The Karush-Kuhn-Tucker conditions for the VI problem (36) are given by

$$\tilde{u}_q^h - \mu^h + \lambda_q^h = 0 \tag{B.1}$$

$$-f_q^h \lambda_q^h = 0 \tag{B.2}$$

where $\mu^h \geqslant 0$ and $\lambda_q^h \geqslant 0$ are the Lagrangian multipliers of constraints (38) and (39), respectively. Based on condition (B.2), if $f_q^h > 0$ then $\lambda_q^h = 0$, and if $f_q^h = 0$ then $\lambda_q^h \geqslant 0$. Hence, conditions (B.1) and (B.2) lead to the following condition

$$\begin{cases} \tilde{u}_q^h = \mu^h & \text{if } f_q^h > 0 \\ \tilde{u}_q^h \leqslant \mu^h & \text{if } f_q^h = 0 \end{cases} \tag{B.3}$$

According to condition (B.3), for any two JATPs $q \neq e$ with $f_q^h > 0$ and $f_e^h > 0$, we have

$$\tilde{u}_q^h = \tilde{u}_e^h. \tag{B.4}$$

From (37), we obtain

$$\sum_{m=1}^{M^h}\sum_{x=1}^{X^h} \eta_x^{hm} u_{qx}^{hm} - \frac{1}{\theta^h}\left(1 + \ln f_q^h\right) - CF_q^h = \sum_{m=1}^{M^h}\sum_{x=1}^{X^h} \eta_x^{hm} u_{ex}^{hm} - \frac{1}{\theta^h}\left(1 + \ln f_e^h\right) - CF_e^h. \tag{B.5}$$

Based on $\theta^h > 0$, we can derive

$$\ln f_e^h = \ln f_q^h + \left(\sum_{m=1}^{M^h}\sum_{x=1}^{X^h} \theta^h \eta_x^{hm} u_{ex}^{hm} - \theta^h CF_e^h\right) - \left(\sum_{m=1}^{M^h}\sum_{x=1}^{X^h} \theta^h \eta_x^{hm} u_{qx}^{hm} - \theta^h CF_q^h\right). \tag{B.6}$$

This leads to

$$f_e^h = f_q^h \frac{\exp\left(\sum_{m=1}^{M^h}\sum_{x=1}^{X^h} \theta^h \eta_x^{hm} u_{ex}^{hm} - \theta^h CF_e^h\right)}{\exp\left(\sum_{m=1}^{M^h}\sum_{x=1}^{X^h} \theta^h \eta_x^{hm} u_{qx}^{hm} - \theta^h CF_q^h\right)}. \tag{B.7}$$

Substituting (B.7) into constraint (38) gives

$$f_q^h \frac{\sum_{e\in Q^h} \exp\left(\sum_{m=1}^{M^h}\sum_{x=1}^{X^h} \theta^h \eta_x^{hm} u_{ex}^{hm} - \theta^h CF_e^h\right)}{\exp\left(\sum_{m=1}^{M^h}\sum_{x=1}^{X^h} \theta^h \eta_x^{hm} u_{qx}^{hm} - \theta^h CF_q^h\right)} = F^h, \tag{B.8}$$

which leads to the JATP choice model (32). This completes the proof. □

Proof of Property 1. Because there are no intra-household interactions between individuals, we can treat each individual in the system as a separate household, and the sizes of all households equal one. Then, the mapping (37) can be rewritten as

$$\tilde{u}_q^h(\mathbf{f}) = \sum_{m=1}^{1}\sum_{x=1}^{X^h} \eta_x^{hm} u_{qx}^{hm}(\mathbf{f}) - \frac{1}{\theta^h}\left(1 + \ln f_q^h\right) - CF_q^h. \tag{B.9}$$

Substituting (B.9) into (36) results in a VI problem whose solution is equivalent to the JATP flow pattern derived from the following choice model:

$$\chi_q^h = \frac{\prod_{m=1}^{1}\prod_{x=1}^{X^{hm}} \exp\left(\theta^h \eta_x^{hm} u_{qx}^{hm}\right)}{\sum_{e\in Q^h}\prod_{m=1}^{1}\prod_{x=1}^{X^{hm}} \exp\left(\theta^h \eta_x^{hm} u_{ex}^{hm}\right)}. \tag{B.10}$$

As the choice model (B.10) corresponds to only one member in the household, its solution satisfies an SUE principle. This completes the proof. □

Proof of Property 2. When $\theta^h \to +\infty, \forall h$, (37) shows that the mapping $\tilde{u}_q^h = u_q^h + CF_q^h, \forall h, q$. In addition, as $\theta^h \to +\infty$, the estimated $\tilde{\eta}_x^{hm} \to +\infty$. Due to (29), the value of η_x^{hm} can be arbitrarily set (e.g., $\eta_x^{hm} = 1$). If we ignore the commonality factor (i.e., $CF_q^h = 0$), the condition (B.3) can be rewritten as

$$\begin{cases} u_q^h = \mu^h & \text{if } f_q^h > 0 \\ u_q^h \leqslant \mu^h & \text{if } f_q^h = 0 \end{cases} \tag{B.11}$$

The above condition satisfies the deterministic HO principle in Vo et al. (2020a). This completes the proof. □

Proof of Property 3. When $\theta^h \to 0, \forall h$, from (27) we have

$$\lim_{\theta^h\to 0} \chi_q^h = \lim_{\theta^h\to 0} \frac{\exp\left(-\theta^h CF_q^h\right)\prod_{m=1}^{M^h}\prod_{x=1}^{X^{hm}} \exp\left(\theta^h \eta_x^{hm} u_{qx}^{hm}\right)}{\sum_{e\in Q^h}\exp\left(-\theta^h CF_e^h\right)\prod_{m=1}^{M^h}\prod_{x=1}^{X^{hm}} \exp\left(\theta^h \eta_x^{hm} u_{ex}^{hm}\right)} = \frac{1}{|Q^h|}. \tag{B.12}$$

This completes the proof. □

Proof of Property 4. When $\eta_x^{hm} < \eta_z^{hn}$, from (34) and (35), it is straightforward to verify that

$$\frac{\partial \chi_q^h}{\partial u_{qz}^{hn}} > \frac{\partial \chi_q^h}{\partial u_{qx}^{hm}} > 0 \tag{B.13}$$

$$\frac{\partial \chi_q^h}{\partial u_{ez}^{hn}} < \frac{\partial \chi_q^h}{\partial u_{ex}^{hm}} < 0 \quad \forall e \neq q \in Q^h. \tag{B.14}$$

The above relations indicate that the utility improvement obtained from type x activities by member m of household type h choosing JATP q has smaller effects on both the increased probability of household type h choosing JATP q (positive effect) and the decreased probability of household type h choosing any other JATP $e \neq q$ (negative effect) than does the utility improvement obtained from type z activities by member n of household type h choosing JATP q. This completes the proof. □

Proof of Proposition 2. First, we know that the feasible set of JATP flow patterns Ω is compact. Second, the link disutility functions $c_a^{hmg}(k)$ for car users and $\hat{c}_b^{hmg}(k)$ for transit passengers are continuous with the link flows as the road link travel time and the in-vehicle congestion discomfort functions are strictly increasing (**A6** and **A7**). Thus, mapping $\tilde{\mathbf{u}}(\mathbf{f})$ is continuous with JATP flow pattern $\mathbf{f}$. According to Brouwer's fixed-point theorem, this completes the proof. □

Proof of Proposition 3. For any two solutions $\mathbf{f}^{(1)*} \in \Omega$ and $\mathbf{f}^{(2)*} \in \Omega$ to the VI problem (36), we have

$$\tilde{\mathbf{u}}(\mathbf{f}^{(1)*}) \left(\mathbf{f}^{(1)*} - \mathbf{f}\right) \geqslant 0 \quad \forall \mathbf{f} \in \Omega \tag{B.15}$$

$$\tilde{\mathbf{u}}(\mathbf{f}^{(2)*}) \left(\mathbf{f}^{(2)*} - \mathbf{f}\right) \geqslant 0 \quad \forall \mathbf{f} \in \Omega. \tag{B.16}$$

Let $\mathbf{f} = \mathbf{f}^{(2)*}$ and substitute it into (B.15), and let $\mathbf{f} = \mathbf{f}^{(1)*}$ and substitute it into (B.16). Adding the resultants yields

$$\left(\tilde{\mathbf{u}}(\mathbf{f}^{(1)*}) - \tilde{\mathbf{u}}(\mathbf{f}^{(2)*})\right) \left(\mathbf{f}^{(1)*} - \mathbf{f}^{(2)*}\right) \geqslant 0. \tag{B.17}$$

According to condition (B.17), the uniqueness of a solution to the VI problem (36) in terms of the JATP pattern (i.e., $\mathbf{f}^{(1)*} = \mathbf{f}^{(2)*}$) can be established through contradiction to the following strictly monotonicity (decreasing) condition

$$\left(\tilde{\mathbf{u}}(\mathbf{f}^{(1)}) - \tilde{\mathbf{u}}(\mathbf{f}^{(2)})\right) \left(\mathbf{f}^{(1)} - \mathbf{f}^{(2)}\right) < 0 \quad \forall \mathbf{f}^{(1)} \neq \mathbf{f}^{(2)} \in \Omega. \tag{B.18}$$

First, let us rewrite (B.18) in an expanded form

$$\sum_{h=1}^{H} \sum_{q \in Q^h} \left(\tilde{u}_q^h(\mathbf{f}^{(1)}) - \tilde{u}_q^h(\mathbf{f}^{(2)})\right) \left(f_q^{h(1)} - f_q^{h(2)}\right) < 0 \quad \forall \mathbf{f}^{(1)} \neq \mathbf{f}^{(2)} \in \Omega. \tag{B.19}$$

Because the scale factors η_x^{hm} for all h, m, x, are homogeneous, which is denoted as η, the mapping (37) can be rewritten as

$$\tilde{u}_q^h(\mathbf{f}) = \eta u_q^h - \frac{1}{\theta^h}\left(1 + \ln f_q^h\right) - CF_q^h. \tag{B.20}$$

Based on (10), we can rewrite (B.20) as

$$\tilde{u}_q^h(\mathbf{f}) = \eta \left[\sum_{m=1}^{M^h} \sum_{g=1}^{G^h} \sum_{k=1}^{K} \left(\sum_{i \in I} \sum_{s \in S} u_{is}^{hmg}(k) \delta_{qis}^{hmg}(k) - \sum_{w \in W} \sum_{p \in P^w} c_{pw}^{hmg}(k) \xi_{qpw}^{hmg}(k) - \sum_{w \in W} \sum_{p \in \hat{P}^w} \hat{c}_{pw}^{hmg}(k) \hat{\xi}_{qpw}^{hmg}(k)\right)\right] - \frac{1}{\theta^h}\left(1 + \ln f_q^h\right) - CF_q^h. \tag{B.21}$$

Substituting (15) and (18) into (B.21) yields

$$\tilde{u}_q^h(\mathbf{f}) = \eta \sum_{m=1}^{M^h} \sum_{g=1}^{G^h} \sum_{k=1}^{K} \left(\sum_{i\in I} \sum_{s\in S} u_{is}^{hmg}(k) \delta_{qis}^{hmg}(k) - \sum_{w\in W} \sum_{p\in P^w} \sum_{a\in A} \sum_{k'=k}^{K} c_a^{hmg}(k') \xi_{qpwak}^{hmg}(k') \right.$$
$$\left. - \sum_{w\in W} \sum_{p\in \hat{P}^w} \sum_{b\in B} \sum_{k'=1}^{K} \hat{c}_b^{hmg}(k') \hat{\xi}_{qpwbk}^{hmg}(k') \right) - \frac{1}{\theta^h} \left(1 + \ln f_q^h\right) - CF_q^h. \quad \text{(B.22)}$$

Because the disutility functions of access, egress, and transfer links are flow-independent, we have

$$\tilde{u}_q^h(\mathbf{f}^{(1)}) - \tilde{u}_q^h(\mathbf{f}^{(2)}) = \eta \sum_{m=1}^{M^h} \sum_{g=1}^{G^h} \sum_{k=1}^{K} \left[\sum_{i\in I} \sum_{s\in S} \left(u_{is}^{hmg}(k)^{(1)} - u_{is}^{hmg}(k)^{(2)} \right) \delta_{qis}^{hmg}(k) \right.$$
$$- \sum_{w\in W} \sum_{p\in P^w} \sum_{a\in A} \sum_{k'=1}^{K} \left(c_a^{hmg}(k')^{(1)} - c_a^{hmg}(k')^{(2)} \right) \xi_{qpwak}^{hmg}(k')$$
$$\left. - \sum_{w\in W} \sum_{p\in \hat{P}^w} \sum_{b\in B_4} \sum_{k'=1}^{K} \left(\hat{c}_b^{hmg}(k')^{(1)} - \hat{c}_b^{hmg}(k')^{(2)} \right) \hat{\xi}_{qpwbk}^{hmg}(k') \right] - \frac{1}{\theta^h} \left(\ln f_q^{h(1)} - \ln f_q^{h(2)} \right). \quad \text{(B.23)}$$

According to (11), (16), and (19), (B.23) can be rewritten as

$$\tilde{u}_q^h(\mathbf{f}^{(1)}) - \tilde{u}_q^h(\mathbf{f}^{(2)}) = -\eta \sum_{m=1}^{M^h} \sum_{g=1}^{G^h} \sum_{k=1}^{K} \left[\sum_{i\in I} \sum_{s\in S} \left(\varpi_{is}(k)^{(1)} - \varpi_{is}(k)^{(2)} - \tilde{\varpi}_{is}(k)^{(1)} + \tilde{\varpi}_{is}(k)^{(2)} \right) \delta_{qis}^{hmg}(k) \right.$$
$$- \sum_{w\in W} \sum_{p\in P^w} \sum_{a\in A} \sum_{k'=k}^{K} \gamma \left(t_a(k')^{(1)} - t_a(k')^{(2)} \right) \xi_{qpwak}^{hmg}(k')$$
$$\left. - \sum_{w\in W} \sum_{p\in \hat{P}^w} \sum_{b\in B_4} \sum_{k'=1}^{K} \hat{\gamma}_4 \left(\hat{t}_b(k')^{(1)} \psi_b(k')^{(1)} - \hat{t}_b(k')^{(2)} \psi_b(k')^{(2)} \right) \hat{\xi}_{qpwbk}^{hmg}(k') \right] - \frac{1}{\theta^h} \left(\ln f_q^{h(1)} - \ln f_q^{h(2)} \right). \quad \text{(B.24)}$$

Then, by substituting (B.24) into (B.19), we have

$$- \eta \sum_{i\in I} \sum_{s\in S} \sum_{k=1}^{K} \left(\varpi_{is}(k)^{(1)} - \varpi_{is}(k)^{(2)} - \tilde{\varpi}_{is}(k)^{(1)} + \tilde{\varpi}_{is}(k)^{(2)} \right) \underbrace{\sum_{h=1}^{H} \sum_{q\in Q^h} \sum_{m=1}^{M^h} \sum_{g=1}^{G^h} \left(f_q^{h(1)} - f_q^{h(2)} \right) \delta_{qis}^{hmg}(k)}_{\left(v_{is}(k)^{(1)} - v_{is}(k)^{(2)} \right)}$$
$$- \eta\gamma \sum_{a\in A} \sum_{k'=1}^{K} \left(t_a(k')^{(1)} - t_a(k')^{(2)} \right) \underbrace{\sum_{w\in W} \sum_{p\in P^w} \sum_{k=1}^{K} \sum_{h=1}^{H} \sum_{q\in Q^h} \sum_{m=1}^{M^h} \sum_{g=1}^{G^h} \left(f_q^{h(1)} - f_q^{h(2)} \right) \xi_{qpwak}^{hmg}(k')}_{\left(v_a(k')^{(1)} - v_a(k')^{(2)} \right)}$$
$$- \eta\hat{\gamma}_4 \sum_{b\in B_4} \sum_{k'=1}^{K} \left(\hat{t}_b(k')^{(1)} \psi_b(k')^{(1)} - \hat{t}_b(k')^{(2)} \psi_b(k')^{(2)} \right) \underbrace{\sum_{w\in W} \sum_{p\in \hat{P}^w} \sum_{k=1}^{K} \sum_{h=1}^{H} \sum_{q\in Q^h} \sum_{m=1}^{M^h} \sum_{g=1}^{G^h} \left(f_q^{h(1)} - f_q^{h(2)} \right) \hat{\xi}_{qpwbk}^{hmg}(k')}_{\left(\hat{v}_b(k')^{(1)} - \hat{v}_b(k')^{(2)} \right)}$$
$$- \sum_{h=1}^{H} \sum_{q\in Q^h} \frac{1}{\theta^h} \left(\ln f_q^{h(1)} - \ln f_q^{h(2)} \right) \left(f_q^{h(1)} - f_q^{h(2)} \right) < 0. \quad \text{(B.25)}$$

Based on (51)–(55), from (B.25) we have

$$Z_1(\mathbf{f}^{(1)}, \mathbf{f}^{(2)}) - Z_2(\mathbf{f}^{(1)}, \mathbf{f}^{(2)}) + Z_3(\mathbf{f}^{(1)}, \mathbf{f}^{(2)}) + Z_4(\mathbf{f}^{(1)}, \mathbf{f}^{(2)}) + Z_5(\mathbf{f}^{(1)}, \mathbf{f}^{(2)}) > 0 \quad \forall \mathbf{f}^{(1)} \neq \mathbf{f}^{(2)} \in \Omega. \quad \text{(B.26)}$$

This completes the proof. □

References

Allahviranloo, M., Axhausen, K., 2018. An optimization model to measure utility of joint and solo activities. Transportation Research Part B 108, 172–187.

Arentze, T.A., Timmermans, H.J.P., 2004a. A learning-based transportation oriented simulation system. Transportation Research Part B 38, 613–633.

Arentze, T.A., Timmermans, H.J.P., 2004b. Multistate supernetwork approach to modelling multi-activity, multimodal trip chains. International Journal of Geographical Information Science 18, 631–651.

Arentze, T.A., Timmermans, H.J.P., 2005. Representing mental maps and cognitive learning in micro-simulation models of activity-travel choice dynamics. Transportation 32, 321–340.

Ashiru, O., Polak, J.W., Noland, R.B., 2004. Utility of schedules: Theoretical model of departure-time choice and activity-time allocation with application to individual activity schedules. Transportation Research Record: Journal of the Transportation Research Board 1894, 84–98.

Auld, J., Mohammadian, A.K., 2012. Activity planning processes in the Agent-based Dynamic Activity Planning and Travel Scheduling (ADAPTS) model. Transportation Research Part A 46, 1386–1403.

Barbieri, D.M., Lou, B., Passavanti, M., Hui, C., Hoff, I., Lessa, D.A., Sikka, G., Chang, K., Gupta, A., Fang, K., et al., 2021. Impact of covid-19 pandemic on mobility in ten countries and associated perceived risk for all transport modes. PLoS One 16, e0245886.

Beck, M.J., Hensher, D.A., 2020. Insights into the impact of COVID-19 on household travel and activities in Australia–The early days under restrictions. Transport policy 96, 76–93.

Bekhor, S., Toledo, T., Prashker, J.N., 2008. Effects of choice set size and route choice models on path-based traffic assignment. Transportmetrica 4, 117–133.

Bernardo, C., Paleti, R., Hoklas, M., Bhat, C.R., 2015. An empirical investigation into the time-use and activity patterns of dual-earner couples with and without young children. Transportation Research Part A 76, 71–91.

Bhat, C.R., Goulias, K.G., Pendyala, R.M., Paleti, R., Sidharthan, R., Schmitt, L., Hu, H.H., 2013. A household-level activity pattern generation model with an application for Southern California. Transportation 40, 1063–1086.

Bhat, C.R., Guo, J., Srinivasan, S., Sivakumar, A., 2004. Comprehensive econometric microsimulator for daily activity-travel patterns. Transportation Research Record: Journal of the Transportation Research Board 1894, 57–66.

Boyce, D., Lee, D.H., Ran, B., 2001. Analytical models of the dynamic traffic assignment problem. Networks and Spatial Economics 1, 377–390.

Bradley, M., Vovsha, P., 2005. A model for joint choice of daily activity pattern types of household members. Transportation 32, 545–571.

Cantelmo, G., Viti, F., 2019. Incorporating activity duration and scheduling utility into equilibrium-based dynamic traffic assignment. Transportation Research Part B 126, 365–390.

Cascetta, E., Nuzzolo, A., Russo, F., Vitetta, A., 1996. A modified logit route choice model overcoming path overlapping problems. Specification and some calibration results for interurban networks, in: Transportation and Traffic Theory. Proceedings of The 13th International Symposium On Transportation And Traffic Theory, Lyon, France, 24-26 July 1996.

Chen, H.K., Hsueh, C.F., 1998. A model and an algorithm for the dynamic user-optimal route choice problem. Transportation Research Part B 32, 219–234.

Chow, J.Y.J., Djavadian, S., 2015. Activity-based market equilibrium for capacitated multimodal transport systems. Transportation Research Part C 59, 2–8.

Chow, J.Y.J., Nurumbetova, A.E., 2015. A multi-day activity-based inventory routing model with space–time–needs constraints. Transportmetrica A 11, 243–269.

Covidfuture, 2020. How will COVID-19 change our world? https://covidfuture.org/. Accessed: 2020-11-21.

Dafermos, S.C., 1982. Relaxation algorithms for the general asymmetric traffic equilibrium problem. Transportation Science 16, 231–240.

De Vos, J., 2020. The effect of COVID-19 and subsequent social distancing on travel behavior. Transportation Research Interdisciplinary Perspectives 5, 100121.

Department for Transport, 2017. National Travel Survey: England. https://assets.publishing.service.gov.uk/government/uploads/system/uploads/attachment_data/file/729521/national-travel-survey-2017.pdf. Accessed: 2020-07-29.

Dubernet, T., Axhausen, K.W., 2015. Implementing a household joint activity-travel multi-agent simulation tool: first results. Transportation 42, 753–769.

Ettema, D., Bastin, F., Polak, J., Ashiru, O., 2007. Modelling the joint choice of activity timing and duration. Transportation Research Part A 41, 827–841.

Ettema, D., Timmermans, H.J.P., 2003. Modeling departure time choice in the context of activity scheduling behavior. Transportation Research Record: Journal of the Transportation Research Board 1831, 39–46.

Friesz, T.L., Harker, P.T., Tobin, R.L., 1984. Alternative algorithms for the general network spatial price equilibrium problem. Journal of Regional Science 24, 475–507.

Fu, X., Lam, W.H.K., 2014. A network equilibrium approach for modelling activity-travel pattern scheduling problems in multi-modal transit networks with uncertainty. Transportation 41, 37–55.

Fu, X., Lam, W.H.K., 2018. Modelling joint activity-travel pattern scheduling problem in multi-modal transit networks. Transportation 45, 23–49.

Fu, X., Lam, W.H.K., Meng, Q., 2014. Modelling impacts of adverse weather conditions on activity–travel pattern scheduling in multi-modal transit networks. Transportmetrica B 2, 151–167.

Gan, L.P., Recker, W., 2008. A mathematical programming formulation of the household activity rescheduling problem. Transportation Research Part B 42, 571–606.

Gan, L.P., Recker, W., 2013. Stochastic preplanned household activity pattern problem with uncertain activity participation (SHAPP). Transportation Science 47, 439–454.

Gliebe, J.P., Koppelman, F.S., 2002. A model of joint activity participation between household members. Transportation 29, 49–72.

Gliebe, J.P., Koppelman, F.S., 2005. Modeling household activity–travel interactions as parallel constrained choices. Transportation 32, 449–471.

Gupta, S., Vovsha, P., 2013. A model for work activity schedules with synchronization for multiple-worker households. Transportation 40, 827–845.

Gupta, S., Vovsha, P., Livshits, V., Maneva, P., Jeon, K., 2014. Incorporation of escorting children to school in modeling individual daily activity patterns of household members. Transportation Research Record: Journal of the Transportation Research Board 2429, 20–29.

Habib, K.N., Carrasco, J.A., Miller, E.J., 2008. Social context of activity scheduling: Discrete–continuous model of relationship between "with whom" and episode start time and duration. Transportation Research Record: Journal of the Transportation Research Board 2076, 81–87.

Hess, S., Rose, J.M., 2012. Can scale and coefficient heterogeneity be separated in random coefficients models? Transportation 39, 1225–1239.

Hong Kong Census and Statistics Department, 2017. https://www.statistics.gov.hk/pub/B10500012018QQ02B0100.pdf. Accessed: 2021-05-02.

Huang, H.J., Lam, W.H.K., 2002. Modeling and solving the dynamic user equilibrium route and departure time choice problem in network with queues. Transportation Research Part B 36, 253–273.

Janson, B.N., 1991. Dynamic traffic assignment for urban road networks. Transportation Research Part B 25, 143–161.

Kang, J.E., Recker, W., 2013. The location selection problem for the household activity pattern problem. Transportation Research Part B 55, 75–97.

Kato, H., Matsumoto, M., 2009. Intra-household interaction in a nuclear family: A utility-maximizing approach. Transportation Research Part B 43, 191–203.

Kim, J., Rasouli, S., Timmermans, H.J.P., 2018. Social networks, social influence and activity-travel behaviour: a review of models and empirical evidence. Transport Reviews 38, 499–523.

Lai, X., Lam, W.H.K., Su, J., Fu, H., 2019. Modelling intra-household interactions in time-use and activity patterns of retired and dual-earner couples. Transportation Research Part A 126, 172–194.

Lam, W.H.K., Huang, H.J., 2002. A combined activity/travel choice model for congested road networks with queues. Transportation 29, 5–29.

Lam, W.H.K., Yin, Y., 2001. An activity-based time-dependent traffic assignment model. Transportation Research Part B 35, 549–574.

Leblanc, L.J., 1973. Mathematical programming algorithms for large scale network equilibrium and network design problems. Ph.D. thesis. Northwestern University, Evanston, IL.

Li, Q., Liao, F., Timmermans, H.J., Huang, H., Zhou, J., 2018. Incorporating free-floating car-sharing into an activity-based dynamic user equilibrium model: A demand-side model. Transportation Research Part B 107, 102–123.

Li, Z.C., Lam, W.H.K., Wong, S.C., 2014. Bottleneck model revisited: An activity-based perspective. Transportation Research Part B 68, 262–287.

Li, Z.C., Lam, W.H.K., Wong, S.C., 2017. Step tolling in an activity-based bottleneck model. Transportation Research Part B 101, 306–334.

Li, Z.C., Lam, W.H.K., Wong, S.C., Sumalee, A., 2010. An activity-based approach for scheduling multimodal transit services. Transportation 37, 751–774.

Li, Z.C., Zhang, L., 2020. The two-mode problem with bottleneck queuing and transit crowding: How should congestion be priced using tolls and fares? Transportation Research Part B 138, 46–76.

Liao, F., 2016. Modeling duration choice in space–time multi-state supernetworks for individual activity-travel scheduling. Transportation Research Part C 69, 16–35.

Liao, F., 2019. Joint travel problem in space–time multi-state supernetworks. Transportation 46, 1319–1343.

Liao, F., Arentze, T.A., Timmermans, H.J.P., 2011. Constructing personalized transportation networks in multi-state supernetworks: a heuristic approach. International Journal of Geographical Information Science 25, 1885–1903.

Liao, F., Arentze, T.A., Timmermans, H.J.P., 2013a. Incorporating space-time constraints and activity-travel time profiles in a multi-state supernetwork approach to individual activity-travel scheduling. Transportation Research Part B 55, 41–58.

Liao, F., Arentze, T.A., Timmermans, H.J.P., 2013b. Multi-state supernetwork framework for the two-person joint travel problem. Transportation 40, 813–826.

Liao, F., Rasouli, S., Timmermans, H., 2014. Incorporating activity-travel time uncertainty and stochastic space–time prisms in multistate supernetworks for activity-travel scheduling. International Journal of Geographical Information Science 28, 928–945.

Lin, T., Wang, D., 2014. Social networks and joint/solo activity–travel behavior. Transportation Research Part A 68, 18–31.

Liu, J., Kang, J.E., Zhou, X., Pendyala, R., 2018. Network-oriented household activity pattern problem for system optimization. Transportation Research Part C 94, 250–269.

Liu, P., Liao, F., Huang, H.J., Timmermans, H.J.P., 2015. Dynamic activity-travel assignment in multi-state supernetworks. Transportation Research Part B 81, 656–671.

Liu, P., Liao, F., Huang, H.J., Timmermans, H.J.P., 2016. Dynamic activity-travel assignment in multi-state supernetworks under transport and location capacity constraints. Transportmetrica A 12, 572–590.

Liu, P., Liao, F., Tian, Q., Huang, H.J., Timmermans, H., 2020. Day-to-day needs-based activity-travel dynamics and equilibria in multi-state supernetworks. Transportation Research Part B 132, 208–227.

Lyu, J., Liao, F., Rasouli, S., Timmermans, H., 2021. Activity-travel scheduling in stochastic multi-state supernetworks with spatial and temporal correlations. Transportmetrica A (in press) doi:https://doi.org/10.1080/23249935.2021.1937374.

Mahmassani, H.S., Mouskos, K.C., 1988. Some numerical results on the diagonalization algorithm for network assignment with asymmetric interactions between cars and trucks. Transportation Research Part B 22, 275–290.

Najmi, A., Rey, D., Waller, S.T., Rashidi, T.H., 2020. Model formulation and calibration procedure for integrated multi-modal activity routing and network assignment models. Transportation Research Part C 121, 102853.

Nourinejad, M., Chow, J.Y.J., Roorda, M.J., 2016. Equilibrium scheduling of vehicle-to-grid technology using activity based modelling. Transportation Research Part C 65, 79–96.

Ouyang, L.Q., Lam, W.H.K., Li, Z.C., Huang, D., 2011. Network user equilibrium model for scheduling daily activity travel patterns in

congested networks. Transportation Research Record: Journal of the Transportation Research Board 2254, 131–139.
de Palma, A., Lindsey, R., Picard, N., 2015. Trip-timing decisions and congestion with household scheduling preferences. Economics of Transportation 4, 118–131.
Parady, G., Taniguchi, A., Takami, K., 2020. Travel behavior changes during the COVID-19 pandemic in Japan: Analyzing the effects of risk perception and social influence on going-out self-restriction. Transportation Research Interdisciplinary Perspectives 7, 100181.
Paulus, P.B., Annis, A.B., Seta, J.J., Schkade, J.K., Matthews, R.W., 1976. Density does affect task performance. Journal of Personality and Social Psychology 34, 248.
Public Transport Research Group, 2020. Long term impacts of COVID-19 on travel demand. https://publictransportresearchgroup.info/portfolio-item/covid-19-long-terms-impacts/. Accessed: 2020-11-09.
Ramadurai, G., Ukkusuri, S., 2010. Dynamic user equilibrium model for combined activity-travel choices using activity-travel supernetwork representation. Networks and Spatial Economics 10, 273–292.
Recker, W.W., 1995. The household activity pattern problem: general formulation and solution. Transportation Research Part B 29, 61–77.
Roorda, M.J., Carrasco, J.A., Miller, E.J., 2009. An integrated model of vehicle transactions, activity scheduling and mode choice. Transportation Research Part B 43, 217–229.
Roorda, M.J., Miller, E.J., Habib, K.N., 2008. Validation of TASHA: A 24-h activity scheduling microsimulation model. Transportation Research Part A 42, 360–375.
SCDHE's Key Indicators, 2021. https://scdhec.gov/covid19/covid-19-key-indicators. Accessed: 2021-10-04.
Shamshiripour, A., Rahimi, E., Shabanpour, R., Mohammadian, A.K., 2020. How is covid-19 reshaping activity-travel behavior? evidence from a comprehensive survey in chicago. Transportation Research Interdisciplinary Perspectives 7, 100216.
Sheffi, Y., 1985. Urban transportation networks. volume 6. Prentice-Hall, Englewood Cliffs, NJ.
Sinha, S.P., Sinha, S.P., 1991. Personal space and density as factors in task performance and feeling of crowding. The Journal of Social Psychology 131, 831–837.
Siripirote, T., Sumalee, A., Ho, H.W., Lam, W.H.K., 2015. Statistical approach for activity-based model calibration based on plate scanning and traffic counts data. Transportation Research Part B 78, 280–300.
Srinivasan, S., Bhat, C.R., 2008. An exploratory analysis of joint-activity participation characteristics using the American time use survey. Transportation 35, 301–327.
Sumalee, A., Tan, Z., Lam, W.H.K., 2009. Dynamic stochastic transit assignment with explicit seat allocation model. Transportation Research Part B 43, 895–912.
Swait, J., Louviere, J., 1993. The role of the scale parameter in the estimation and comparison of multinomial logit models. Journal of Marketing Research 30, 305–314.
Tong, C.O., Wong, S.C., 1999. A stochastic transit assignment model using a dynamic schedule-based network. Transportation Research Part B 33, 107–121.
Transport Department, 2011. Hong Kong Travel Characteristics Survey. https://www.td.gov.hk/filemanager/en/content_4652/tcs2011_eng.pdf. Accessed: 2020-07-29.
US National Household Travel Survey, 2017. https://nhts.ornl.gov/assets/2017_nhts_summary_travel_trends.pdf. Accessed: 2021-05-02.
Vo, D.K., Lam, W.H.K., Chen, A., Shao, H., 2020a. A household utility optimum approach for modeling joint activity-travel in congested road networks. Transportation Research Part B 134, 93–125.
Vo, D.K., Qian, K., Lam, W.H.K., Sumalee, A., 2020b. Modeling joint activity-travel patterns in pedestrian networks with use of wi-fi data. Asian Transport Studies 6, 100007.
Weiss, A., Habib, K.N., 2018. A generalized parallel constrained choice model for intra-household escort decision of high school students. Transportation Research Part B 114, 26–38.
Worldometer's Coronavirus Update, 2020. https://www.worldometers.info/coronavirus/. Accessed: 2020-12-14.
Wu, Z.X., Lam, W.H.K., 2003. Combined modal split and stochastic assignment model for congested networks with motorized and nonmotorized transport modes. Transportation Research Record: Journal of the Transportation Research Board 1831, 57–64.
Zhang, J., Kuwano, M., Lee, B., Fujiwara, A., 2009. Modeling household discrete choice behavior incorporating heterogeneous group decision-making mechanisms. Transportation Research Part B 43, 230–250.
Zhang, J., Timmermans, H.J.P., Borgers, A., 2005. A model of household task allocation and time use. Transportation Research Part B 39, 81–95.
Zhang, W., Susilo, Y.O., Termida, N.A., 2016. Investigating the interactions between travellers' familiar areas and their multi-day activity locations. Journal of Transport Geography 53, 61–73.